

## Tu-Pos326

**FACTORS AFFECTING SINGLE-VESICLE AMPEROMETRIC SIGNALS: A THEORETICAL STUDY.** ((Chow, R.H. and Ch. Heinemann)) Max Planck Inst. für biophysikalische Chemie, Am Fassberg, D-3400 Göttingen, Germany.

Recently carbon-fiber microelectrodes have been used for electrochemical detection of catecholamine release from single vesicles of adrenal chromaffin cells (Wightman et al, 1991, PNAS 88:10754-10758; Chow et al, 1992, Nature 356:60-63). Using Monte Carlo simulations incorporating realistic geometry, we have analysed some of the factors influencing the shape of the oxidation current transient: the diffusion constant  $D$ , the distance  $x$  from the release site to the detecting surface, and the time course of release. The main part of experimental traces were readily fit assuming instantaneous release of molecules from the cell surface, but required either that  $x \geq 1 \mu\text{m}$  (larger than expected) or that  $D \gg 5.5 \times 10^{-6} \text{ cm}^2/\text{s}$  ( $D$  of freely diffusing catecholamine). This observation points to either 1) irregular carbon fiber surfaces or cell infoldings, 2) retarded diffusion, perhaps due to a slowly diffusing complex, or 3) non-instantaneous release, perhaps reflecting the kinetics of dilation of the fusion pore or escape from a matrix. When  $D$  was adjusted to  $3 \times 10^{-7} \text{ cm}^2/\text{s}$  to fit the main part of the data traces, the simulations still did not show the slow initial onset seen in many of the experimental traces. This slow "foot" signal was previously suggested to be due to the slow leak of molecules out of the narrow fusion pore that initially connects the vesicle lumen with the outside, and that later dilates to complete exocytosis. Simulations of altered time courses for release of molecules confirmed that details of the release time course are best appreciated near the detector, with the shape of the rising phase being most informative.

## Tu-Pos328

**VOLTAGE-DEPENDENT SWELLING OF A SECRETORY GRANULE MATRIX.** ((Chaya Nanavati and Julio M. Fernandez)) Dept. of Physiol. and Biophys., Mayo Clinic, Rochester, MN 55905.

Nature has designed the secretory granule matrix for the rapid delivery of biologically active peptides and transmitters. This matrix is a miniature biopolymer consisting of a polyanionic polymer network which traps peptides and transmitters when condensed, and releases them upon exocytotic decondensation. The physical mechanisms that trigger matrix swelling and secretory product release are, however, still unknown. Upon exocytotic fusion the secretory granule matrix is transiently subjected to strong electric fields. Therefore, we designed experiments to study the effects of an electric field on the polymer matrix from the mast cell secretory granule and discovered a host of novel, unexpected properties. The matrix responded to positive and negative voltages by condensing or swelling. These condensing and swelling cycles were reversible and could be repeated several hundred times. The swelling was accompanied by a large increase in conductance. Thus, electrically, the matrix resembled a diode with a conductance which was at least a hundredfold higher at negative potentials. This conductance was super-ohmic, and up to six times greater than that predicted by simple electrodiffusion. In addition to passing a current, a swollen matrix exerted pressures on the order of a hundred pounds per square inch. All these responses took place within a few milliseconds of application of the electric field. We propose that this voltage-dependent swelling of the secretory granule matrix may play a role in the exocytotic release of secretory products.

## Tu-Pos327

**WHAT HAPPENS TO A FUSION ZONE AFTER FUSION PORES ARE CREATED IN IT?** ((Y.K. Wu, R.A. Sjodin, K. Foster\*, and A.E. Sowers\*)) Dept. Biophys. Univ. Maryland Sch Med, Baltimore, MD 21201, and \*Dept. Bioengineering, Univ. Penn., Philadelphia, PA 19104.

We have shown by thin section electron microscopy (BJ 60:1026-1037) that in a contact zone induced between erythrocyte ghosts by dielectrophoresis, the use of an electrofusion protocol converts the contact zone into a fusion zone (FZ) containing from 1-225 fusion pores per  $\mu\text{m}^2$ . Also, after creation, both the i) FZ stability, and ii) the time-dependent diameter expansion rates of the fusion zone are strongly dependent on an intact spectrin network. Using computer-assisted analysis on video-recorded phase optics images of fusion zone diameters, we have found that the FZ diameter vs. time dynamics has two, or three, distinct phases (I-III) in erythrocyte ghosts with an intact or heat-disrupted (42 °C, 20 min), respectively, spectrin network. These phases, revealed by FZ diameter vs. time measurements under some combinations of various electric pulse parameters, temperatures (4-33 °C) during measurements, heat treatment temperatures (39-50 °C), and dielectrophoretic force ( $E_{ac} = 3.25, 4.25, \& 5.25 \text{ V/mm}$ ), and under certain conditions, were remarkably independent from one another, yet the durations of Phase I (1.0-1.2 sec) and Phase II (4.0 sec) were remarkably invariant regardless of the variable studied. This suggested the existence of a complex but dissectable interplay of biomechanical factors (see also other abstract by Sowers, et al.). Supported by ONR and NSF.

## Tu-Pos329

**COMPARTMENTALIZATION OF ATP WITHIN CHOLINERGIC NERVE TERMINALS.** ((Dixon J. Woodbury and Marie Kelly)) Department of Physiology, Wayne State University School of Medicine, Detroit, MI 48201.

Within nerve terminals of the electric organ of *Torpedo*, acetylcholine (ACh) is distributed between at least two compartments. About 60% is "bound", i.e., trapped within sub-cellular organelles such as synaptic vesicles, and 40% is "free." The free ACh is generally believed to be cytosolic ACh. Solsona et al. have shown that the distribution of ATP within nerve terminals is similar to that of ACh (Solsona, Salto, and Ymborn, 1991, *BBA* 1095:57-62). In synaptosomes, the bound population is distinguished from free because it is not released into solution following a freeze and thaw (F/T) cycle. The F/T cycle fractures cell membranes but, synaptic vesicles (SVs) are thought to be too small for rupture. Nevertheless, free ATP and ACh represent cytosolic amounts only if SVs do not release ATP or ACh during the freeze/thaw cycle.

We have found that synaptic vesicles, isolated from electric organ of *Torpedo*, release significant amounts of ATP (and presumably ACh) following F/T. In solutions low in  $\text{Ca}^{++}$  and high in sucrose about 15% of the ATP is released following each initial F/T cycle, but about 50% of the total trapped ATP is not released even after 8 F/T cycles. When SVs are re-suspended in *Torpedo* ringer, about 30% of the trapped ATP is released after each F/T cycle, with less than 15% remaining after 8 F/T cycles. Based on these data, previous estimates of cytosolic ATP and ACh should be decreased from about half of the total pool to less than a fourth.

## INTERCELLULAR COMMUNICATION

## Tu-Pos330

**NOVEL EFFECTS OF DEUTERIUM OXIDE ON NITRIC-OXIDE RELATED VASODILATION AND  $[\text{Ca}^{2+}]_i$  IN VASCULAR ENDOTHELIAL CELLS.** ((R. Wang, L. Oster, J. de Champlain and R. Sauvé)) GRSNA and GRTEM, Département de Physiologie, Université de Montréal, Montréal, Québec, Canada H3C 3J7. (Spon. by G. Roy)

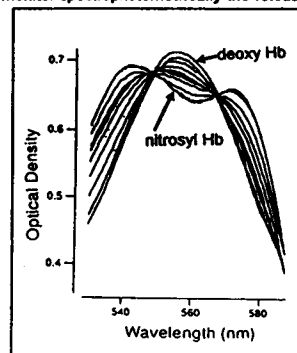
Intake of deuterium oxide ( $\text{D}_2\text{O}$ ) in drinking water has been reported to prevent or attenuate the development of hypertension in spontaneously hypertensive rats. The possibility that  $\text{D}_2\text{O}$  might alter  $[\text{Ca}^{2+}]_i$  in vascular endothelial cells, which in turn could modulate the release of nitric oxide (NO), was investigated in the present study. It was observed that  $\text{D}_2\text{O}$  relaxed pre-contracted rat mesenteric arterial beds in an endothelium-dependent manner. This effect of  $\text{D}_2\text{O}$  could be inhibited by a NO synthase inhibitor, L-NAME. In cultured bovine aortic endothelial cells,  $\text{D}_2\text{O}$  induced a biphasic increase in  $[\text{Ca}^{2+}]_i$ , with a characteristic initial transient increase followed by various patterns of sustained  $[\text{Ca}^{2+}]_i$  increase. The sustained phase was entirely dependent on the extracellular calcium entry. These data demonstrated a direct effect of  $\text{D}_2\text{O}$  on  $[\text{Ca}^{2+}]_i$  in vascular endothelial cells, which may be responsible for the endothelium-dependent, presumably NO mediated, vasodilatation induced by  $\text{D}_2\text{O}$  in precontracted vessels. A putative use of  $\text{D}_2\text{O}$  as a novel tool for the functional study of the endothelium-dependent regulation of the vascular tone can be envisioned since the  $\text{D}_2\text{O}$  effect would be independent of receptor binding mechanisms at the cell membrane level.

## Tu-Pos331

**CAGED NITRIC OXIDE (NO): RUTHENIUM NITROSYL TRICHLORIDE AS A PHOTSENSITIVE PRECURSOR OF NO AND ITS BIOLOGICAL APPLICATIONS.**

Nadir Bettache, John E. T. Corrie, Tom Carter, John Williams, David Ogden, Tim V. P. Bliss and David R. Trentham. National Institute for Medical Research, Mill Hill, London, NW7 1AA, U.K.

Ruthenium nitrosyl trichloride ( $\text{Ru}(\text{NO})\text{Cl}_3$ ) is a photosensitive precursor of nitric oxide (NO), an important mediator in several physiological processes. Hemoglobin ( $\text{Hb}[\text{Fe}(\text{II})]$ ) was used to monitor spectrophotometrically the release of NO from  $\text{Ru}(\text{NO})\text{Cl}_3$  after illumination at pH 7 and 21°C. As shown in the figure, repetitive exposure of "caged NO" to light ( $\lambda = 300-350 \text{ nm}$ ) converted deoxy Hb to nitrosyl Hb. Following a laser pulse, NO bound to deoxy Hb within 5 ms. The NO product quantum yield was estimated to be 0.012 at 320 nm. Photorelease of 10-25 nM NO from 5-10  $\mu\text{M}$  caged NO induced half-maximal relaxation of rabbit aorta. The rat hippocampal slice was also used to study the effect of NO. Photorelease of NO from 100  $\mu\text{M}$   $\text{Ru}(\text{NO})\text{Cl}_3$  produced a depression of NMDA receptor-mediated synaptic responses but did not induce long-term potentiation.



## Tu-P03332

**MODULATION OF CONNEXIN43 DURING THE CELL CYCLE OF CULTURED SMOOTH MUSCLE CELLS.** (X-D. Huang, K. L. March and M. L. Pressler) Krannert Institute of Cardiology, Indiana University & Roudebush VAMC, Indianapolis, IN

Alterations in gap junction (GJ) communication may be involved in transformation of smooth muscle (SM) cells from a contractile to a proliferative phenotype. We previously reported that cell coupling is interrupted during mitosis. We now report localization of connexin43 (CX43) during the cell cycle using immunocytochemistry combined with flow cytometry. Cultured bovine aortic SM (BASM) cells ( $\leq 7$  passages) were examined at various times after serum replation and compared to cells blocked in S and M phases by aphidicolin ( $3 \mu\text{M}$ ) and demecolcin ( $0.34 \mu\text{M}$ ) respectively. During the cell cycle, there were sequential changes in immunoreactive CX43. In G0/G1 cells, CX43 was observed in a speckled pattern over the membrane and cytoplasm. During S phase, little CX43 was found in the membrane but instead localized to perinuclear vesicular structures. During metaphase-telophase, immunoreactive staining of CX43 virtually disappeared only to reappear several hours after cell division. Preliminary studies show co-localization of CX43 and clathrin in some of the vesicular structures. The results suggest that the mechanism of uncoupling during mitosis may involve uptake of CX43 into cytoplasmic vesicles.

## Tu-P03334

**TISSUE SPECIFIC REGULATION OF GAP JUNCTION FUNCTION AND EXPRESSION BY OLEIC ACID** (K.K. Hirsch, B.N. Minnich, M.V. Olsen and J.M. Burt) Dept. of Physiology, Univ. of Arizona, Tucson, AZ 85724.

The present study examined the long-term effects of oleic acid (OA) on gap junction (GJ) mediated coupling (measured via Lucifer Yellow dye transfer technique) and connexin expression (by Northern analysis) in neonatal rat heart and A7r5 cells (aortic smooth muscle cell line). Extent of coupling was assessed in both cell types incubated at  $37^\circ\text{C}$  for 4, 8 and 24 h with various concentrations of OA in media containing 10% fetal calf serum. Coupling between A7r5 cells was dose-dependently decreased from 90 to 54% by  $0.25 \mu\text{M}$  OA. Higher concentrations of OA ( $50\text{-}150 \mu\text{M}$  OA) did not further decrease coupling in A7r5 cells. In heart cells, coupling was dose-dependently decreased from 95 to 0% with  $0\text{-}150 \mu\text{M}$  OA, with  $25 \mu\text{M}$  OA reducing coupling to only 84%. For both cell types, the effects of OA were maximal at 4 h and sustained throughout 24 h. The different effects of OA in these two cell types could not be attributed to differential incorporation of OA into cellular membranes. The effects of 25 and  $100 \mu\text{M}$  OA on coupling between A7r5 cells was fully reversed after vigorous washing with 0.5% BSA. Coupling between heart cells was only partially restored in similarly treated cells. With regard to connexin expression, there was a dose-dependent increase in Cx40 mRNA levels in A7r5 cells treated for 24 h with 25, 50 or  $100 \mu\text{M}$  OA (23, 100 and 266%, respectively). Cx43 mRNA levels in A7r5 and heart cells were not consistently affected by OA although we occasionally saw a small increase at high OA concentration. These data suggest that OA affects coupling in a tissue- and connexin-specific manner and mRNA levels in a connexin-specific manner. Supported by: Am. Heart Assoc. Az. Affil. G2-2992, Az. Dis. Contr. Res. Comm. and HL31008.

## Tu-P03336

**TEMPERATURE-DEPENDENCE OF EMBRYONIC CARDIAC GAP JUNCTION CHANNEL ACTIVITY.** (Y.-H. Chen and R.L. DeHaan) Department of Anatomy and Cell Biology, Emory University School of Medicine, Atlanta, GA 30322.

The effects of temperature on the conductance and voltage-dependent kinetics of cardiac gap junction channels between pairs of 7-day embryonic chick ventricle myocytes have been investigated over the range of  $14\text{-}27^\circ\text{C}$ , using the whole-cell double patch-clamp technique. At  $22\text{-}27^\circ\text{C}$  junctional channels had a maximal unitary conductance state near 240 pS and five smaller sub-conductance states in 40 pS increments (Chen and DeHaan, J. Membr. Biol. 127:95, 1992). Cooling decreased junctional conductance ( $G_j$ ), reduced the frequency of channel openings, and shifted the openings from larger to smaller conductance states. The mean slope of the change in  $G_j$  with temperature was  $300 \text{ pS}/^\circ\text{C}$ , yielding a temperature coefficient ( $Q_{10}$ ) of  $4.3 \pm 1.8$  ( $n=12$ ). Temperature also affected the voltage-dependent kinetics of the channels. At  $22\text{-}27^\circ\text{C}$   $G_j$  decayed in response to an 80 mV step in transjunctional voltage with a bi-exponential time course, and recovered along a symmetrical bi-exponential curve. Cooling reduced the fast decay time constant but increased both recovery time constants. These data indicate that the large conductance states (160, 200, 240 pS) are more sensitive to cooling than the smaller states, and that the activation energy required to open channels to the larger states is greater than that needed for smaller openings. (Supported by Grant NIH P01-HL27385 to RLD).

## Tu-P03333

**SPECIES DIFFERENCES IN CARDIAC CONDUCTION VELOCITY. MODULATION OF EXPRESSION OR DISTRIBUTION OF CX43 ?** (P.N. Münster, C.A. Brodhecker\*, G.E. Sandusky\* & M.L. Pressler) Krannert Institute of Cardiology & Roudebush VAMC, Indiana University and \*Lilly Research Labs, Indianapolis, IN 46202

We have previously reported that cardiac conduction velocity ( $\theta$ ) in mammalian Purkinje strands varies with the species size: small animals (e.g. cat) have 2.4-fold slower conduction than large animals (e.g. sheep). These interspecies differences in  $\theta$  may be a natural example of the functional effects of changes in number and/or distribution of gap junction channels. We used an affinity-purified antibody to residues 367-379 of connexin43 to determine 1) the amount of immunoreactive CX43 per mg total protein and 2) the distribution of CX43 in sections of ventricular muscle (VM) and Purkinje fiber bundles. Western blots of 100  $\mu\text{g}$  samples of VM extract revealed similar amounts of CX43/mg protein in mouse, dog and sheep. However, immunohistochemical staining of these same species showed changes in the distribution of CX43 as one ascended the phylogenetic scale: in larger animals, more CX43 localized in end-end junctions than side-side junctions. In addition, larger animals (e.g. sheep) had denser staining of CX43 between Purkinje myocytes. Studies are in progress to provide further details of the factors which determine the site of localization of the CX43 channels in the myocyte membrane.

## Tu-P03335

**PROTEIN KINASE C REGULATION OF JUNCTIONAL CONDUCTANCE BETWEEN CELL PAIRS EXPRESSING EXOGENOUS CONNEXIN43.** (Gregory E. Morley, Raisa Perzova, Justus Anumonwo, Jose F. Ek, Steven Taffet, Mario Delmar and Jose Jalife). SUNY/Health Science Center, Syracuse NY 13210.

Junctional conductance ( $G_j$ ) of connexin43 (Cx43) channels expressed in cells such as cardiac myocytes is known to be modulated by a variety of intracellular factors, including protein kinases. Activation of the protein kinase C (PKC) phosphorylation pathway has been reported to cause an increase in  $G_j$  of cardiac cell pairs. Yet, recent studies have shown that PKC activation decreases mean unitary junctional conductance in cell pairs expressing Cx43; in the absence of changes in open probability or channel number, the latter result would suggest that macroscopic  $G_j$  may actually decrease upon PKC stimulation. The purpose of the present study was to identify the effects of PKC activation on macroscopic  $G_j$  of cells expressing exogenous Cx43. Communication-deficient neuroblastoma cells (N2A) were transfected with Cx43 cDNA and cell pairs were patch-clamped in the dual voltage-clamp configuration.  $G_j$  was measured by holding both cells at  $-40 \text{ mV}$  and pulsing cell 1 to  $-90 \text{ mV}$  for 1 sec once every 20 seconds. PKC was activated by continuous superfusion of 200 nM of 12-O-tetradecanoylphorbol-13-acetate (TPA). PKC activation led to a 30-100% decrease in  $G_j$ . The experiments were repeated in *Xenopus* oocyte cell pairs injected with Cx43 mRNA. The results in the oocyte system were very similar to those obtained from N2A cells. Overall, the data show that TPA leads to a decrease in macroscopic  $G_j$ . Experiments under way will assess the effect of TPA on a Cx43 mutant lacking the intracellular PKC consensus sequences. Our results should lead to a better understanding of PKC-mediated regulation of intercellular communication in the heart.

## Tu-P03337

**INSIDE-OUTSIDE AND TRANSJUNCTIONAL VOLTAGE DEPENDENCE OF RAT CONNEXIN 43 CHANNELS EXPRESSED IN PAIRS OF XENOPUS OOCYTES.** (L.C. Barrio, A. Handler and M.V.L. Bennett) Neurología Experimental, Hospital Ramón y Cajal, 28034-Madrid, Spain, and \*Neuroscience, AECOM, Bronx, NY-10461, USA.

cRNA of rat connexin 43 (Cx43) was injected in pairs of *Xenopus* oocytes which endogenous expression was previously blocked with an antisense oligomer (30mer) of *Xenopus* connexin 38. After 12-48 hours, electrical coupling was measured using double voltage clamp technique. As a consequence of the peculiar architecture of intercellular channels they are under the influence of two electrical fields, i.e., the inside-outside ( $V_{in}$ ) and transjunctional ( $V_j$ ) potentials, changes of either one may modulate the junctional conductance ( $g_j$ ). Varying simultaneously the holding potential ( $V_{in}$ ) in both oocytes which were clamped at same membrane potential (i.e.,  $V_j=0$ ), the  $g_j$  increased with hyperpolarizations and decreased with depolarizations of membrane potential, jumping  $V_{in}$  from  $-80 \text{ mV}$  to  $20 \text{ mV}$  reduced the  $g_j$  to its half value; the time courses of  $g_j$  changes followed a single exponential fashion with slow time constants (c.5s). Graded transjunctional voltage steps (up  $\pm 100 \text{ mV}$ ) applied in each cell of the pair increased and decreased slightly the instantaneous  $g_j$  (defined with a clamped timing c.5ms) for positive and negative polarities, respectively. Boltzmann parameters were  $A=0.03$  and  $G_{max}=G_{min}=0.1$ . A slow  $g_j$  decay was also present for  $V_j$  steps, as  $V_j$  magnitude increased steady-state  $g_j$  fell to lower level and was reached with faster time constant.  $G_j$  was reduced to 35% of its maximum level for  $V_j = \pm 100 \text{ mV}$  with time constant of several hundred of milliseconds ( $\sim 500 \text{ ms}$ ). Boltzmann parameters were  $A=0.07$  and  $V_{1/2} = \pm 55 \text{ mV}$ . When the same  $V_j$  steps were delivered at different holding potentials, the relationship of steady-state  $g_j$  to  $V_j$  was unaffected. In pairs with higher levels of electrical coupling ( $\sim 5\text{-}10 \text{ nS}$ ), a progressive reduction of voltage sensitivity of  $g_j$  was a persistent finding.

In summary, i)  $g_j$  of rat connexin 43 junctional channels showed  $V_{in}$  and  $V_j$  dependence; ii) the sensitivity to  $V_j$  was more pronounced than to  $V_{in}$ ; iii) both types of voltage dependence may operate independently; iv) two types of gating may be present each of them with its specific voltage dependence, i.e.,  $V_j$  or  $V_{in}$ , and with different kinetics properties; and v) the increase of coupling degree over determined  $g_j$  level reduced its voltage sensitivity. Supported by FISS 92/0440 grant to L.C.B.

**Tu-P0333**

SINGLE-CHANNEL ANALYSIS OF A TRANSJUNCTIONAL VOLTAGE DEPENDENT GAP JUNCTION CHANNEL EXPRESSED IN SCHWANN CELLS

Chanson M., Rook M.B., Chandross K.J., Kessler J.A. and Spray D.C.

Under dual whole cell recording conditions, gap junctional currents measured between Schwann cells in culture exhibit a steep voltage dependence to transjunctional potential. Indeed, when a difference of potential is applied between two coupled cells, the junctional current decreased with time to a steady-state level that is equal to zero for driving forces  $> 40$  mV. Since most of these cell pairs showed low junctional conductance, recording of single gap junction channel activity at various driving forces and under equilibrium conditions was possible without the use of uncoupling agents. Amplitude distribution of transitions between open and closed states at different transjunctional potentials indicated that 80% of the Schwann cells were connected by a single population of gap junction channels with an unitary conductance ( $\gamma$ ) of 40 pS;  $\gamma$  was not affected by voltage. The probability of one channel to be open ( $P_o$ ) out of the total number of channels present in the junctional membrane was determined by using a binomial distribution.  $P_o$  decreased with increasing driving force following a Boltzmann relation with  $V_o$  (the transjunctional potential at which half of the channels closed) = 15 mV. According to the best fit,  $P_o$  in the absence of driving force could be estimated to be 0.435. The decrease in  $P_o$  is associated with a decrease of the mean open time of the channels, the time constants ranging from 1.62 sec at a driving force of 20 mV to 0.36 sec at 60 mV. These results indicate that the 40 pS gap junction channels expressed by Schwann cells behaved independently and that their gating can be described by a first order kinetic model of channel transitions between open and closed states.

**Tu-P0334**

CROSSLINKING STUDIES OF RAT AND MOUSE LIVER CONNEXINS IN PURIFIED FORM AND IN PLASMA MEMBRANES. ((M. Kordel<sup>1</sup>, B.J. Nicholson<sup>2</sup> & A.L. Harris<sup>1</sup>)) <sup>1</sup>Dept. Biophysics, Johns Hopkins Univ., Baltimore, MD 21218, <sup>2</sup>Dept. Biol., SUNY, Buffalo, NY 14260

Connexin32 (Cx32) and connexin26 (Cx26) co-localize to the same gap junctional areas in mouse liver, as shown by immunohistochemistry (Nature 329:732). We use chemical crosslinking in combination with immunaffinity purification of Cx32 to investigate whether these two connexins are present in the same channel structures. When Cx32 is immunaffinity purified from octylglucoside-solubilized liver membranes using a monoclonal antibody specific for Cx32, Cx26 co-purifies with the Cx32 (always for mouse, variably for rat), suggesting that Cx26 is present in the same structures that contain Cx32. To confirm this, the affinity-purified connexin was incubated with the cleavable lysine-specific crosslinker dithiobis(succinimidylpropionate) (DSP). Western blots of SDS-PAGE stained with connexin-specific antibodies showed that with increasing incubation times with DSP, the amount of hexameric connexin increased and the amount of monomeric and dimeric connexin decreased. Under reducing conditions that cleave DSP, Western blots showed the reappearance of monomeric Cx32 and Cx26, with concomitant reduction in hexameric connexin. To address the possibility of connexin monomer exchange between oligomeric structures during the time between membrane solubilization and affinity purification (~1 hr @4°C), plasma membranes were exposed to DSP, and then solubilized with octylglucoside and affinity purified for Cx32 as before. Western blots showed hexameric connexin as previously. Cleavage of the DSP resulted in reappearance of monomeric Cx26 and Cx32 along with reduction in hexameric connexin. These data strongly suggest that in mouse liver Cx32 and Cx26 are present in the same channel structures. Supported by NIH grants GM36044 & BRSG S07 RR07041 and ONR grant N00014-90-J-1960.

**Tu-P0342**

DIFFERENTIAL REGULATION OF CONNEXINS IN VASCULAR SMOOTH MUSCLE BY SEROTONIN (5-HT). ((L.K. Moore, M.V. Olsen, and J.M. Burt)) Univ. of Arizona, Tucson, AZ 85724

Gap junctions (GJ) form low resistance pathways between neighboring cells and thereby provide for coordination of tissue function. In vascular smooth muscle (VSM) these channels are believed to be important in maintenance of and coordination of changes in vessel tone and consequently may be of critical importance in vascular pathophysiology. 5-HT affects vessel tone in a bed specific manner and has been linked to the occurrence of vasospasm and other disease processes which may also involve abnormal GJ function or expression. VSM cells from human and pig coronary, rat mesentery, rat aorta and the A7r5 VSM cell line expressed different connexins and formed channels with distinct unitary conductances. VSM from mesenteric vessels expressed Cx43 and a 70pS channel (patch solution for all experiments contained 67mM CsCl and 67mM K-glutamate as the principle current carrying ions). A7r5 cells expressed Cx43 and Cx40 and channels with conductances of 70, 108, and 141pS. Rat probes for Cx43 and Cx40 suggested the presence of both Cx40 and Cx43 messages in pig coronary, but sometimes revealed two bands. The coronary cells exhibited 70pS channels. Brief exposure (<10min) to 1  $\mu$ M 5-HT resulted in a substantial although sometimes transient increase, on the order of 30%, in macroscopic conductance in all cell types. Treatment of cells in culture with 5-HT for 24 hours resulted in an increase in Cx43 and Cx40 mRNA levels in A7r5 cells and an increase in Cx43 mRNA in the pig coronary cells. However, in treated mesentery cells Cx43 mRNA levels were decreased. Such differences in connexin expression and GJ channel function between these VSM cell types may contribute to the differences in susceptibility of these vessel types to vasospasm and to the abnormal function associated with different vascular diseases. Supported by: HL31008, Am. Heart Assoc. Az. Affil, and Az. Dis. Control Res. Comm.

**Tu-P0339**

INTERCELLULAR COMMUNICATION IN MOUSE LEYDIG CELLS ((W.A. Varanda & A.C. Campos de Carvalho)) Dept. of Physiology, USP, 14049 Ribeirão Preto, and Institute of Biophysics, UFRJ, 21941 Rio de Janeiro, Brazil

Leydig cells can be dissociated into clusters and pairs of cells by gentle mechanical disruption of the mouse testes. Lucifer yellow injected into one cell of a cluster readily diffuses to other cells. Use of the double whole cell patch-clamp technique indicates a high degree of electrical coupling between cell pairs. In 60 pairs studied 30% displayed junctional conductance ( $g_j$ ) in the range of 1-6 nS, 31% had  $g_j$  between 6-12 nS, and 30% between 12-30 nS. Eventhough in several pairs voltage dependence could not be detected, in general, junctional conductance was voltage dependent for transjunctional voltages exceeding 50mV. Inside-out voltage dependence of  $g_j$  was not present. As expected octanol uncoupled the cells. Cell pairs tend to uncouple spontaneously making possible recordings of single channel currents. Channel mean open time is around 1 sec. Several levels of conductance can be distinguished in the records, ranging from 11 to 60 pS. The most frequent values correspond to conductances of 34 and 45 pS. Western blots of Percoll gradient purified Leydig cells using connexin specific antibodies indicate that Cx43 is expressed in these cells, while Cx26 and Cx32 are not.

**Tu-P0341**

DOPAMINE INCREASES DYE COUPLING IN FIBROBLASTS OVEREXPRESSING CONNEXIN43. ((M.A. Segerberg, A. Hotz-Wagenblatt, G.A. Weiland)) Dept. of Pharmacology, and Dept. of Biochemistry, Cell and Molecular Biology, Cornell University, Ithaca, N.Y. 14850

NIH3T3 mouse embryonic fibroblast cells which were induced to overexpress connexin43, the heart gap junction protein, were examined for permeability to the fluorescent dye Lucifer Yellow. The average number of permeable interfaces in overexpresser cells was two to three times higher than in control NIH3T3 cells. Dopamine, 10  $\mu$ M, increased coupling approximately two- to three-fold in both controls and overexpressers. The effect of dopamine was blocked by 100 nM haloperidol, a dopamine antagonist. A mutation in the connexin43 gene which eliminated nearly all the intracellular C-terminus, thus preventing phosphorylation(s) of serines or tyrosines in this portion of the molecule, was also introduced into 3T3 cells. Cells with mutant connexin43 showed increased dye permeability compared to control cells, but were unresponsive to dopamine. We conclude that phosphorylation of C-terminal tyrosines or serines may be required for dopamine sensitivity.

**Tu-P0343**

cAMP ENHANCING MANEUVERS INCREASE CALCIUM-DEPENDENT GRANULE EXOCYTOSIS IN PANCREATIC  $\beta$  CELLS. ((K. Gillis and S. Mislser)), The Jewish Hospital of St. Louis, St. Louis, MO 63110.

Enhanced cytosolic cAMP is associated with increased glucose-induced,  $Ca^{2+}$ -dependent insulin secretion by pancreatic islet  $\beta$  cells. We have reinvestigated this effect by measuring membrane capacitance increases ( $\Delta C_m$ ) from single rat  $\beta$  cells. (1) Using the perforated patch variant of whole cell recording, bath application of the phosphodiesterase inhibitor isobutylmethylxanthine (IBMX) results in larger  $\Delta C_m$ 's in response to widely spaced single voltage clamp pulses (0.033 Hz). This is associated with a 20% average increase in the inciting  $Ca^{2+}$  current. Also, the depression of  $\Delta C_m$  responses seen during a short train of voltage clamp pulses (0.2 Hz) is reduced. (2) Using conventional whole cell recording with a free  $Ca^{2+}$  concentration of ~1.5  $\mu$ M in the pipette, and the cell clamped at -70 mV to prevent depolarization dependent  $Ca^{2+}$  entry, the rate of rise of  $C_m$  after cell "pop-in" was enhanced by the presence of 150  $\mu$ M cAMP in the pipette. These results suggest that maneuvers which raise cytosolic cAMP may contribute to the enhancement of depolarization induced secretion by mobilization of granules into an available pool, as well as by enhancing  $Ca^{2+}$  entry. (Support: NIH DK37380).

## Tu-Pos344

## CONDUCTION BLOCK IN ISOLATED PURKINJE FIBERS AFTER SLIGHT LOCAL INCREASE OF INTERNAL RESISTIVITY.

(P. Daleau and J. Délèze) Laboratoire de Physiologie Cellulaire, U.A.290 CNRS, Université de Poitiers, Poitiers, France.

Coupling between cardiac cells influences conduction velocity which may lead to reentrant excitation. Therefore, studies were undertaken to determine the value of Purkinje fiber internal resistivity (R<sub>i</sub>) at which conduction block occurs. When an uncoupler (heptanol or ouabain) was superfused in the central compartment of a three compartment single mannitol gap, kinetics of the increase in R<sub>i</sub> were measured using a sub-threshold current clamp method. Substitution of mannitol by Tyrode in the central compartment enabled us to study conduction through the central gap of an action potential fired in a side compartment. We verified whether inhibition of I<sub>Na</sub> or a 30mV depolarization in the middle compartment was not able to block conduction, and determined the time to block due to application of uncouplers. 3.5 mM heptanol produced a conduction block in about 1 min (depolarization being less than 5 mV). Although 3.5mM heptanol strongly increased R<sub>i</sub> to a maximum value of 892±239% from baseline (mean±SD; n=6) in 5 to 10min, the time to block corresponds to an R<sub>i</sub> value of only 140 to 180% of control. Conduction was restored during washout of heptanol when R<sub>i</sub> was in the range of 140 to 240% of baseline. 10<sup>-6</sup>M ouabain produced a three fold increase in R<sub>i</sub> in 4 to 5 hours. As with heptanol, R<sub>i</sub> had reached only twice its baseline value at the time corresponding to conduction block. Thus, we have shown that a conduction block may be produced by a slight local increase in R<sub>i</sub>. We speculate that increased R<sub>i</sub> in cardiac fibers, as occurs during ischemia, may rapidly lead to R<sub>i</sub> discontinuity and conduction block.

## IMPORT INTO INTRACELLULAR ORGANELLES

## Tu-Pos345

## AN INTACT N-TERMINAL SEQUENCE OF RHODANESSE IS NOT REQUIRED FOR MITOCHONDRIAL BINDING AND IMPORT. ((B. Hu, J.M. Chirgwin, and P.M. Horowitz)) U. Texas Health Science Center, Dept. Biochemistry, San Antonio, TX 78230.

Rhodanese is a mitochondrial matrix enzyme which is biosynthetically imported from the cytoplasm without amino terminal cleavage. Wild type rhodanese (labeled in vitro by transcription/translation of bovine rhodanese cDNA in a pET vector) was added to purified yeast mitochondria. Import was judged successful by resistance of the labeled rhodanese to proteinase K, unless the mitochondria were permeabilized with deoxycholate. Treatment of the mitochondria with valinomycin abolished import. A series of deletion mutants, Δ1-10, Δ1-16, and Δ1-23, retaining the initiator methionine at -1, all bound to mitochondria as judged by cosedimentation, but only Δ1-10 was successfully imported. The results indicate that the amphipathic α-helix seen in the X-ray structure from residues 11 to 22 is necessary for import but that the preceding nonhelical residues are nonessential.

## Tu-Pos347

## DIRECT MEASUREMENT OF CALCIUM UPTAKE INTO THE ENDOPLASMIC RETICULUM OF PERMEABILIZED COS-1 CELLS EXPRESSING A SARCOPLASMIC RETICULUM CALCIUM PUMP. ((M.C. Klein, C.M. Sumbilla and M.F. Schneider)), Dept. of Biological Chemistry, Univ. of Maryland School of Medicine, Baltimore, MD 21201

COS-1 cells were transfected with DNA for the chick sarcoplasmic reticulum Ca-ATPase (SERCA1 of Campbell et al, J. Biol. Chem., 266, 1991) and plated on microscope cover slips. The cells were heavily loaded with fura-2 by exposure to 3 μM fura-2-AM for 0.5-1 hr, 30 °C in phosphate-buffered saline. The surface membrane was then permeabilized by 0.005% saponin in an 'intracellular' solution. All of the cytoplasmic and nuclear fura-2 diffused away, leaving behind fura-2 trapped inside internal stores. An image intensifier and video camera/frame grabber were used to record fluorescence images at excitation wavelengths of 380 and 358 nm. The resulting Ca<sup>2+</sup> images showed uniformly low [Ca<sup>2+</sup>] in all regions where the [fura-2] was high enough to measure reliable ratios. Upon exposure to solutions containing 1-10 μM free [Ca<sup>2+</sup>] and 5 mM Mg-ATP, peripheral regions of the cell accumulated Ca<sup>2+</sup> non-uniformly, as indicated by a decrease in the fluorescence at 380 nm and no change in the 358 nm signal. The accumulated Ca<sup>2+</sup> could be released by 5 μM ionomycin; 10 μM Mn<sup>2+</sup> did not quench the fluorescence. Non-transfected and mock-transfected cells never exhibited appreciable Ca<sup>2+</sup> uptake. This procedure thus provides a means for monitoring and imaging the calcium content in internal stores of permeabilized cells. Supported by NIH.

## Tu-Pos346

## COOPERATIVE EQUILIBRIA BETWEEN TRANSFERRIN AND IRON ACCEPTOR SITES OF RETICULOCYTE ENDOSOMES. ((P.R. Dellacroce, J.J. Lorio, Y.C. Ho, J.K. Abdul-Rahman, J.A. Watkins, and J. Glass)) Center of Excellence for Cancer Research, Treatment, and Education, Hematology/Oncology Section, LSU-MC-Shreveport, LA 71130.

Transferrin (Tf) binds iron (Fe) with a very high affinity (K<sub>a</sub>) and serves to deliver Fe to cells via an endocytic process during which the K<sub>a</sub> of Tf for Fe, when Tf is bound to its receptor (R<sub>Tf</sub>), must be greatly diminished. To directly measure the apparent K<sub>a</sub> of Tf for Fe upon formation of the Tf-R<sub>Tf</sub> complex, endocytic vesicles enriched in <sup>125</sup>I labeled Tf bound to R<sub>Tf</sub> were isolated from rabbit reticulocytes. The vesicles were permeabilized with 0.1% CHAPS to preserve the <sup>125</sup>I-Tf-R<sub>Tf</sub> complex, and were incubated to equilibrium with <sup>59</sup>Fe citrate (1:1000 Fe:citrate) in equilibrium dialysis chambers with 140 mM NaCl, 2 mM NaHCO<sub>3</sub>, 20 mM HEPES, 0.025% CHAPS, pH 6.0. At pH 7.0, the binding affinity of the Tf-R<sub>Tf</sub> complex for Fe was 5x10<sup>18</sup> M<sup>-1</sup> compared to 1x10<sup>21</sup> M<sup>-1</sup> for pure Tf with cooperativity constants of 0.2 and 0.3, respectively. The binding affinity of the Tf-R<sub>Tf</sub> complex for Fe at pH 6.0 was 4x10<sup>16</sup> M<sup>-1</sup> compared to 1x10<sup>19</sup> M<sup>-1</sup> for pure Tf with cooperativity constants of 0.05 and 0.08, respectively. The difference among binding constants between Tf at pH 7.0 and Tf-R<sub>Tf</sub> at pH 6.0 indicates iron dissociation is made more favorable by 6.25 kcal for the N-terminal site and 8.7 kcal for the C-terminal site. Using conditions for endosome preparation which yield the intact <sup>59</sup>Fe, <sup>125</sup>I-Tf-R<sub>Tf</sub> complex, the 2-3 intravesicular iron binding sites per Tf had an apparent binding constant of 7x10<sup>16</sup> M<sup>-1</sup>, 2.8x10<sup>16</sup> M<sup>-1</sup>, 1.4x10<sup>16</sup> M<sup>-1</sup> with a cooperativity constant of 1.6. The negative cooperativity for the Tf-R<sub>Tf</sub> complex and the positive cooperativity for the acceptor sites suggest that iron dissociation from Tf in vesicles is highly favorable.

## Tu-Pos348

## CALCIUM ACCUMULATION BY ORGANELLES WITHIN PERMEABILIZED RAT BRAIN SYNAPTOSOMES IS AFFECTED BY EGTA CONCENTRATION. ((J.E. MOORE, K. NUTT, AND R.F. ABERCROMBIE)) Department of Physiology, Emory University School of Medicine, Atlanta, GA 30322.

Because calcium uptake into intracellular organelles is dependent on free calcium ion concentration, most studies have used calcium chelators like EGTA to hold free calcium constant. We examined whether EGTA had any effect on <sup>45</sup>Ca<sup>2+</sup> uptake. Permeabilized synaptosomes (.25mg/ml saponin) were incubated in an intracellular ionic media at pH 7.4 (20mM Hepes), 37°C, and 3mM ATP for either 1, 10, 30, or 60 seconds in the presence of four different EGTA concentrations (0, 10, 100, or 1000μM). In all cases, free calcium was held at ~0.7μM, which was checked with calcium sensitive mini-electrodes. We found that <sup>45</sup>Ca<sup>2+</sup> uptake increased with time up to 30 seconds, and that this increase could be abolished by the addition of the calcium ionophore A23187. With no EGTA, ionophore sensitive <sup>45</sup>Ca<sup>2+</sup> uptake increased 0.02±0.003 μmol/g protein. In the presence of 10μM EGTA, uptake increased 0.1±0.014 μmol/g protein; in 100μM EGTA, uptake increased 0.25±0.05 μmol/g protein; and in 1000μM EGTA, ionophore sensitive calcium uptake increased 1.0±0.25 μmol/g protein in 30 s. This uptake was ATP dependent and not affected by KCN plus oligomycin-B. Our interpretation is that a mobile buffer like EGTA may enhance calcium uptake by overcoming diffusion limitations in the space surrounding the uptake sites. Supported by NIH NS-19194.

## Tu-Pos349

CHLORIDE ACTIVITY IN THE ENDOSOMAL COMPARTMENT OF SWISS 3T3 FIBROBLASTS MEASURED BY RATIO IMAGING MICROFLUORIMETRY (J. Biwersi, K. Zen, L.-B. Shi and A.S. Verkman)) Cardiovascular Research Institute, U.C.S.F., San Francisco, CA 94143

It has been proposed that inward movement of Cl accompanies proton pump-induced acidification in endocytic vesicles. To test this hypothesis, we have developed a ratio imaging method to measure Cl activity in individual endocytic vesicles in living cells. A fluorescent dextran was synthesized containing the chromophores 6-phenylquinoline (Cl sensitive) and lucifer yellow (Cl insensitive). The indicator was internalized by fluid-phase endocytosis. Cl activity was measured by a ratio imaging method using hardware and software developed recently to measure pH in individual endocytic vesicles (Zen, Biwersi, Periasamy & Verkman, J. Cell. Biol. 119:99-110, 1992). When calibrated in endosomes in intact cells using digitonin, the ratio (R) of phenylquinoline-to-lucifer yellow fluorescence decreased from 1.0 to 0.47 as [Cl] was increased from 0 to 100 mM; the [Cl] when R = 0.75 was 18 mM. The time course of endosomal [Cl] was measured after pulse labeling Swiss 3T3 fibroblasts with the dextran (15 mg/ml) for 1 min at 37 °C. [Cl] was 6 mM at 1 min after labeling and increased to 24 mM with a half-time of ~5 min. Endosomal pH decreased to ~5.5 during this time as measured by CF-TMR-dextran. After steady-state [Cl] was reached, addition of the electrogenic protonophore CCCP rapidly decreased endosomal [Cl] to 7 mM. These studies represent the first measurement of ion activity in a subcellular compartment in a living cells.

## Tu-Pos351

INTRACELLULAR OLIGONUCLEOTIDE HYBRIDIZATION DETECTED BY FLUORESCENCE RESONANCE ENERGY TRANSFER (FRET) <sup>1</sup>S. Sixou, <sup>2</sup>D.J. Chin, <sup>1</sup>G.A. Green, <sup>3</sup>B. Giusti, <sup>3</sup>G. Zon, <sup>1</sup>E.C. Szoka Jr., <sup>1</sup>School of Pharmacy, University of California, San Francisco, CA 94143, <sup>2</sup>The Agouron Institute, La Jolla, CA 92037, <sup>3</sup>Lynx Therapeutics, Foster City, CA 94144.

We have demonstrated intracellular hybrid formation between complementary oligonucleotides by FRET, following microinjection of the oligos into cultured cells. Hybrid formation between a 5'-fluorescein labeled 28-mer oligonucleotide (F-PT) and its complementary strand, labeled at the 3' end with rhodamine (R-PD) can be detected by FRET. In solution, the hybrid formed with a half-time of less than 1 minute at 37°C and had a melting temperature of 65°C. When one of the strands was a phosphodiester, the complex could be degraded by DNase I. In addition, the oligos did not interact with non-sequence specific DNA and, once formed, were stable to displacement of the complementary strand by an equal amount of labeled oligonucleotide. To learn about the intracellular hybridization and degradation kinetics of oligonucleotides, the fluorescein labeled oligos were microinjected either as the preformed duplex or as individual strands. As previously described (Chin et al., The New Biologist, 2 : 1091), the oligonucleotides rapidly accumulated in the nucleus and the half-life of a preformed duplex between a phosphorothioate and a phosphodiester complementary pair is about 15 minutes at 37°C in BSC 1 cells. Sequential microinjection of the F-PT and the R-PD (25 minutes delay) resulted in a rapid appearance of energy transfer in the nucleus between the F-PT and R-PD suggesting that hybrid formation of the complex conjugate occurred in the cell. This work has been supported by grants from NIH GM30163 (FCS), NIH (DJC) and from "Association pour la Recherche Thérapeutique" (SS).

## Tu-Pos350

PHOSPHORYLATION OF CARDIAC CALSEQUESTRIN IN ATRIAL TUMOR CELLS AND TRANSFECTED COS-1 CELLS. (Steven E. Cala, Jeffrey J. O'Brian, Adil I. Daud, and Larry R. Jones) Krannert Institute of Cardiology, Indiana University School of Medicine, Indianapolis, IN 46202 and \*DuPont Merck Pharmaceutical Company, Wilmington, DE 19880

Calsequestrin (CSQ) is the major intraluminal sarcoplasmic reticulum (SR) Ca<sup>2+</sup>-binding protein and is enriched in SR terminal cisternae. Cardiac CSQ is phosphorylated by casein kinase II on a cluster of three serine residues (Ser<sup>278,282,286</sup>) *in vitro* and *in vivo*. Several other intraluminal SR and ER proteins are also phosphorylated by casein kinase II, however a physiological role for casein kinase II phosphorylation of these proteins remains to be established. To further investigate the *in vivo* phosphorylation of cardiac CSQ, we have metabolically-labeled transformed atrial cells (AT1), as well as COS-1 cells transiently expressing recombinant cardiac CSQ. Immunoprecipitation using affinity-purified CSQ antibody revealed that CSQ was phosphorylated in both cell types, giving phosphopeptide maps which were indistinguishable from that produced after phosphorylation by casein kinase II. Pulse-chase experiments showed that CSQ phosphorylation peaked at a few hours post-labeling and decayed at a rate much faster than the CSQ protein half-life. CSQ phosphorylation in AT1 cells was largely inhibited by cycloheximide. These data suggest that *in vivo* CSQ phosphorylation occurs directly following protein synthesis. Phosphorylation by casein kinase II may confer targeting information to intraluminal SR and ER proteins.

## PROTEIN SECRETION AND SORTING

## Tu-Pos352

FLUID PHASE ENDOCYTOSIS BY ATRIAL MYOCYTES IN SITU: A NOVEL RYANODINE-INSENSITIVE CALCIUM COMPARTMENT. (E. Page and D. A. Hanck) University of Chicago, Chicago, IL 60637.

We investigated fluid phase endocytosis (FPE) associated with recycling of fused plasmalemmal/secretory granule membranes during atrial natriuretic peptide (ANP) secretion by cardiac myocytes of intact noncontracting adult rat atrial preparations *in vitro*. Measurements included (a) V<sub>f</sub>, the volume of the myocyte endocytotic vesicle compartment (S') which internalizes <sup>14</sup>C-sucrose but was inaccessible to <sup>3</sup>H-methoxyinulin; (b) kinetics of <sup>14</sup>C-sucrose efflux from S'; (c) morphometry of light and electron micrographs to show that endocytosis by nonmyocytes contributes negligibly to V<sub>f</sub>. In presence of 10 μM ryanodine and over a wide range of ANP secretory rates, V<sub>f</sub> was not significantly different from its control value in unstretched atria at 37°C (0.31 ± 0.2 ml/g dry atrium (mean ± SE, n = 12)), remaining unchanged in stretched and unstretched atria, in 0.2 mM and 1.4 mM [Ca<sup>2+</sup>]<sub>out</sub> and in solutions whose osmolarity was varied from the isotonic by from -58 mosmoles below to +100 mosmoles above the isosmolar value. V<sub>f</sub> was increased by 40% in 3 mM neomycin and decreased by 40% after alpha-1-adrenergic stimulation. Assuming S' internalizes Ca at the extracellular concentration of 1.4 mM, its Ca<sup>2+</sup> content (in endocytotic vesicles) would be 0.43 μmoles/g dry atrium, which approximately equals the published total Ca content of atrial granules (Somlyo et al, 1988). We suggest that endocytotic vesicles, interacting with nascent atrial granules, serve as the source of atrial granule Ca content, thereby creating a novel ryanodine-insensitive Ca pathway whose inward loop consists of FPE vesicles and whose outward loop includes externalization of Ca during exocytosis of ANP from atrial granules. Supported by USPHS HL-10502.

## Tu-Pos353

EFFECTS OF THE MEMBRANE BARRIER, MASS ACTION AND INTERNAL BINDING ON RELEASE OF PROTEIN FROM SECRETION GRANULES ((K.K. Goncz, M.M. Moronne and S. S. Rothman)) UCSB, Berkeley, CA 94720; LBL, Berkeley, CA 94720; UCSF, San Francisco, CA 94143.

It has been known for many years that proteins contained in isolated secretion (zymogen) granules extracted from pancreatic acinar cells are released into the suspending medium in response to mass action\*. In the current study we explore the permeability properties of the enclosing membrane to these proteins. Granules suspended in isologous medium immediately after isolation were imaged over a period of up to 4 hours, without the use of stains or fixative, with 3.64 nm X-rays at 50 nm resolution using scanning transmission X-ray microscopy. From the X-ray absorption data, the protein content and rate of protein efflux from individual granules were calculated. While maintaining their structural integrity, on average, granules continuously decreased in size and protein mass towards a final protein concentration value characteristic of each preparation. We can calculate the protein permeability coefficients (P) for individual granules using the relationship:  $P = \frac{F}{A \cdot (C_{in} - C_{out})}$  (F) protein efflux, (A) granule membrane area and (C) free protein concentration (activity). However, to do so we must determine [C]<sub>in</sub>. It is known that much of the intragranular protein is held in an aggregated, "inactive" form and therefore the calculated total protein concentration does not provide an accurate measure of [C]<sub>in</sub>. To obtain this information we must know the partition coefficient (PC) between bound and free intragranular protein at equilibrium. From previous data we calculated PC=10<sup>4</sup>. Applying this value, a permeability coefficient value of 2-6 x 10<sup>-6</sup> cm/sec was obtained. This is a large value of P for proteins and suggests a membrane transporter or pore to facilitate movement. \*Goncz et al., Biochim. Biophys. Acta. 1109:7-12 (1992).

## Tu-P03354

**pH-Dependent Association of Chromogranin A with Secretory Vesicle Membrane and A Membrane Binding Region of Chromogranin A.** Seung Hyun Yoo  
Laboratory of Cellular Biology, National Institute on Deafness and other Communication Disorders, National Institutes of Health, Bethesda, MD 20892

Chromogranin A is a low affinity, high capacity  $Ca^{2+}$  binding protein, postulated to be responsible for the  $Ca^{2+}$  buffering role of secretory vesicles and has been found only in the soluble portions of the vesicular proteins. Contrary to the generally accepted notion of chromogranin A existing as a free-floating soluble protein, chromogranin A bound to the secretory vesicle membrane at the intravesicular pH of 5.5 and freed from the membrane when the pH was raised to a more physiological pH of 7.5.

To identify the vesicle membrane binding region in chromogranin A, chromogranin A peptides representing various portions of the protein were synthesized and used for the vesicle membrane binding studies. A segment in the N-terminal region (residues 18 to 37) was shown to bind to the vesicle membrane in a pH-dependent manner. This pH-dependent vesicle membrane binding property of chromogranin A appears to be of fundamental physiological importance with regard to the roles of chromogranin A in secretory vesicle biogenesis, particularly in segregating secretory vesicle membranes from others in the *trans*-Golgi network, and also in transmitting extravesicular signals such as inositol 1,4,5-trisphosphate or inositol 1,3,4,5-tetrakisphosphate for  $Ca^{2+}$  release or uptake to the inside of vesicles.

## Tu-P03356

**NON-QUANTAL SECRETION DURING TRANSIENT VESICLE FUSION**  
G. Alvarez de Toledo\*, R. Fernández-Chacón\* & J.M. Fernández\* \*Departamento de Fisiología Médica y Biofísica. Universidad de Sevilla. 41009 Sevilla. SPAIN. †Department of Physiology & Biophysics. Mayo Clinic. Rochester, MN 55905. USA

During exocytotic fusion, a water-filled pore connects the lumen of a secretory vesicle with the extracellular environment, providing a path for the release of neurotransmitter and other secretory products. Patch-clamp experiments have shown that vesicle fusion does not occur as an all-or-none event, but can develop slowly in a fluctuating manner or can be transient. These observations raised the possibility that non quantal release, an unexplained phenomenon of common occurrence in synaptic transmission, might be observed during such incomplete transient fusion events. To test this hypothesis we have combined patch clamp measurements of the activity of single exocytotic fusion pores in beige mouse mast cells with the electrochemical detection of secretory products released during the exocytotic events. Our results show that the release starts as soon as a fusion pore forms, being linearly related to the pore conductance (Fig. A). Furthermore, we also observed a significant release during transient fusion events (Fig. B) The rate of release during transient and irreversible fusion events was very similar, suggesting that the mechanisms underlying secretion are very similar for both types of events. These results demonstrate, for the first time, the release of secretory products by a vesicle without undergoing complete fusion and may represent the basis for a non-quantal mechanism of release of secretory products.



## Tu-P03358

**EFFECT OF COATOMER COMPLEX ON INOSITOL HEXAKISPHOSPHATE BINDING OF ISOLATED GOLGI MEMBRANES**  
(J.-P. Xie and B. Fleischer) Dept. of Mol. Biol., Vanderbilt Univ., Nashville, TN 37235. (Spon. by S. Nath)

Binding of inositol polyphosphates by clathrin assembly protein AP-2 is associated with potassium ion-selective channel activity of this protein [A.P. Timmerman et al., Proc. Nat'l. Acad. Sci. USA 89, 8976 (1992)]. Coatomer is a distinct type of non-clathrin coat protein complex involved in the formation of specific Golgi intercompartmental transport vesicles. Treatment of isolated rat liver Golgi membranes with a bovine brain cytosol fraction in the presence of 2 mM  $Mg^{2+}$ , 0.25 mM ATP, an ATP regenerating system, and 1 mM guanosine triphosphate (GTP) results in a small (20%) increase in inositol hexakisphosphate ( $IP_6$ ) binding of the reisolated Golgi membranes. A greater (150%) increase of  $IP_6$  binding is obtained when 20  $\mu$ M GTP $\gamma$ S is substituted for GTP in the reaction mixture, a condition known to cause accumulation of coated transport vesicles. A parallel increase in  $\beta$ COP, a component of the coatomer complex, was found in the treated Golgi.  $\beta$ COP was estimated on Western blots of treated membranes using a specific monoclonal antibody (mAb3A5, kindly provided by Dr. T. Kreis). These studies indicate that formation of transport vesicles from Golgi membranes involves inositol polyphosphate binding proteins. (Supported by NSF Grant DCB-8908128)

## Tu-P03355

**SINGLE SECRETORY EVENTS RECORDED BY ELECTROCHEMICAL METHODS FROM RAT PINEAL CELLS.**

((A. Marin and L. Tabares)) Dept. of Physiology and Biophysics, School of Medicine, University of Seville (Spain). (sponsor J.L. López-Barneo).

Indolamine release from single isolated rat pineal cells were studied using a carbon-fiber electrode as an electrochemical detector. The fiber was subjected to a potential of +650 mV and positioned very close to the cell surface. In order to detect on line changes on the oxidation current at the tip surface, the electrode signal was continuously monitored by an I-V converter. An extracellular pulse of acetylcholine (ACh) was applied through a patch pipette to stimulate serotonin secretion. After a delay (several minutes), one or more transients of electronic currents were detected. These signals appeared as spike-like changes with a fast rising phase and a slower decay to the base line. The rise time of the fastest transients were about 100 ms, and the width of the spikes at half amplitude varied between 200 and 1200 ms. Typically, the amplitude of the spikes with fast rising phases were between 100-250 pA. Some spikes were preceded by a slower and smaller current (foot), which electronic charge represented only a small fraction of the recorded charge during the spike (i.e. 6%).

The possible effect of ACh on the ionic permeabilities of pineal cells was also investigated by means of the patch clamp technique. When a single pulse of ACh (20  $\mu$ M) was applied to a cell under whole cell, clamped at 0 mV, with a delay of about 15 s one or more outward  $K^+$  transient currents were recorded. The current started to develop slowly and reached a maximum amplitude of 70-90 pA in 3-4 s. After the peak, the current slowly decreased in 10-14 s.

These experiments show that ACh promotes the outflow of  $K^+$ , and triggers the secretion of oxidizable substances from pineal cells. These data may represent the first evidence for exocytotic serotonin release from rat pineal cells.

## Tu-P03357

**MULTIPLE COMPONENTS OF EXO- AND ENDOCYTOSIS IN SINGLE MELANOTROPHS OF THE RAT PITUITARY.** (W. Almers, P. Thomas<sup>2</sup>, J.G. Wong<sup>3</sup>)<sup>1</sup> Max-Planck-Inst. f. Med. ResearCh, Heidelberg, Germany, <sup>2</sup> Univ. of California, Davis and <sup>3</sup> Univ. of Washington, Seattle, WA

To study final steps in the secretory pathway, we have monitored exocytosis after step increases in cytosolic  $[Ca]$ . The membrane capacitance, C, was used as an assay of cell surface area.  $[Ca]$  was measured with fura-2 or fura-pra, and increased by flash photolysis of 10 mM DM-nitrophen + 8-9 mM Ca. Mg-ATP was absent, hence Mg-ATP dependent enzymes are not expected to function. Stepping  $[Ca]$  from 0.1 to 50  $\mu$ M caused two waves of exocytosis. First, C increased by 200fF (representing 300 vesicles) with a time constant of about 40 ms. As in neurons, a small subset of vesicles is prepared for rapid exocytosis. This exocytic burst depended steeply on  $[Ca]$ , was half-maximal at 30  $\mu$ M, and unaffected by internal pH 6.2. Next, C continued to increase by 0.8-1.5 pF (1200-2500 vesicles) with time constants of the order of a few s. Half-maximal at 10 - 50  $\mu$ M  $[Ca]$ , this component was shifted to 20 fold higher  $[Ca]$  by internal pH 6.2. At  $[Ca] < 100 \mu$ M, no slow phase was seen. Instead C fell rapidly (time constant  $< 1$ s), often below the value measured before the  $[Ca]$  step, in a rapid, excessive burst of endocytosis. When  $[Ca]$  increased transiently, excess endocytosis followed only the first transient; after later transients, endocytosis exactly removed the membrane added during the exocytic burst. Excess endocytosis probably removes membrane added during previous, undetected episodes of exocytosis. Evidently, the plasma membrane can accumulate membrane marked for rapid endocytosis. The approach described here provides a way to follow Ca-stimulated membrane traffic in single cells at millisecond resolution.

## Tu-P03359

**RECOMBINANT DOPAMINE BETA-HYDROXYLASE WITHOUT SIGNAL SEQUENCE IS BOTH MEMBRANE-BOUND AND SOLUBLE.**

((K. R. Gibson, P. G. Vanek<sup>‡</sup>, W. D. Kaloss\*, G. B. Collier\*, J. C. Connaughton<sup>†</sup>, M. Angelichio<sup>‡‡</sup>, G. P. Livi<sup>‡‡</sup> and P. J. Fleming\*))  
\*Georgetown University Medical Center, Department of Biochemistry, 3900 Reservoir Rd, N.W., Washington, D.C. 20007; †Laboratory of Molecular Oncology, National Cancer Institute, Frederick, MD 21701; ‡Oncor, Inc., 209 Perry Parkway, Gaithersburg, MD 20877; ‡‡SmithKline Beecham, 709 Swedeland Road, King of Prussia, PA.

The endogenous signal sequence for bovine dopamine beta-hydroxylase was replaced with a heterologous signal sequence. The expression of the recombinant enzyme in *Drosophila melanogaster* Schneider II cells was verified by Western blotting and enzyme activity. Subcellular analysis shows that the recombinant enzyme exists as both a soluble and a membrane-bound form in these cells. N-terminal sequence analysis of purified recombinant enzyme demonstrates complete removal of the signal sequence. These data demonstrate that the endogenous uncleaved signal sequence is not required for membrane binding.

This project was supported in part by PHS grant GM 27695 (to P.J.F.). KRG was supported by research fellowship MH 10223.

**Tu-P03360**

**HIGH-LEVEL EXPRESSION OF A K<sup>+</sup> CHANNEL FUSION PROTEIN FOR RAPID PURIFICATION FROM MAMMALIAN CELLS.** ((RH Spencer<sup>1</sup>, J Aiyar, S Grissmer, O Beske, GA Gutman, and KG Chandry)). Dept. Physiol. & Biophys. and <sup>2</sup>Dept. Microbiol. & Mol. Gen., UC Irvine, CA 92717.

Although mutagenesis strategies have defined functional domains in K<sup>+</sup> channels, the biochemical characterization of these proteins, a prerequisite for physicochemical analysis of the 3-dimensional structure, has been largely ignored. In order to develop a rich source of homogeneous K<sup>+</sup> channels for subsequent purification, we have employed a vaccinia viral vector (pTM1) to express a K<sup>+</sup> channel fusion protein, Kv1.3/His/G10, in mammalian cells. The fusion construct consists of a histidine repeat (His<sub>6</sub>), a sequence from gene 10 of the T7 phage, and an enterokinase cleavage site, fused in-frame to the NH<sub>2</sub>-terminus of the *Shaker*-related Kv1.3 protein. The pTM1 vector provides the promoter and terminator from T7 as well as sequences for cap-independent translation. Transfection of the construct into rat basophil leukemic cells, followed by infection with a recombinant vaccinia virus containing T7 RNA polymerase, resulted in high level expression of the channel protein (15,000 per/cell). The expressed Kv1.3/His/G10 channel activated at -30 mV, was use-dependent, and was half-blocked by 10 mM TEA or ~5 nM CTX, like the native Kv1.3 channel. The His<sub>6</sub> repeat of the fusion protein will enable purification using metal chelate chromatography, while anti-G10 antibodies could be used for immunoaffinity purification. This expression system potentially offers an efficient and rapid means for K<sup>+</sup> channel purification. Supported by AID4783, AHA/92-59, Cancer Research Inst., UCI, and a grant from Pfizer Inc.

**Tu-P03362**

**EXAMINATION OF K<sup>+</sup> CHANNEL BIOSYNTHESIS: EVIDENCE FOR GLYCOSYLATION AND COTRANSLATIONAL SUBUNIT ASSEMBLY OF Kv1.1.** ((Karen K. Deal, David M. Lovinger, and Michael M. Tamkun)) Depts. of Molecular Physiology & Biophysics and Pharmacology, Vanderbilt Medical School, Nashville, TN 37232

While the integration of electrophysiological and molecular techniques have provided great insight into structure/function relationships, K<sup>+</sup> channel cell biology is only in its infancy. To examine mechanisms involved in Kv1.1 biosynthesis, immune precipitations were conducted on Triton X-100 extracts of [<sup>35</sup>S]met-labeled mouse L-cells expressing 1,000-8,000 functional channels. Immune precipitation of Kv1.1 protein from tunicamycin treated cells yielded a core peptide of 53kD, while control cells produced a tightly associated 57-59kD doublet on SDS-PAGE. The 57kD band is the major species present in cells metabolically labeled for 20', the 59kD band is first observed at 40', and the two proteins are equally present beyond 2 hrs. Only the 59kD band is Endo H sensitive. Pulse-chase studies reveal that both species have an identical half-life of ~12 hrs. Isolation of cell surface channels via a biotinylation approach produced a diffuse band (57-59kD) suggesting additional glycosylation was not required to move to the cell surface. Subunit assembly was addressed utilizing an *in vitro* translation system and taking advantage of the ability of *Shaker*-like K<sup>+</sup> channels to form heterotetramers. When Kv1.1 and Kv1.4 were cotranslated in a microsomal system, isoform specific antisera against either channel coprecipitated both proteins. Such coprecipitation is an operational definition of subunit assembly. Assembly was detected at early time points (15') and the ratio of coprecipitated isoforms was constant during the synthesis period. Together these results suggest that: 1) in transfected L-cells mature Kv1.1 protein is glycosylated but this process is slower, less complete than for other proteins expressed in these cells and 2) assembly of heteromeric channels is cotranslational, taking place in the ER.

**Tu-P03364**

**THE ARABIDOPSIS KATI cDNA CONFERS FUNCTIONAL EXPRESSION OF AN INWARD-RECTIFYING POTASSIUM CHANNEL IN XENOPUS OOCYTES.** ((J.I. Schroeder<sup>1</sup>, D.P. Schachtman<sup>1</sup>, W.J. Lucas<sup>2</sup>, J.A. Anderson<sup>3</sup> and R.F. Gaber<sup>3</sup>)). <sup>1</sup>Dept. of Biology and Center for Molecular Genetics, University of California, San Diego, La Jolla, CA 92093-0116. <sup>2</sup>Dept. of Botany, University of California, Davis, CA 95616. <sup>3</sup>Dept. of Biochemistry, Molecular Biology and Cell Biology, Northwestern University, Evanston, IL 60208.

Inward-rectifying K<sup>+</sup> channels located in the plasma membrane of higher plant and animal cells play an essential role in excitability and cellular homeostasis. The cDNAs, *KATI* and *AKTI*, have recently been cloned from the higher plant *Arabidopsis thaliana* by the complementation of *Saccharomyces cerevisiae* mutants deficient in K<sup>+</sup> uptake. Despite some structural similarities of *KATI* and *AKTI* to outward-rectifying K<sup>+</sup> channels, these plant genes completely restored K<sup>+</sup> uptake to yeast mutants. Research on guard cells has shown that K<sup>+</sup> uptake into higher plant cells can be ascribed to proton-pump driven K<sup>+</sup> influx through inward-rectifying K<sup>+</sup> channels. We show that a single messenger RNA transcript from the *Arabidopsis thaliana KATI* cDNA confers the functional expression of hyperpolarization-activated K<sup>+</sup> channels in *Xenopus* oocytes. The time- and voltage-dependence of *KATI*-induced K<sup>+</sup> currents is similar to inward-rectifying K<sup>+</sup> channel currents in higher plant cells. The channels encoded by *KATI* are highly selective for K<sup>+</sup> over other monovalent cations, are blocked by tetraethylammonium (TEA<sup>+</sup>) and barium, and have a single channel conductance of 28±7 pS with 118 mM K<sup>+</sup> in the external solution. These functional characteristics, typical of inward-rectifying K<sup>+</sup> channels in eukaryotic cells, demonstrate that *KATI* encodes a functional inward-rectifying K<sup>+</sup> channel.

**Tu-P03361**

**RAPID TURNOVER AND GLUCOCORTICOID-INDUCED EXPRESSION OF A VOLTAGE-GATED K<sup>+</sup> CHANNEL IN CLONAL PITUITARY CELLS.**

((K.Takimoto, R.Gealy, \*J.S.Trimmer, and E.S.Levitan)) Dept. of Pharmacology, Univ. of Pittsburgh, Pittsburgh, PA15261, and \*Dept. of Biochemistry and Cell Biology, SUNY, Stony Brook, NY11794

We have been testing the hypothesis that hormones and neurotransmitters can produce long-term changes in cell excitability by regulating K<sup>+</sup> channel gene expression. Previously, we reported that glucocorticoids rapidly increased Kv1.5 K<sup>+</sup> channel mRNA in clonal and normal pituitary cells. Here we present the mechanism and consequence of this change in channel mRNA in GH<sub>4</sub> rat pituitary tumor cells. Using nuclear run-on assays, we found that dexamethasone induced gene transcription ~2.5 fold. This increase in gene transcription was also observed in the presence of cycloheximide, an inhibitor of protein synthesis. Antibodies specific for Kv1.5 polypeptide were used to measure expression of Kv1.5 protein. Immunoblots indicated that the level of the 76 kD immunoreactive protein decreased with cycloheximide with a half life of ~4 h. In contrast, dexamethasone increased the immunoreactive protein ~3 fold within 12 h. Thus, dexamethasone rapidly increases Kv1.5 protein by directly activating channel gene transcription. Hormonal regulation of K<sup>+</sup> channel gene expression constitutes a novel mechanism for producing long-term changes in the electrical activity of excitable cells.

**Tu-P03363**

**HETEROLOGOUS EXPRESSION OF THE HUMAN POTASSIUM CHANNEL Kv2.1 IN CLONAL MAMMALIAN CELLS BY DIRECT CYTOPLASMIC MICROINJECTION OF cRNA.**

((Deborah L. Lewis, Fernando Soler, Roger D. Zühke, Rolf H. Joho & Stephen R. Ikeda)) Department of Pharmacology & Toxicology, Medical College of Georgia, Augusta, GA 30912-2300 and Department of Cell Biology and Neuroscience, University of Texas Southwestern Medical Center at Dallas, Dallas, TX 75235-9039.

The cloned human delayed rectifying K<sup>+</sup> channel Kv2.1 (DRK1) was expressed in clonal mouse fibroblasts (L-cells) and rat basophilic leukemia cells (RBL-1) by direct cytoplasmic microinjection of complementary RNA (cRNA). Within six hours, cells microinjected with Kv2.1 cRNA expressed a large sustained outward current as determined from whole-cell patch-clamp recordings. Nearly 100% of cells injected with cRNA expressed outward current. Cells which were not injected, injected with water, or injected with 0.1% fluorescein dextran alone (the co-injection marker) did not express overt time-dependent outward currents. Current density was 30-70 pA/pF when measured at a potential of +50 mV. Steady-state activation and inactivation parameters for Kv2.1 were similar when expressed in either L-cells or RBL-1 cells. These results are the first to demonstrate that functional ion channel proteins can be expressed in mammalian clonal cell lines by direct cytoplasmic microinjection of cRNA.

**Tu-P03365**

**HIGH-LEVEL EXPRESSION OF WILD TYPE AND C-TERMINUS CHIMERIC HUMAN K<sup>+</sup> CHANNEL GENES (hPCN1-KV1.5) IN STABLE MAMMALIAN CELL LINES:**

**CHARACTERIZATION OF CHANNEL FUNCTION, DETECTION OF THE GENE PRODUCT AND FLUORESCENCE-ACTIVATED CELL SORTING USING TWO SITE-DIRECTED ANTIBODIES.** ((A. Malayev, L.H. Philipson, A. Kuznetsov, C. Chang, and D.J. Nelson)) University of Chicago, Chicago, IL 60637

We have recently reported the cloning and expression of a delayed rectifier K<sup>+</sup> channel (hPCN1/KV1.5) isolated from a human insulinoma cDNA library which is also present in normal human islets, brain, and heart (Philipson, L., et al. *PNAS* 88:53 (1991)). The hPCN1 cDNA driven by the CMV promoter was co-transfected into CHO cells with a neomycin resistance gene. One of several stable clones (8C4) positive for hPCN1 message by Northern blot analysis of total cellular RNA was further analyzed. Using whole cell voltage-clamp technique a large outward K<sup>+</sup> current was observed in 8C4 cells but not controls after depolarization to voltages more positive than -25mV. Activation kinetics were similar to that reported after microinjection of cRNA into *Xenopus* oocytes (Philipson et al, *ibid*); however, in contrast to the non-inactivating current observed in the oocyte, time-dependent current inactivation was observed in outside-out patches from the CHO cells. A chimeric gene (hPCN1-cp) was constructed by fusing a cDNA encoding an 32-amino acid epitope, the human proinsulin c-peptide, to the 3' end of the coding region of hPCN1. The resulting hPCN1-cp construct was also expressed in a stable CHO cell line (C33) which exhibited levels of outward current indistinguishable from the 8C4 line. Specific immunochemical detection was observed with anti-human c-peptide antibody at dilutions to 1:16,000. Western blots of membrane proteins from C33 cells revealed two bands of approximately 82 and 78 kd. The upper band was entirely eliminated by digestion with N-glycanase, suggesting that the hPCN1-cp protein was incompletely glycosylated in these cells. Cells expressing the hPCN1 channel could also be sorted by FACS from non-expressing cells using a specific anti-peptide antibody directed at the first extracellular loop. Supported by NIH Grants RO1 GM36823 and PO1 NS24575 (DJN).

**Tu-Pos366**

**INACTIVATION OF HETEROMULTIMERIC POTASSIUM CHANNELS COMPOSED OF INACTIVATING AND NON INACTIVATING SUBUNITS.** (T.E.Lee, A. Kuznetsov, L. Philipson, D. Nelson) University of Chicago, Chicago, IL 60637

We have examined inactivation rates of heteromultimeric K<sup>+</sup> channels expressed by micro injection of cRNA for a human I<sub>K</sub> (hPCN1/Kv1.5) and a human I<sub>A</sub> (hPCN2/Kv1.4) into *Xenopus* oocytes. We also constructed and characterized a tandem cDNA which was formed by linking the 5' end of hPCN1 to the 3' end of hPCN2. From the simple ball and chain model for inactivation one would predict that the inactivation rate is a function of balls per tetrameric channel. A channel formed from hPCN2 message contains four balls, a channel formed from the tandem construct or from a 1:1 co-injection contains two balls, and a heteromultimeric channel formed in a 32:1 (hPCN1:hPCN2) co-injection ratio should contain only one ball. Voltage clamp protocols were devised to isolate heteromultimeric current which took advantage of differential inactivation and steady-state inactivation. We found that, as predicted, our tandem construct (n=8) inactivated at half the rate of hPCN2 current (n=6). Unexpectedly, we found that heteromultimeric current isolated from 1:1 (n=2), 2:1 (n=7), 4:1 (n=5), 8:1 (n=6), 16:1 (n=4), and 32:1 (n=9) hPCN1:hPCN2 co-injections inactivated at the same rate as the tandem construct. It was clear that protein expression ratios reflected amounts of RNA co-injected since no pure hPCN2 current could be detected and the amount of pure hPCN1 current increased as predicted with increasing injection ratios (hPCN1 was 14% of total current for 1:1 (n=3), 28%±2 for 2:1 (n=6), 39%±2 for 4:1 (n=5), 50%±4 for 8:1 (n=6), 68%±8 for 16:1 (n=4), 70%±2 for 32:1 n=6). Evidence that the heteromultimer characterized in the 32:1 co-injection is different from the tandem was provided by steady-state inactivation experiments. The half inactivation voltage was -45.2 mV±0.7 (n=11) for the tandem and -38.7mV±0.3 (n=5) for fast inactivating current from a 32:1 co-injection. Therefore, heteromultimers formed from hPCN1 and hPCN2 which should have one ball per functional tetramer inactivate similarly to those which should have two balls, and do not show a linear decrease in inactivation rate as might be expected from the ball and chain model. Supported by NIH Grants RO1 GM36823 and PO1 NS24575 (DJN).

**Tu-Pos368**

**MODULATION OF K<sup>+</sup> CHANNEL mRNA IN PRIMARY HUMAN T LYMPHOCYTES.** ((M. Price, B. Freedman, R. Swanson, K. Folander and C. Deutsch)) Dept. of Physiology, University of Pennsylvania, Phila., PA and Merck Sharp & Dohme Res. Labs., West Point, PA.

The voltage-gated K<sup>+</sup> current observed in whole-cell patch-clamp of human peripheral T lymphocytes first increases following stimulation with mitogen (Matteson and Deutsch, 1984; Deutsch et al., 1986) due to increased number of channels (Deutsch et al., 1991), and then decreases. We have used a single-stranded DNA probe to investigate the steady-state levels of K<sup>+</sup> channel (Kv1.3) mRNA in human peripheral blood T cells. The predominant transcript is 9.5 kb. This message is maintained at a maximal steady-state level for the first few hours of stimulation with phytohemagglutinin and declines by 30 hours, consistent with the findings of Cai et al., 1992. Similar results were obtained using phorbol ester and ionomycin stimulation. While K<sup>+</sup> channel mRNA decreases, IL2 receptor mRNA increases monotonically to a maximal steady-state level by approx. 36 hours, reflecting typical kinetics of cell cycle progression. Steady-state levels of K<sup>+</sup> channel transcripts are modulated by charybdotoxin and high extracellular [K<sup>+</sup>], both of which depolarize T cells (Grinstein and Smith, 1990; Leonard et al., 1992) and inhibit stimulated proliferation and IL2 production (Price et al., 1988; Freedman et al., 1992). Supp. by GM 41467.

**Tu-Pos370**

**THE L401V MUTATION IN Kv3.1 DOES NOT ALTER SINGLE CHANNEL CONDUCTANCE OR K<sup>+</sup>/Rb<sup>+</sup> SELECTIVITY.** ((J. Ayer, S. Grisamer, and K. G. Chandy)) Dept. Physiol. & Biophys. Univ. Cal. Irvine, CA 92717.

The loop between transmembrane segments S5 and S6 (P-region) has been proposed to form the pore of voltage-gated K<sup>+</sup> channels (Hartman et al. *Science* 251:942,1991). In a Kv2.1/Kv3.1 chimera containing the Kv3.1 pore, Kirsch et al. (*Neuron* 8:499,1992; *Biophys. J.* 62:136,1992) showed that substitution of a single leucine to valine in the pore greatly altered single channel conductance (γ) and K<sup>+</sup>/Rb<sup>+</sup> selectivity, but not sensitivity to internal TEA (TEA<sub>i</sub>). However, residues that appear to be important in chimeras may not have the same significance in native proteins. To ascertain whether this indeed was the case we generated the identical mutation in native Kv3.1, and examined various channel properties. Unlike the chimera, the L401V Kv3.1 mutant channel had a γ of 27 pS and a K<sup>+</sup>/Rb<sup>+</sup> selectivity ratio of 0.5; properties identical to the native Kv3.1 channel. Furthermore, unlike the chimera, sensitivity of the L401V Kv3.1 mutant to TEA<sub>i</sub> increased substantially (half-block 3 mM) compared to the TEA<sub>i</sub>-resistant native Kv3.1. These data suggest that residue(s) outside the P-region, present in the chimera, but not in native Kv3.1, may be critical determinants of single channel conductance and K<sup>+</sup>/Rb<sup>+</sup> selectivity. Studies are in progress to find these residues. Supported by grants from Pfizer Inc., A124783 and the American Heart Association 92-59.

**Tu-Pos367**

**DIFFERENTIAL MODULATION OF 2 HUMAN POTASSIUM CHANNELS (Kv1.4, Kv1.5) BY CAMP AND THEOPHYLLINE.** ((S. S. Po, M. M. Tamkun, D. J. Snyders, P. B. Bennett)). Department of Pharmacology, Vanderbilt University School of Medicine, Nashville, TN 37232-2171.

The effects of theophylline (TH) and 8Br-cAMP on two potassium channels cloned from human heart (hKv1.4 and hKv1.5) were investigated in *Xenopus* oocytes by 2-electrode voltage clamp methods. Kv1.4 rapidly inactivates, probably by an N-type mechanism. Kv1.5 is predominantly a delayed rectifier exhibiting C-type (S6) slow inactivation and lacks the amino acid sequences corresponding to the proposed "ball" inactivation region. Incubation with 3 mM TH for 24 hours followed by recording in TH-free solutions increased the recovery time constant of Kv1.4 from 4.2 ± 0.3 to 7.7 ± 0.3 sec. (n=23, p < 0.05). Kv1.5 recovery was increased by 265% (τ<sub>recovery</sub> = 154 ± 31 (C) and 563 ± 99 (TH) msec, n=15, p < 0.05). However, levels of expressed current for Kv1.4 decreased (8 ± 0.75 μA/μF → 5.7 ± 0.87 μA/μF, n=23) while Kv1.5 increased (14.8 ± 0.15 μA/μF → 25.8 ± 3.7 μA/μF, n=16). In contrast, acute exposure to 8-Br-cAMP (100 μM) increased the recovery time constant of Kv1.4 by 53 ± 15 % (-120 mV; paired, n=4, p < 0.05) and decreased that of Kv1.5 by 32 ± 9 % (-120 mV; paired, n=4, p < 0.05). Slope factors and V<sub>1/2</sub> of inactivation curves of both Kv1.4 and Kv1.5 were unchanged. The rate of apparent macroscopic inactivation of Kv1.4 at all voltages was unchanged. Our results suggest both short and long term regulation of channel kinetics and expression levels, and that these two human potassium channels are regulated in at least two distinct ways. Supported by HL40608 and HL46681.

**Tu-Pos369**

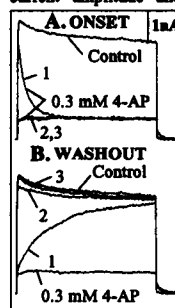
**IS A DEFECTIVE K<sup>+</sup> CHANNEL GENE (Kv3.1) RESPONSIBLE FOR THE LONG QT SYNDROME? (R. Wymore, N. Jenkins, C. Wagner-McPherson, J. Wasmuth, T. Wymore, G. Gutman, K.G. Chandy))** Department of Physiology and Biophysics, UC Irvine, CA 92717

The long QT syndrome (LQT) is an autosomal dominant disease in which repolarization after a cardiac action potential is altered such that the QT interval, as observed on an EKG of a patient, is lengthened. QT interval lengthening can lead to arrhythmias, fainting and sudden death (Ward, *J. Irish Med. Assoc.* 54:1,1964; Romano, *Lancet* 1658,1965). The genetic locus of LQT has been mapped to within ~10 cM of the H-rus protooncogene on human chromosome 11p15.5 (Keating, et al. *Science* 252:704,1991). Since delayed rectifier voltage-gated potassium (K<sup>+</sup>) channels contribute to membrane repolarization after a cardiac action potential, and because class III antiarrhythmics, and other cardiac K<sup>+</sup> channel blockers, prolong the QT interval, we have attempted to discern if any of the 14 known K<sup>+</sup> channel genes (Chandy et al. *Nature* 352:26,1991) are plausible candidates for the defective LQT gene. We have localized the *Shaw*-related Kv3.1 gene to human chromosome 11, and to mouse 7 in a region homologous with human chromosome 11p15.4. Ried et al. (*Genomics* in press, 1992) have sublocalized Kv3.1 to human 11p15, which would place it within ~8 cM of H-rus. Thus, Kv3.1, a delayed rectifier which we have shown by PCR analysis to be expressed in the heart, is a possible candidate for the defective LQT gene. The only other K<sup>+</sup> channel gene on human 11, Kv1.4, is localized in the mouse to a region homologous to human 11p13, and is therefore unlikely to be a candidate. Furthermore, the Kv1.4 gene product expresses an A-type K<sup>+</sup> current which would not be expected to contribute significantly to the QT interval. Studies are under way to more precisely locate Kv3.1 in relation to H-rus and other markers near the LQT locus. In addition we are attempting to identify Kv3.1-related polymorphisms which would be useful for linkage studies. Supported by A124783.

**Tu-Pos371**

**4-AP BLOCK OF RCK1 K<sup>+</sup> CURRENTS EXPRESSED IN SOL-8 CELLS: RELATIONSHIP BETWEEN BLOCK AND CHANNEL ACTIVATION.** ((N. A. Castle<sup>1</sup>, D. E. Logothetis<sup>1</sup> and G. K. Wang<sup>2</sup>)) <sup>1</sup>Anesthesia Research Labs., Brigham & Women's Hospital; <sup>2</sup>Dept. Cardiology, Childrens Hospital; Boston, MA

4-aminopyridine (4-AP) block of K<sup>+</sup> channels has been reported to be state dependent. We examined the blocking action of 4-AP on the cloned delayed rectifier K<sup>+</sup> channel RCK1 expressed in sol-8 cells. 4-AP was superfused onto the cell 2 min before applying a 500 ms pulse to +50 mV (HP -70 mV) to activate the channels. During the first pulse after application of 4-AP there was a small reduction in peak current amplitude and an apparent increase in the rate of inactivation (Fig A pulse



1). However, subsequent pulses (2,3) applied every 15 s showed maximal block throughout the pulse. During the first pulse following a 10 min washout of 4-AP in the absence of channel activation, the current at the beginning of the depolarizing pulse was similar to that observed during maximal block. However, during the pulse the current increased in an exponential manner to an amplitude similar to that seen in the absence of 4-AP (Fig B pulse 1). Subsequent pulses (2,3) elicited currents with profiles similar to that observed in control. These results suggest that 4-AP requires the channel to open before block can occur and that 4-AP can be trapped when the channel closes. Thus, both block and unblock of 4-AP require wild type RCK1 channels to be activated. The mode of 4-AP block of mutant RCK1 channels is presently being investigated.

**Tu-PoS372****STATE OF EXPRESSION AFFECTS BIOPHYSICAL PROPERTIES OF I<sub>K</sub>K EXPRESSED IN XENOPUS OOCYTES.**

((A.E. Busch\*, M.D. Varnum#, J.P. Adelman# and J. Maylie\*)) \*Dept. of Obstet. & Gynecol. and #Vollum Institute, Oregon Health Sciences University, Portland, OR 97201 (Spon. by J.J. Faber)

The slowly activating, voltage-dependent potassium current I<sub>K</sub>K is encoded by a protein with a molecular structure very different from other voltage-gated potassium channels. The potassium channel proteins out of the *Shaker*, *Shab*, *Shaw* and *Shal* families (and their mammalian homologues) contain six membrane-spanning regions, while the I<sub>K</sub>K-protein has only one putative transmembrane domain. Although regulation of I<sub>K</sub>K by second messengers has been well characterized, nothing is known about how this protein forms a channel and the mechanisms involved in channel activation. Furthermore there is no understanding about the subunit stoichiometry of the I<sub>K</sub>K channels. The very different molecular structure as well as activation kinetics of I<sub>K</sub>K suggest a fundamentally different gating mechanism, which may involve subunit assembly. In such case the biophysical properties of I<sub>K</sub>K should be affected by the density of the I<sub>K</sub>K protein expressed in the membrane. Here we show that expression of I<sub>K</sub>K protein increases from day 2 to day 7 after mRNA injection, reflected by an increase of the maximal conductance. Concurrent with the increase of the maximal conductance the conductance-voltage relationship is shifted to more negative potentials, while the activation of I<sub>K</sub>K is accelerated. For the *Shaker* related rat potassium channel RBK1, however, the activation kinetics and conductance-voltage relationship are not affected by the state of channel expression. These results are consistent with the hypothesis that I<sub>K</sub>K channel formation and activation might involve subunit assembly.

**Tu-PoS374****EXPRESSION OF THE I<sub>SK</sub> POTASSIUM CHANNEL PROTEIN IN RAT MYOMETRIUM AT DIFFERENT STAGES OF PREGNANCY STUDIED BY WESTERN BLOTTING.** ((M.B. Boyle, L.A.M. Heslip and L. B. MacKay)) The University of Texas Medical Branch, 301 University Blvd., Galveston, Texas 77555-1062.

Expression of the I<sub>SK</sub> protein was studied in myometrial tissue from pregnant and non-pregnant estrogen-treated rat myometrium. When I<sub>SK</sub> mRNA is injected into *Xenopus* oocytes, it induces the expression of a slowly activating K current detectable after a few days. In the rat uterus, the expression of this mRNA is higher at term than at mid gestation and is stimulated by estrogen. We now report that the expression of I<sub>SK</sub> protein may increase between mid-gestation and late pregnancy. Using an antibody made against a fusion protein containing the C-terminus of the I<sub>SK</sub> protein we detected a 21 kD protein on Western blots of rat uterine tissue. When total homogenates of uterus from three-day-estrogen-treated and estrogen-deprived ovariectomized rats were compared on Western blots, the intensity of the 21 kD band was similar for the two treatments. This finding contrasts with earlier studies of the mRNA, in which it was shown that the I<sub>SK</sub> mRNA is much more abundant in uterus from estrogen-treated rats. The I<sub>SK</sub> protein appeared to be present in similar amounts in myometrium and endometrium from estrogen-treated rats. In order to examine I<sub>SK</sub> protein levels during pregnancy, microsomal fractions were prepared from rat myometrium dissected from the uterus at different stages of pregnancy. The 21 kD band was detected on blots of pregnant rat myometrium at day 16 and at day 22 (delivering rats). The intensity of the band was similar in all samples from day 22 rats. The intensity of the 21 kD band tended to be lower in the samples from day 16 rats, but this result was variable. In five out of seven day-16 rats, the intensity of the 21 kD band was less than in the day 22 rats (n=6). These findings suggest that the I<sub>SK</sub> protein is regulated in the rat myometrium during pregnancy, becoming more abundant at term when estrogen would be expected to increase.

**Tu-PoS376****THE TOXIN HELOTHERMINE FROM MEXICAN BEADED LIZARD AFFECTS K CHANNELS IN RAT CEREBELLUM GRANULE CELLS**((V. Magnelli, M. Mobile G. Prestipino, L. Lagostena, J. Mochca-Morales\* and L.D. Possani\*)). Istituto di Cibernetica e Biofisica, CNR, Genova, Italy. \*Instituto de Biotecnologia/UNAM, Cuernavaca, México.

A novel toxin has been recently isolated from the venom of the Mexican beaded lizard *Heloderma horridum horridum*. We tested this toxin on K channels from newborn rat cerebellum granule cells with patch-clamp technique in whole-cell configuration. Currents were evoked from -80 mV holding potential with test pulses from -60 to 60 mV. Bath application of HLTX in concentration values ranging between 0.08 μM and 1.6 μM reduced both peak and steady-state currents with different percentage. The effect was voltage dependent with a blocking percentage higher for more depolarized potentials. The effect was completely reversible after washing HLTX out of the bath and it occurred within 4 minutes. Dose-response curve showed a sigmoidal course (K<sub>d</sub> = 0.4 μM). The major effect on peak current, suggests the use of HLTX as a possible tool for discriminating different components of K current. Experiments with classical K channel blockers are in progress to determine HLTX role.

**Tu-PoS373****CHEMICAL CROSSLINKING INDUCES PERSISTENT ACTIVATION OF I<sub>K</sub>K EXPRESSED IN XENOPUS OOCYTES.**

((M. D. Varnum\*, A. E. Busch#, J. Maylie# and J. P. Adelman\*)) \*Vollum Institute and #Dept. of Obstet. & Gynecol., OHSU, Portland, OR 97201.

MinK is a voltage-dependent potassium channel remarkable for its succinct structure and slowly activating current, I<sub>K</sub>K. In order to investigate the quaternary structure of this unique channel and how its structure may relate to slow activation, we have engineered rat minK cDNA to encode the FLAG antigenic sequence at the COOH-terminus of the channel protein. MinK-FLAG mRNA expressed in *Xenopus* oocytes elicited currents which closely resembled those of wild-type I<sub>K</sub>K. We applied a membrane impermeable crosslinking agent dithiobis(sulfosuccinimidyl propionate) (DTSSP) which covalently links primary amine groups. Repetitive depolarizations in the presence of DTSSP (250 μM) gradually increased the quasi-instantaneous current-voltage relation and decreased the time-dependence of I<sub>K</sub>K. Subsequently, channels remained persistently activated, independent of membrane voltage, even after prolonged washout. This current was inhibited by specific channel blockers. In addition, the DTSSP-induced effect was dependent upon depolarization. When the membrane potential was held at -100 mV during application of the crosslinker and washout, no change in I<sub>K</sub>K was observed. DTSSP had no obvious effect on oocytes expressing a divergent K channel, RBK1. Acylation without crosslinking, using the related compound Sulfo-NHS-ester, also produced no significant change in I<sub>K</sub>K. These results suggest that activation of I<sub>K</sub>K may involve a mechanism that is substantially different than that of *Shaker*-like K channels, and that this conformational change can be stabilized by chemical crosslinking. We are currently examining possible subunit interactions of DTSSP-treated channel proteins by immunoprecipitation and SDS-PAGE.

**Tu-PoS375****Charybdotoxin (ChTX) and TEA Sensitive K<sup>+</sup> Currents in Highly Ca<sup>2+</sup> Dialyzed Vascular Myocytes.** Robert H. Cox and Martin Morad, The Graduate Hospital and Dept. of Physiology, University of Pennsylvania, Philadelphia, PA, 19146.

In enzymatically dispersed rabbit portal vein myocytes dialyzed with 10mM BAPTA, whole cell K<sup>+</sup> currents were measured. These currents activated around -20mV, had a characteristic noisy appearance at potentials above +20mV, and increased with increasing voltage. Whole cell currents measured at test potentials between 0 and +60mV from holding potentials of -40 or -80mV were inhibited by both 0.5mM TEA (by 58±12%) and by 50nM ChTX (by 65±11%). Difference currents were obtained by subtraction of individual current traces at various voltages. They activated around 0mV, increased rapidly with voltage, were independent of holding potential, and showed little inactivation. Whole cell K<sup>+</sup> currents decreased 11±7% with only 0.1mM Cd<sup>2+</sup> (I<sub>Ca</sub> blocked) and 63±12% with 0.1mM Cd<sup>2+</sup> plus 0.5mM TEA. These currents decreased 42±12% with only 5mM Ni<sup>2+</sup> (block I<sub>Ca</sub> and Na:Ca exchange blocked) and 69±13% with 5mM Ni<sup>2+</sup> plus 0.5mM TEA. Cytoplasmic free [Ca<sup>2+</sup>] in cells dialyzed with 10mM BAPTA plus 0.1mM Fura-2 yielded values below 10nM. These results provide evidence for the existence of a voltage dependent, TEA and ChTX inhibited K<sup>+</sup> current under conditions of low cytoplasmic [Ca<sup>2+</sup>] (< 10nM) in portal vein myocytes.

**Tu-PoS377****DENDROTOXIN INHIBITS SODIUM AND TRANSIENT POTASSIUM CURRENTS IN MURINE HIPPOCAMPAL NEURONS.**

((X.Y. Li and J.J. McArdle)) Dept. of Pharmacology & Toxicology, New Jersey Medical School-UMDNJ, Newark, NJ 07103-2714. (Spon. by J.J. McArdle)

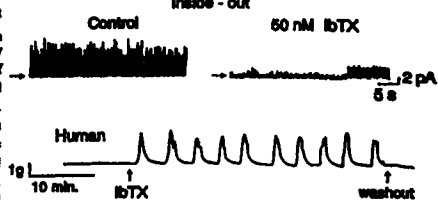
Dendrotoxin (DTX) is believed to specifically block the delayed rectifier potassium current of rat hippocampal neurons. We used the whole-cell configuration of the patch voltage-clamp technique to examine the effects of DTX on sodium current (I<sub>Na</sub>) as well as fast (I<sub>A<sub>f</sub></sub>) and slow (I<sub>A<sub>s</sub></sub>) inactivating transient potassium currents of hippocampal neurons isolated from adult mice. As expected, 1 μM TTX completely inhibited I<sub>Na</sub>. Surprisingly, 2.8 nM DTX also inhibited I<sub>Na</sub> by 57 ± 14 % of the control amplitude (n=9). For 3 neurons in which the transient K current was dominated by I<sub>A<sub>f</sub></sub>, 5.6 nM DTX caused a 65 ± 17 % decline of this current. In contrast, for 4 neurons in which the transient current was dominated by I<sub>A<sub>s</sub></sub>, 5.6 nM DTX had no significant effect. For 6 neurons having both I<sub>A<sub>f</sub></sub> and I<sub>A<sub>s</sub></sub>, DTX selectively suppressed I<sub>A<sub>f</sub></sub>. I<sub>A<sub>f</sub></sub>, I<sub>A<sub>s</sub></sub> and I<sub>A<sub>t</sub></sub> were also selectively inhibited by 10 mM TEA and 5 mM 4-AP, respectively. Our data demonstrate that DTX inhibits I<sub>Na</sub> as well as I<sub>A<sub>f</sub></sub>, suggesting a DTX binding site on both the Na and slowly inactivating transient K channel. The channel responsible for I<sub>A<sub>f</sub></sub> may lack this site or possess one which does not influence function. NIAAA AA08025 and NIH NS31040.

## Tu-Pos378

CALCIUM-ACTIVATED K CHANNELS AS MODULATORS OF HUMAN MYOMETRIAL CONTRACTILITY. ((C. Oberst, K. Aewer, B. M. Sanborn, E. Stefani and L. Toro)) Dept. Mol. Physiol. & Biophys. BCM, Dept. of Biochem. & Molec. Biol. UT Med. Sch. Houston, Texas, 77030.

The role of  $Ca^{2+}$  activated potassium ( $K_{Ca}$ ) channels in the regulation of the membrane potential, intracellular free calcium ( $Ca^{2+}$ ), and contraction in uterine smooth muscle was investigated. In cell-attached patches from a human myometrial cell line, membrane depolarization activated a  $179 \pm 4$  pS K channel which was sensitive to internal  $Ca^{2+}$  ( $n=8$ ). The channel activity was blocked by cesium tetrodotoxin (TbTX), a potent and selective blocker of  $K_{Ca}$  channels ( $n=4$ ). This blockage had important physiological consequences. TbTX depolarized the cells by  $9.8 \pm 2.8$  mV ( $n=3$ ), as measured with the potential-sensitive dye bisacryl. In Fura-2 loaded cells, blockage of  $K_{Ca}$  channels with TbTX caused a dose-dependent increase in  $Ca^{2+}$ , with an EC50 of 0.79 nM and a maximal increase of  $152 \pm 39\%$ . Blockage of these channels affected contractile activity in both human and estrogen-primed rat myometrial strips. TbTX caused phasic contractions in human myometrial strips and increased both the frequency and force of spontaneous contractions in estrogen-primed rat myometrial strips ( $n=3$ ).

These data suggest that large conductance  $K_{Ca}$  channels actively participate in the control of membrane potential and  $Ca^{2+}$  in myometrium. Thus,  $K_{Ca}$  channels have a significant role on the pattern of myometrial contractile activity. Supported by NIH and AHA-NHL Center grants.



## Tu-Pos380

IDENTIFICATION OF THE MOLECULAR COMPONENTS OF THE CHARYBDOTOXIN RECEPTOR FROM SMOOTH MUSCLE. ((H.-G. Knaus, M. Garcia-Calvo, K. Giangiacomo, O.B. McManus, G.J. Kaczorowski and M.L. Garcia)) Merck Research Laboratories, Rahway, NJ 07065

In both vascular (Garcia-Calvo, et al., 1991, Biochem., 30, 11157) and tracheal smooth muscle sarcolemmal membrane vesicles,  $^{125}I$ -charybdotoxin ( $^{125}I$ -ChTX) can be specifically cross-linked to a membrane protein that has an apparent molecular weight of 31 kDa. Treatment of these preparations with N-glycosidase F causes a time-dependent conversion of the original cross-linked material into an intermediate form of 27 kDa, and subsequently to a final product of 22 kDa. Thus, it appears that the 31 kDa subunit is heavily glycosylated at two different positions by N-linked sugars. When the solubilized ChTX receptor from both trachea and aortic smooth muscle is subjected to purification procedures, a preparation can be obtained which is enriched ca. 3000-fold in ChTX binding activity. Bolton-Hunter radiolabelling of the final preparation followed by SDS-PAGE analysis indicates the presence of two subunits (M.W.'s of 62 and 31 kDa) that fractionate with binding activity. Deglycosylation studies demonstrate that the behavior of the purified 31 kDa subunit upon SDS-PAGE is identical to that of the protein to which ChTX is cross-linked, suggesting that they are the same entity. Fully functional Maxi-K channels can be reconstituted from both purified ChTX receptor preparations, suggesting that this channel is composed of two subunits.

## Tu-Pos382

ANION-ACTIVATED  $K^+$  CHANNEL ROLE IN THE TEMPERATURE-SENSITIVITY OF THE CORNEAL ENDOTHELIAL RESTING POTENTIAL. ((M.A. Watsky and J.L. Rae)) Depts. of Physiology and Biophysics and Ophthalmology, Mayo Foundation, Rochester, MN 55905.

Previous studies have shown that the resting potential ( $E_m$ ) of the corneal endothelium hyperpolarizes following an increase in temperature above  $24^\circ C$ . In the current study, whole-cell perforated patch and on-cell single channel studies were employed to examine the influence of ion channels in this temperature sensitive response. Whole-cell studies comparing currents at  $24^\circ C$  and  $32^\circ C$  revealed a small, outwardly rectifying, slowly activating current with a small degree of voltage dependence and a reversal potential showing  $K^+$  selectivity ( $E_{rev} = -55$  mV). This current had features similar to the whole-cell current seen following addition of  $HCO_3^-$  to these cells. Single channel studies found the only change in channel activity following an elevation in temperature to be an increase in the open probability ( $P_o$ ) of a  $K^+$  channel previously reported in this cell type to be activated by external anions.  $P_o$  ( $-30$  mV) at  $24^\circ C$  and  $32^\circ C = 0.003$  and  $0.06$ , respectively. Increases in  $P_o$  were found at all voltages examined. The increased  $P_o$  for this channel at elevated temperatures is more than enough to account for the magnitude of the hyperpolarization seen in these cells following temperature elevation. Addition of  $HCO_3^-$  along with elevated temperature produced a synergistic effect on the increase in  $P_o$  along with an increased hyperpolarization of the cell. (Supported by NIH grants EY09673, EY03282, EY06005).

## Tu-Pos379

DETERMINATION OF THE TARGET SIZE OF THE CHARYBDOTOXIN RECEPTOR FROM BOVINE AORTIC AND TRACHEAL SMOOTH MUSCLE BY RADIATION INACTIVATION ANALYSIS. ((M. Garcia-Calvo, H.G. Knaus, G.J. Kaczorowski, M.L. Garcia, and E. Kempner)) Merck Research Laboratories, Rahway, NJ 07065 and \*The National Institutes of Health, Bethesda, MD 20892. (Spon. J.P. Reuben)

Radiation inactivation analysis was employed to determine the target size of the charybdotoxin (ChTX) receptor which is part of the Maxi-K channel in bovine aortic and tracheal sarcolemmal membrane vesicles. [ $^{125}I$ ]ChTX binding follows a mono-exponential relationship vs. dose of radiation and loss of activity is due to a decrease in the site density of ChTX receptors. The calculated minimum target size for the membrane-bound receptor in each of these tissues is 88 kDa. Similar experiments with the digitonin-solubilized ChTX receptor from aorta yield a minimum target size of 96 kDa. In the same membrane preparations, the minimum target sizes of 5' nucleotidase and of the  $\alpha_1$  subunit of the L-type  $Ca^{2+}$  channel are 70 kDa and 207 kDa, respectively. These values correlate well with the molecular weights previously determined for these proteins. Since in previous experiments [ $^{125}I$ ]ChTX was specifically cross-linked to a 31 kDa glycoprotein (of which 22 kDa is protein), the current data are consistent with a subunit composition of the Maxi-K channel of either a tetramer of 22 kDa proteins, or of proteins of 22 and ca. 60 kDa. Recent data from this laboratory support the second hypothesis.

## Tu-Pos381

AN ULTRA-RAPIDLY ACTIVATING DELAYED RECTIFIER CARRIES SUSTAINED OUTWARD CURRENT IN HUMAN ATRIAL MYOCYTES. ((Z. Wang, B. Ferrini, S. Nattel)) Montreal Heart Institute, Montreal, Quebec, Canada, HIT IC8.

Depolarization of human atrial cells activates a transient outward current, which then inactivates rapidly leaving a sustained current ( $I_s$ ). To determine the ionic mechanism of  $I_s$ , we applied the whole-cell patch-clamp technique to isolated human atrial myocytes. When  $I_s$  was inactivated by a conditioning pre-pulse to  $+40$  mV, depolarizing steps from  $-50$  mV elicited  $I_s$ , which appeared instantaneous at  $36^\circ C$  but was time-dependent at  $25^\circ C$  with activation  $\tau$  varying from  $18 \pm 3$  ms ( $-10$  mV) to  $2.0 \pm 0.2$  ms (at  $+50$  mV).  $I_s$  activated at the plateau voltage range, and its size increased at more positive potentials. The activation curve determined from  $I_s$  current tails was well fitted by a Boltzmann distribution with midpoint and slope factor of  $-5.0 \pm 3.5$  mV and  $10.0 \pm 1.5$  mV ( $n=10$ ), respectively. Partial inactivation of  $I_s$  was observed at potentials positive to  $+40$  mV in 67% cells (20/30, 25% reduction after 500 ms at  $+60$  mV).  $I_s$  was highly sensitive to 4AP, with an  $IC_{50}$  of  $49.6 \pm 1.6$   $\mu M$ , compared to  $2.0 \pm 0.1$  mM for  $I_{Kr}$ . 50  $\mu M$  4AP selectively blocked  $I_s$ , and increased APD by  $66 \pm 11\%$ . The current blocked by 50  $\mu M$  4AP had the same kinetics and voltage-dependence as revealed when  $I_s$  was evoked after  $I_{Kr}$  was inactivated by a conditioning pulse. The dependence of  $I_s$  reversal potential (determined from  $I_s$  tails) on  $[K^+]_o$  (55 mV/decade), along with the fact that no  $I_s$  was seen with  $Cs^+$  substitution for  $K^+$  in the internal solution, confirm its  $K^+$  selectivity. The tail envelope test was satisfied, indicating a single population of channels. The pharmacologic, kinetic, and voltage-dependent properties of  $I_s$  indicate that it is an ultra-rapidly activating delayed rectifier, which has many similarities to previously cloned  $K^+$  channels (HK2, HBK2, hPCN1, and RK4), as well as currents expressed in guinea pig myocytes ( $I_{Kr}$ ) and rat atrium (RAK). This widely-expressed  $K^+$  channel may play an important role in repolarizing human atrial tissue.

## Tu-Pos383

NA-ACTIVATED K CHANNELS, LOCAL ANESTHETICS AND MEMBRANE POTENTIAL IN MYELINATED AXONS. ((W. Vogel, D.-S. Koh and P. Jonas)) Physiol Inst, Aufweg 129, W-6300 Giessen and MPI, Jahnstr. 29, W-6900 Heidelberg, Germany

Using the method of Jonas et al. (PNAS 86:7238-7242, 1989) single-channel recordings from amphibian myelinated axons have been obtained showing among other potassium channels (Pflugers Arch 418:68-73, 1991) a K channel type which was steeply activated (Hill coefficient 2.6) by internal  $Na^+$  ions ( $K_D = 33$  mM) at  $E_m = -90$  mV. Its single-channel conductance was 90 pS in symmetrical 105 mM-K and 34 pS in external Ringer solution. The channel was selective for  $K^+$  over  $Na^+$  ( $P_{Na}/P_K = 0.02$ ). Open probability of the channel was 0.59 at  $E = 40$  mV and 0.37 at  $E = -90$  mV with  $[Na^+]_i = 100$  mM. A typical feature of its gating were frequent subconductance states (about nine). The channel was inhibited by external  $Cs^+$  and  $Ba^{2+}$  ions at millimolar concentrations but it was comparatively insensitive to tetraethylammonium ( $IC_{50} = 21$  mM TEA),  $Cs^+$  and TEA $^+$  reduced the apparent single-channel current, whereas  $Ba^{2+}$  blocked by reducing the open probability. The block by  $Cs^+$  and  $Ba^{2+}$  was more pronounced at negative potentials, whereas the block by TEA was potential-independent. Density of the Na-activated K channels was much higher at the node than at the paranode. Thus  $Na^+$  influx especially during periods of increased neuronal activity may influence the activity of the Na-activated K channel and thereby change membrane potential. 40  $\mu M$  lidocaine also clearly activated this K channel which may explain clinically well-known antiarrhythmic effects of this local anesthetic on heart cells.

**Tu-P03384****POTASSIUM CHANNELS IN THP-1 HUMAN MONOCYTES.**

(R. Grygorczyk and I.W. Rodger.) Merck Frost Centre for Therapeutic Research, Kirkland, Quebec, Canada.

Human monocytic leukemia THP-1 cells after treatment with phorbol esters differentiate into macrophage-like cells. Compared to other human myeloid cell lines (HL-60, U937, KG-1, HEL) they behave more like native monocyte-derived macrophages (J. Auwerx, *Experientia* 47:22-31, 1991). Therefore, the THP-1 cell line represents a useful model for studying the mechanisms involved in macrophage differentiation and for exploring the physiological role(s) of different ion channels. Two types of K<sup>+</sup> channels were characterized in this study cells using whole-cell and excised patch configurations. A depolarization-activated outward K<sup>+</sup> current was observed, which showed half-maximal activation at -15 mV and slow inactivation during depolarizing voltage steps. This current was Ca<sup>2+</sup>-independent and insensitive to charybdotoxin (ChTx, 100 nM). A second K<sup>+</sup> current was observed in whole-cell and cell-attached configurations after stimulation with the calcium ionophore A23187 (2 μM). In excised patches, in symmetrical 150 mM K<sup>+</sup>, this Ca<sup>2+</sup>-activated channel displayed an inwardly rectifying single-channel I-V relationship (30 pS and 15 pS at -100 mV and +100 mV respectively). The channel activity was voltage-independent and was blocked by extracellular ChTx (5 to 20 nM). These two K<sup>+</sup> currents in THP-1 cells display similar characteristics to those reported for human blood monocyte-derived macrophages.

**Tu-P03396**

**CONTRIBUTION OF A DELAYED RECTIFIER CURRENT TO THE MEMBRANE PROPERTIES OF TYPE I SEMICIRCULAR CANAL HAIR CELLS.** ((K.J.Rennie<sup>1</sup> and M.J.Correia<sup>1,2</sup>), Depts. of Otolaryngology<sup>1</sup> and Physiology and Biophysics<sup>2</sup>, University of Texas Medical Branch, Galveston, TX 77555-1063.

We have studied the membrane properties of type I semicircular canal hair cells, enzymatically dissociated from the crista of the king pigeon and Mongolian gerbil. Using perforated patch, whole-cell voltage-clamp, four membrane currents have been identified in type I cells; a delayed rectifier-type potassium current I<sub>K1</sub>, a calcium-activated potassium current (I<sub>KCa</sub>), a cation current and a calcium current. I<sub>K1</sub> is the dominant conductance at zero-current (-70mV) and deactivates at potentials hyperpolarized to -90mV. The type I input resistance ranged from 25-140MΩ in gerbil and pigeon cells. This variation appeared to be due to a variation in the size of I<sub>K1</sub> between cells, because when I<sub>K1</sub> was pharmacologically removed using 5mM external 4-aminopyridine, or internally applied 20mM tetraethylammonium ions, the input resistance in 9 cells was increased to a mean value of 0.4 (±0.05GΩ) and the zero-current potential depolarized by approximately 30mV. In current-clamp, during small positive current steps (≤400pA), the membrane potential reached a peak and then decayed with an exponential time course. Current clamp responses did not resemble the voltage oscillations we have observed in type II semicircular canal hair cells under the same recording conditions, or those reported in conventional ruptured patch whole-cell current clamp.

Supported by NIH grant DC01273

**Tu-P03388**

**ATP-γS MODULATES A CLONED Ca<sup>2+</sup>-DEPENDENT K<sup>+</sup> CHANNEL.** ((M. Esguerra, C.D. Foster, and I.B. Levitan.) Graduate Department of Biochemistry and Center for Complex Systems, Brandeis University, Waltham, MA 02254.

The recent cloning of the *Slowpoke* family of Ca<sup>2+</sup>-dependent K<sup>+</sup> channels (Atkinson et al., 1991; Adelman et al., 1992) has made possible molecular investigations of the regulation of these channels. The C-terminal cytoplasmic motif of *Slowpoke* contains several consensus amino acid sequences for phosphorylation, and phosphorylation is a ubiquitous mechanism for modulation of K<sup>+</sup> channels. We examined whether *Slowpoke* channel activity can be modulated in membrane patches detached from *Xenopus* oocytes expressing the A1C2E1G3 *Slowpoke* variant. In 4 of 4 patches, application of the ATP analog ATP-γS (100-200 μM) to the inside face of the patch led to a twofold increase in channel open probability. These effects did not reverse up to 1 hour after washout of the ATP analog. Our results are consistent with modulation of channel activity by a protein kinase that comes away with the detached patch.

**Tu-P03385**

**A VOLTAGE-DEPENDENT, CALCIUM-ACTIVATED POTASSIUM CURRENT IN RABBIT CORONARY ARTERY VASCULAR SMOOTH MUSCLE CELLS** ((George, M.J., Volk, K.A., Shibata, E.F.)) Dept. of Physiology & Biophysics, University of Iowa, Iowa City, IA 52242.

Vascular smooth muscle cells enzymatically isolated from the rabbit coronary artery show large outward currents upon depolarization. One component of this outward current is a large K<sup>+</sup> efflux. Previous studies from our lab have characterized a voltage-dependent delayed rectifier K<sup>+</sup> current in this cell type that has a small conductance and functions independently of intracellular Ca<sup>2+</sup> concentration. In addition to this current, we have observed a large, Ca<sup>2+</sup>-activated outward current. The properties of this current are consistent with the Ca<sup>2+</sup>-activated potassium current seen in other tissues in regard to its large conductance levels (>10pA at +40mV) as well as its voltage- and Ca<sup>2+</sup>-dependence. Using the inside-out and cell-attached patch clamp techniques, we have determined the slope conductances of this current to be 140 pS with 140mM intracellular and 4.5mM extracellular K<sup>+</sup> and 202 pS with symmetrical (140 mM) potassium.

Calcium-dependence was determined by washing on EGTA-buffered calcium solutions of concentrations within the 0 nM to 1 μM range to inside-out patches. Calcium concentrations of the 10 to 50 nM range were needed to activate this potassium current throughout voltages of 60 to -40 mV. Open times for the channel increased markedly as the calcium concentration increased. Likewise, the open time for the current increased upon depolarizations to more positive potentials. Supported by NIH HL41031 and an EI of AHA to EFS.

**Tu-P03387**

**MACROSCOPIC (CUT-OPEN OOCYTE) AND RECONSTITUTED (BILAYER) SINGLE CHANNEL CURRENTS OF SLOWPOKE Ca-ACTIVATED K CHANNELS** ((R. Olcese, L. Toro, G. Pérez, M. P. Kavanaugh\*, R. A. North\*, J. P. Adelman\* & E. Stefani)) \*Vollum Inst., Oregon Health Sc. Univ., Portland, OR 97201 & Dept. Molecular Physiology & Biophysics, Baylor College of Medicine, Houston, TX 77030.

Slowpoke calcium-activated K channels were recorded from oocytes injected with RNA transcribed from cloned cDNA encoding the slowpoke locus of *Drosophila*. Injected oocytes did not show voltage dependent outward currents when stimulated from a V<sub>PI</sub> = -90 mV to +50 mV. However, outward currents were successfully recorded after injection of intracellular calcium pulses (5 ms) through the recording pipette which contained 1.5 M NaMES and 40 mM CaMES<sub>2</sub>. These currents reached a maximum (10-100 μA) 20-30 s after calcium injection. Thereafter, they spontaneously declined to the basal level due to the calcium buffer capacity of the oocyte. After several calcium injections steady currents could be recorded which were blocked in a dose dependent manner by TEA (1 mM) and were unaffected by charybdotoxin (100 nM). Single channels could be recorded after incorporation into lipid bilayers of oocyte membranes banding at 20:50% sucrose interface of a discontinuous sucrose gradient. Experiments were performed using a 250/50 KCl gradient in the presence of 100 μM free Ca<sup>2+</sup>. Under these conditions, K channels had a conductance of 240 pS and were sensitive to internal calcium. Supported by AHA-National Center and NIH grants.

**Tu-P03389**

**POTASSIUM CHANNEL ACTIVATION CAN BE SLOWED BY MUTATIONS IN THE S4 AND S4-S5 LINKER REGIONS.** C.J. Smith, Maxwell, M. Kanevsky and R.W. Aldrich, Dept. of Molecular and Cellular Physiology and Howard Hughes Medical Institute, Stanford University, Stanford, CA 94305.

Several studies have suggested involvement of the S4 and S4-S5 linker regions in the activation process. We are studying two mutations that slow activation kinetics in a *Shaker* B K channel deletion mutant in which inactivation has been removed. The first is a chimera generated by replacing the S4 of *Shaker* with the S4 of the fly *Shaw* K channel. There is a large positive shift in the conductance-voltage relation of the chimeric channel and a decrease in apparent voltage-dependence of activation. Activation kinetics are greatly slowed, much like the parent *Shaw* K channel, and appear to have a single exponential time course without the normal delay seen in wild type *Shaker* channels, possibly indicating that a single rate-limiting step underlies the opening of this channel. Mutations in the first, second and seventh positively charged residues of *Shaker* that mimic *Shaw* at those positions alter the voltage range of channel activation in a qualitatively similar fashion to the *Shaw* S4 chimera but do not contribute to the slowing of activation kinetics. The second mutation of interest is at position 385 in the S4-S5 linker region. Several hydrophobic substitutions for the highly conserved leucine at this position, including replacement with phenylalanine, lead to modest depolarizing shifts in the voltage range of channel activation and decrease the apparent charge moved during activation. Tyrosine at this position leads to similar changes in the voltage-dependence of channel function but also slows channel activation approximately 5-fold. Since the only difference between these two channels is the -OH group of tyrosine, this result argues that the -OH group plays a role in slowing activation.

**Tu-P03390**

**AMINO TERMINAL ACIDIC RESIDUES INFLUENCE THE DEACTIVATION RATE OF THE  $I_{K1}$  CHANNEL** ((R.E. Hice, K. Folander, R. Swanson, and M.C. Sanguinetti)) Pharmacology Dept., Merck Research Labs, W. Point, PA 19486

Human, mouse, and rat  $I_{K1}$  proteins were expressed in *Xenopus* oocytes by injection of their cRNAs. Despite extensive primary sequence homology (>76% amino acid sequence identity), the human and rodent currents differed in both activation and deactivation rates with no differences in activation threshold (-50 mV). Activation continued throughout very long (100 s) depolarizations at room temp; isochronal currents (30 s depolarizations) were, therefore, compared. Currents elicited by depolarizations to > -10 mV required 3 time constants for exponential fits. The human channel activated more rapidly than did the rodent variants (eg., human  $\tau_1 = 577 \pm 122$ ,  $\tau_2 = 2587 \pm 220$ ,  $\tau_3 = 20005 \pm 1014$  vs. rat  $\tau_1 = 966 \pm 138$ ,  $\tau_2 = 3993 \pm 158$ ,  $\tau_3 = 34266 \pm 1298$  (msec  $\pm$  sem at 0 mV; n=5)). Deactivation rates were fit with 2 time constants and were also more rapid for human currents ( $\tau_1 = 278 \pm 11$ ,  $\tau_2 = 705 \pm 56$ ; rat  $\tau_1 = 373 \pm 32$ ,  $\tau_2 = 1530 \pm 296$ ; mouse  $\tau_1 = 365 \pm 21$ ,  $\tau_2 = 1495 \pm 39$  (msec  $\pm$  sem at -60 mV; n=6-8)). One striking difference between the human and rodent  $I_{K1}$  proteins is that the rodent variants have a higher density of negative charge in their NH<sub>2</sub> terminal domains. Mutations were, therefore, made in the human cDNA to introduce 4 acidic residues into positions corresponding to those in the rat sequence (V21D, Q22E, G29D, S38D). These mutations slowed the deactivation rates of the human channel to values similar to those of the rat and mouse channels (eg.,  $\tau_1 = 389 \pm 4$ ,  $\tau_2 = 1449 \pm 58$  at -60 mV; n=5). These results provide evidence for sequence specific changes in the kinetics of the expressed  $I_{K1}$  currents and specifically demonstrate that acidic residues in the NH<sub>2</sub> terminal domain of the protein influence the rate of deactivation of the channel.

**Tu-P03392**

**FILTER-INDUCED ERRORS IN ESTIMATING THE CONDUCTANCE OF SINGLE CHANNELS WITH NONSTATIONARY FLUCTUATION ANALYSIS.** ((S.D. Silberberg and K.L. Magleby)) Department of Physiology and Biophysics, University of Miami School of Medicine, Miami FL 33101-6430.

The stochastic nature of channel activation contributes to the fluctuations in whole-cell currents. Assuming a homogeneous population of independent channels with a single conducting state, it is possible to estimate the number of channels (*N*) and the magnitude of the unitary current event (*i*) underlying the whole-cell current by using nonstationary fluctuation analysis (Sigworth F.J., *J. Physiol.* 307; 97-129, 1980). We have investigated the effects of filtering on the estimation of *i* and *N* from the analysis of simulated whole-cell currents. Filtering lead to an under-estimation of *i* and an over-estimation of *N*. For example, with 1 kHz filtering and a mean channel open time of 0.2 ms, *i* was under-estimated by 47% and *N* was over-estimated by 37%. Decreasing the filtering to 5 kHz reduced the errors to 14% and 2%, respectively. These errors were found to be due to both the attenuation and broadening of the unitary current induced by the filtering. Some guidelines for minimizing errors with nonstationary fluctuation analysis will be presented. Supported by grants AHA-91G1A/743 and NIH-AR32805, and by The Muscular Dystrophy Association.

**Tu-P03394**

**QUARTZ PIPETTES FOR SINGLE CHANNEL RECORDING** ((J.L. Rae and R.A. Levis)) Mayo Foundation, Rochester, MN 55905 and Rush Medical College, Chicago, IL 60612<sup>†</sup>

Dielectric loss of the glass used to fabricate patch pipettes is a significant source of noise in single channel recording. The power spectral density of dielectric noise is given by  $4kTDC_d(2\pi f)$ , where *D* is the dissipation factor, *C<sub>d</sub>* is the capacitance of the dielectric, and *f* is the frequency in Hz. Since quartz has a far lower dissipation factor than any other material yet used to fabricate patch pipettes and also has a low dielectric constant, it should produce pipettes with the lowest amount of dielectric noise. Here we describe practical aspects of quartz pipette fabrication with a Sutter P-2000 laser based puller and describe the sealability of such pipettes to membranes with and without fire polishing. We demonstrate that quartz pipettes produce significantly less noise than pipettes fabricated from other glasses, although, as anticipated, Sylgard coating is still required for low noise. Noise increases which occur with increasing depth of immersion of the pipette are described and analyzed, and comparisons between quartz and other glasses used for pipette fabrication are presented. Other expected noise sources are analyzed. In addition, we show approaches using silicone (dimethylpolysiloxane) fluid which can further reduce background noise levels below that which can be achieved with quartz pipettes alone.

Supported by NIH Grants EY03282 and EY06005.

**Tu-P03391**

**INTERACTIONS OF SHAKER INACTIVATION PEPTIDES WITH S4-S5 CHIMERAS.** (R.D. Mummell-Leonado, M. Przelak and R.W. Aldrich, Dept. of Molecular and Cellular Physiology and Howard Hughes Medical Institute, Stanford University, Stanford, CA 94305.

Inactivation in Shaker K channels occurs by at least 2 structurally and pharmacologically distinct mechanisms termed N- and C-type inactivation. N-type inactivation involves the NH<sub>2</sub>-terminal region acting as a tethered particle and binding near the internal mouth of the pore. Structure-function studies using a range of synthetic peptides have been carried out to demonstrate the features of the NH<sub>2</sub>-terminal regions that provide for their interaction with a site near the channel pore. These synthetic peptides are now being used as probes to look for residues on the rest of the channel protein which when mutated affect the association and dissociation binding rates in a predictable way based on the mechanism proposed. These residues will be likely candidates for forming the binding site for the inactivation particle. Initially we have focused on the S4-S5 linker region of the channel which has been proposed as a putative 'receptor' for the inactivation particle (Isacoff *et al.*, 1991). This region is highly conserved amongst K channels in the Kv1, 2, 3 and 4 subfamilies. We have made a number of chimeric channels using the ShBΔ6-46 background and substituting the S4-S5 linker regions of K channels from each of the 4 families for the S4-S5 linker region of Shaker. These include the S4-S5 linker regions from drk1, Shab, Shal, Shaw and RKShIIIA (Kv3.2). The binding affinities of the peptides to these chimeric channels are compared to their affinities for the native channels. Shaker and drk1 differ in this region by 6 out of the 15 residues. The NH<sub>2</sub>-terminal peptides from Shaker B, C and Raw3 had a much lower affinity for binding to drk1 than for binding to ShBΔ6-46. The association rates were 100-fold lower in each case. The dissociation rates were actually slightly reduced compared to ShBΔ6-46. The binding affinity of ShB peptide to the drk1 linker chimera was also much lower than for ShBΔ6-46, whereas the peptides bound to the Shaw-linker chimera with very similar affinities to ShBΔ6-46. (Isacoff *et al.*, 1991. *Nature*:353, 86-90)

**Tu-P03393**

**RECTIFICATION OF INWARDLY RECTIFYING POTASSIUM CHANNELS IN THE MURINE MACROPHAGE CELL LINE J774.1: DEPENDENCE ON INTERNAL MAGNESIUM AND CHANNEL GATING** ((K.L. Coulter and C.A. Vandenberg)) Dept. of Biological Sciences and Neuroscience Research Institute, University of California, Santa Barbara, CA 93106.

The mechanism of rectification of the inwardly rectifying potassium channel in the macrophage-like cell line J774.1 was examined using single-channel recording techniques. Voltage ramps and voltage jumps applied to single inward rectifier channels in cell-attached patches produced currents that rectified strongly with a marked reduction in current at a potential near *E<sub>K</sub>* and no detectable current at more positive potentials. Single-channel rectification was eliminated upon excision of inside-out patches into a magnesium-free (but not magnesium-containing) solution, suggesting that internal block by magnesium causes rapid, single-channel rectification. In the absence of internal magnesium, a slower, time-dependent closing of the channel was observed at positive potentials. This slower gating process also appears to contribute to the rectification of this channel. (Supported by NIH grant HL 41656 and the American Heart Assoc., California Affiliate.)

**Tu-P03395**

**BROWNIAN DYNAMICS REPRESENTATION OF A "POTASSIUM-LIKE" CHANNEL** ((Eric Jakobsson)) Department of Physiology and Biophysics, National Center for Supercomputing Applications, University of Illinois, Urbana, Illinois 61801

The behavior of a multiply-occupied cation-selective channel has been computed by Brownian dynamics. The length, cross-section, ion-ion repulsion force, and ionic mobility within the channel are all estimated from data and physical reasoning. The only free parameter was a partition energy at the mouth of the channel, defining the free energy in the channel compared to the bath. Varying that parameter alone, keeping all others fixed, gave the full range of single channel conductances seen experimentally for potassium channels. Setting the partition energy at -12 kT made the computed channel look much like a squid axon potassium channel with respect to magnitude of conductance, shape of the I-V curve, Using flux ratio exponents, decrease of current with extracellular ion accumulation, and saturation at high ion concentration in the bathing solution. The model included no preferred binding sites (local free energy minima) for ions in the channel. Therefore it follows that none of the above-mentioned properties of potassium channels are strong evidence for the existence of such sites. Partially supported by NIH.

## Tu-P03396

**Calcium-dependent inactivation of cardiac calcium channel  $\alpha_1$ ,  $\beta_2$  subunits and a deletion mutant of  $\alpha_1$ , expressed in *Xenopus* oocytes.** ((A. Neely, X. Wei, L. Birnbaumer & E. Stefani)) Dept. of Molec. Physiol. & Biophys., Baylor Coll. of Med. Houston, Texas 77030.

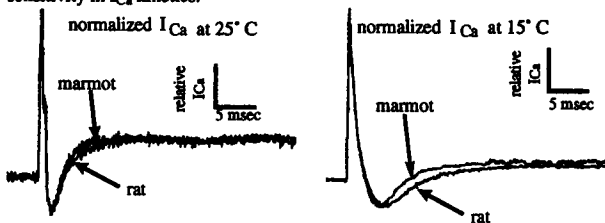
Dihydropyridine sensitive  $\text{Ca}^{2+}$  channels inactivate by  $\text{Ca}^{2+}$  binding to a yet unknown intracellular site. In an attempt to identify the site and further clarified the mechanisms involved we developed the experimental conditions to study  $\text{Ca}^{2+}$ -induced inactivation from expressed calcium channels. In  $\text{Ca}^{2+}$  buffering conditions which prevent activation of endogenous  $\text{Ca}^{2+}$ -dependent  $\text{Cl}^-$  currents, cardiac  $\alpha_1$  and  $\beta_2$  subunit expressed in *Xenopus* oocytes induced inward currents that rapidly inactivates in 5 mM  $\text{Ca}^{2+}$  but not in 10 mM  $\text{Ba}^{2+}$ . Intracellular  $\text{Ca}^{2+}$  was buffered by pre-injecting the oocytes with 35 nl of 55 mM BAPTA-K. Currents were further isolated in  $\text{Cl}^-$ -free recording solutions and recorded under voltage-clamp using the cut-open oocyte technique. Rates of inactivation increased with peak currents in single and paired pulses experiments. This  $\text{Ca}^{2+}$ -dependent inactivation was also dependent on voltage. During single depolarizing steps comparable peak inward currents had a faster inactivation rate at more negative potentials ( $0.02 \text{ ms}^{-1}$  at  $-10 \text{ mV}$  and  $0.005 \text{ ms}^{-1}$  at  $+20 \text{ mV}$ ). This anomalous voltage-dependence together with its persistence with BAPTA puts the  $\text{Ca}^{2+}$  binding near the channel inner mouth. Moreover, using a deletion mutant of the  $\alpha_1$  subunit which carries larger current than the parent form (A. Neely et al., this meeting), we are able to show that  $\text{Ca}^{2+}$ -induced inactivation does not depend on the presence of auxiliary subunit.

## Tu-P03398

**VENTRICULAR CALCIUM CURRENTS FROM A HIBERNATOR SHOW LESS TEMPERATURE DEPENDENCE.**

((X. Gong†, G.L. Florant††, and R.L. White†)) Depts. †Physiology & ††Biology, Temple University, Philadelphia, PA 19140. (Spon. by L. Horn)

Hibernation involves a reduction in body temperature to near ambient (often about  $2^\circ \text{C}$  in winter). As body temperature falls, the heart slows but resting potential is maintained and the heart continues to contract in hibernating mammals. We compared L-type calcium currents ( $I_{\text{Ca}}$ ), recorded from voltage-clamped ventricular myocytes isolated from either rat or marmot (*Marmota*). At  $25^\circ \text{C}$ ,  $I_{\text{Ca}}$  decayed with a time constant near 1.9 msec in either rat or marmot cardiac myocytes. When temperature was lowered to  $15^\circ \text{C}$ ,  $I_{\text{Ca}}$  in marmot decayed with a significantly faster time constant ( $2.43 \pm 0.18 \text{ msec}$ ) than  $I_{\text{Ca}}$  in rat ( $3.37 \pm 0.23 \text{ msec}$ ). These data suggest a differential temperature sensitivity in  $I_{\text{Ca}}$  kinetics.



## Tu-P03400

**SINGLE L-TYPE  $\text{Ca}^{2+}$  CHANNELS IN HUMAN VASCULAR SMOOTH MUSCLE - MODULATION BY INTRACELLULAR NUCLEOTIDES AND  $\text{Ca}^{2+}$**

K. Grochner and W.R. Kukovetz, Dept. of Pharmacology und Toxicology, Univ. of Graz, Austria.

L-type voltage-dependent  $\text{Ca}^{2+}$  channels were studied in the membrane of smooth muscle cells isolated from human umbilical vein. The effects of intracellular nucleotides and  $\text{Ca}^{2+}$  were studied at the level of single channels using the inside-out configuration of the patch clamp technique. With  $\text{Ba}^{2+}$  (80 mM) as charge carrying cation in the pipette and 140 mM KCl, 1 mM  $\text{MgCl}_2$  and 0.1  $\mu\text{M}$  free  $\text{Ca}^{2+}$  (buffered with EGTA) in the solution facing the cytoplasmic side of patches, channels initially exhibited a behavior similar to those in on-cell patches i.e. activation started at potentials above  $-30 \text{ mV}$ , slope conductance was 22 pS and reversal potential was about  $+50 \text{ mV}$ . However, channel activity in inside-out patches showed slow rundown resulting in silent patches within 5 to 10 min. Addition of Bay K 8644 to either the bath or pipette solution enhanced channel activity but did not prevent rundown. Addition of GTP (200  $\mu\text{M}$ ) to the bath solution clearly slowed rundown, whereas ATP (1 mM) did not. Administration of ATP (1 mM) in the presence of GTP (200  $\mu\text{M}$ ), however, enhanced channel activity in inside-out patches. The combined presence of both nucleotides resulted in fairly stable channel activity over up to 30 min. Under these conditions, channel activity was clearly dependent on the free  $\text{Ca}^{2+}$  concentration at the cytoplasmic face of the patches. Elevation of free  $\text{Ca}^{2+}$  up to 100  $\mu\text{M}$  reversibly reduced open probability and clearly enhanced inactivation of the channels. Our results demonstrate significant modulatory effects of intracellular ATP, GTP and  $\text{Ca}^{2+}$  on L-type  $\text{Ca}^{2+}$  channels of human vascular smooth muscle.

## Tu-P03397

**Fast and slow activation in a modified cardiac calcium channel  $\alpha_1$  subunit expressed in *Xenopus* oocytes.** ((A. Neely, X. Wei, L. Birnbaumer & E. Stefani)) Dept. of Molec. Physiol. & Biophys., Baylor Coll. Med., Houston, Texas 77030.

The cardiac  $\text{Ca}^{2+}$  channel  $\alpha_1$  subunit is sufficient to express voltage-dependent  $\text{Ba}^{2+}$  currents. Co-expression of  $\beta$  subunit increases current density and accelerates current onset (Wei et al., *J. Biol. Chem.* 266, 2194-21947, 1991). Using the cut-open oocyte clamp technique, we characterized the activation kinetics of  $\text{Ba}^{2+}$  currents (10 mM) through  $\text{Ca}^{2+}$  channels for  $\alpha_1$  subunit expressed alone or combined with the  $\beta_2$  subunit. Currents from  $\alpha_1$  alone activate following a single exponential with a time constant of about 10 ms and maximum inward currents at  $+30 \text{ mV}$ . In contrast, currents potentiated by co-expression of  $\beta_2$  subunit, activate at more negative potentials with a time constant of 1-3 msec. In some cases, in  $\alpha_1$ - $\beta_2$  expression, a slow component was resolved. This may be tentatively explained by a fraction of  $\alpha_1$  channels lacking  $\beta_2$  subunit. We also studied and  $\alpha_1$  subunit with a deletion at the carboxy terminal which expressed ionic currents significantly larger than parental  $\alpha_1$ . This deletion exhibits both slow and fast kinetics of activation. At  $+10 \text{ mV}$ , the fast component accounts for about 50% of the current while at  $+30 \text{ mV}$ , a component of about 20 ms could be as much as 3 folds larger than the fast component. In summary,  $\text{Ca}^{2+}$  channels can express 2 activation modes (fast and slow) and the co-expression of  $\alpha_1$  with  $\beta_2$  subunit favors the fast mode. Furthermore, the dual mode of activation is encoded in the  $\alpha_1$  subunit and kinetic heterogeneity may reflect a modulation process sensitive to the  $\beta_2$  subunit.

## Tu-P03399

**THE FATTY ACID DOCOSAHEXAENOIC ACID INHIBITS L-TYPE CALCIUM CURRENT.** ((A.R. Ritzenhouse, H. Hallaq, A. Leaf, & P. Hess)) Dept. of Cellular and Molecular Physiology, Harvard Medical School, Boston, MA 02115.

Docosahexaenoic acid (DHA), a C22:6  $\omega$ -3 fatty acid found in high concentrations in fish oil, protects cardiovascular tissues from cytotoxicity during periods of acute ischemia, though the exact mechanism by which this is accomplished is unclear. Recently Hallaq et al. (PNAS, 1992, 89: 1760) reported that concentrations of DHA without effects of its own blocked the agonist and antagonist effects of dihydropyridines (DHPs) on cardiac muscle contraction. It also noncompetitively inhibited the binding of  $^3\text{H}$ -nitrendipine to cardiac myocytes, indicating that its site of action may be the L-type Ca channel. Here, we report that DHA acts as a modulator of L-type Ca current in undifferentiated PC12 cells, a pheochromocytoma cell line that contains mainly L-type Ca channels. Bath application of 5  $\mu\text{M}$  and 10  $\mu\text{M}$  DHA decreased whole cell Ba currents  $36 \pm 7\%$  ( $n=10$ ) and  $78 \pm 4\%$  ( $n=3$ ) respectively. Arachidonic acid (5  $\mu\text{M}$ ; C20:4  $\omega$ -6) also decreased the peak current  $64 \pm 6\%$  ( $n=7$ ) while oleic acid (10  $\mu\text{M}$ ; C18:1  $\omega$ -9) had no significant effect ( $n=3$ ). Unlike the DHP antagonist (-)-202-791, the ability of DHA (5  $\mu\text{M}$ ) to inhibit L-type current appears independent of holding potential; the inhibition of the Ba current was not significantly different when cells were held at  $-90 \text{ mV}$  ( $46 \pm 7\%$ ;  $n=7$ ) or  $-60 \text{ mV}$  ( $31 \pm 11\%$ ;  $n=9$ ). In addition, neither 1  $\mu\text{M}$ , a concentration that had no effect of its own, nor 5  $\mu\text{M}$  DHA blocked the effects of the DHP agonist (+)-202-791 (100 nM).

The effects of DHA at the single channel level were consistent with its effects at the whole cell level. 10  $\mu\text{M}$  DHA puffed onto cells decreased the mean average current ( $67\% \pm 7\%$ ) and the open probability ( $67 \pm 11\%$ ) of multichannel patches ( $n=6$ ) recorded in the cell-attached patch configuration in the presence of 500 nM (+)-202-791. Mode 1 and 2 activity decreased in the presence of DHA, but were still apparent. Similar results were observed when the DHP agonist was absent. These results indicate that particular fatty acids may be endogenous modulators of the L-type Ca channel.

## Tu-P03401

**Ca-DEPENDENT FACILITATION OF Ca CURRENT IN CARDIAC MYOCYTES IS REVERSED BY PROTEIN KINASE INHIBITORS.**

((Weilong Yuan and Donald M. Bers)) Loyola Univ Chicago, Maywood, IL 60153.

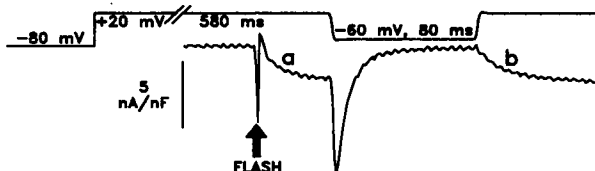
Repetitive activation of Ca current ( $I_{\text{Ca}}$ ) from  $E_m = -90 \text{ mV}$  in rabbit ventricular myocytes induces facilitation or a "staircase" of  $I_{\text{Ca}}$  which depends on Ca entry (rather than voltage) and takes several seconds to accumulate and dissipate (e.g. Hryshko & Bers, *Am. J. Physiol.* 259:H951-H961, 1990). That is,  $I_{\text{Ca}}$  at the 10<sup>th</sup> pulse at 1-2 Hz ( $I_{10}$ ) is greater than at the 1<sup>st</sup> ( $I_1$ , see Figs). This is partly due to more rapid  $I_{\text{Ca}}$  inactivation at  $I_1$  (e.g.  $\tau_{\text{fast}} \sim 5 \text{ ms}$  at  $I_1$  and 15 ms at  $I_{10}$ ). We studied the effects of relatively selective inhibitors of the calmodulin- and cAMP-dependent protein kinases on this  $I_{\text{Ca}}$  staircase (i.e.  $I_{10} < I_1$ ), but the effects differed. The decrease in  $I_{\text{Ca}}$  amplitude with KN-62 (e.g. at  $I_{10}$ ) was attributable primarily to a progressive decrease in Ca channel availability (i.e. slower  $I_{\text{Ca}}$  recovery from inactivation).  $I_1$  still inactivated more rapidly than  $I_{10}$ . With H-89,  $I_{10}$  amplitude was also less than  $I_1$ , possibly for the same reason, but in addition the faster inactivation of  $I_{\text{Ca}}$  at  $I_1$  was also largely suppressed. Phosphorylation sensitive to H-89 may contribute to the more rapid inactivation of  $I_{\text{Ca}}$  after rest (during  $I_1$ ). Phosphorylation sensitive to both H-89 and KN-62 may contribute to the rapidity of  $I_{\text{Ca}}$  recovery from inactivation at  $E_m = -90 \text{ mV}$ .



## Tu-P00402

EVIDENCE FOR DHP BLOCK OF A FAST REACTION PARTICIPATING IN THE GATING OF THE SLOW L-TYPE CALCIUM CURRENT OF SKELETAL MUSCLE. ((W. Melzer, P. Eßlinger, D. Feldmeyer and B. Pohl)) Dept. Cell Physiology, Ruhr-University Bochum, D-4630 Bochum, FRG

The slow L-type  $\text{Ca}^{2+}$  current of skeletal muscle attains a fast gating mode once it is activated by a conditioning depolarisation indicating the participation of slow and fast reactions in the gating of the channel. We studied the DHP effect on these reactions by using flash photolysis of nifedipine in voltage clamped cut muscle fibers of the frog. The current activated by a light flash was the faster the later the flash was applied after the onset of membrane depolarization. Yet, the limiting speed of the flash-induced activation (a) was still considerably lower than expected from the photolysis reaction and almost identical with the fast mode activation observed in a subsequent test depolarization (b). We conclude that nifedipine selectively blocks a rapid step of the channel gating.

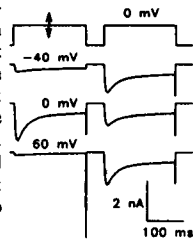


## Tu-P00404

A SIMPLE MODEL OF V- and  $\text{Ca}^{2+}$ -DEPENDENT INACTIVATION OF L-TYPE  $\text{Ca}^{2+}$  CHANNELS.

((R. Shirokov, R. Lewis & E. Ríos)) Rush Univ., Chicago, IL 60612

Two independent inactivation mechanisms are postulated, based on observations on charge 2 (Shirokov et al., this meeting). The model assumes diffusion limited binding of  $\text{Ca}^{2+}$  to a site near the channel mouth, which controls a V-independent gate. The channel is largely inactivated by its own current. The inactivation kinetics are determined by the latency to first opening. The model simulates many properties of the  $\text{Ca}^{2+}$  channel including, as shown in the figure: 1) fast current-dependent and slow V-dependent components in current decay; 2) the availability of current measured in a double-pulse protocol has a minimum after conditioning at voltages of maximal current (Tillotson & Eckert); 3) the deactivation of the channel is very fast at negative voltages, although the mean open time at high voltages is large and weakly V-dependent. The model is also consistent with the high sensitivity of the closed channels to inactivation by internal  $\text{Ca}^{2+}$ , demonstrated experimentally, and reproduces the complex kinetics of recovery from inactivation. Supported by NIH and AHA-Chicago.

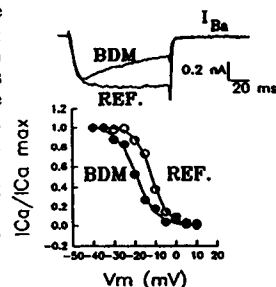


## Tu-P00406

BDM ENHANCES VOLTAGE DEPENDENT INACTIVATION OF L-TYPE CALCIUM CHANNEL IN HEART. ((Ferreira, G., Maggi, M., Pizarro, G. and Brum, G.)) Depto. de Biofísica, Fac. de Medicina, Montevideo, Uruguay. (Spon. by K. Barany)

The effect of the chemical phosphatase butanodione monoxime (BDM) on L-type Ca channel whole-cell currents in guinea pig cardiac myocytes was studied. Extracellularly applied, 20 mM BDM increased the rate of current inactivation both for Ca or Ba as charge carriers. The Ca current elicited by clamp depolarizations from -40 to +20 mV was reduced 20.6%  $\pm$  4.2, whereas the current at the end of the pulse (100 ms) was reduced 85.1%  $\pm$  3.8 (n=10). The steady state inactivation curve was shifted to negative voltages and its slope slightly decreased by the drug. Boltzmann fit parameters were in reference  $V_{1/2} = -11.7$  mV,  $k = -3.9$  mV; in BDM  $V_{1/2} = -19.3$  mV,  $k = -4.9$  mV; n=3. We conclude that the drug enhanced voltage dependent inactivation, although it is unclear if this is due to its phosphatase action.

Partially funded by grants from PEDECIBA and the CSIC.



## Tu-P00403

$\text{Ca}^{2+}$ -DEPENDENT POTENTIATION AND INACTIVATION OF SINGLE CARDIAC L-TYPE  $\text{Ca}^{2+}$  CHANNEL CURRENTS UNDER SIMULTANEOUS OPTICAL MONITORING OF INTRACELLULAR CALCIUM CONCENTRATIONS. ((Y. Hirano and M. Hiraoka)) Department of Cardiovascular Diseases, Medical Research Institute, Tokyo Medical and Dental University, Tokyo, JAPAN

Activities of L-type  $\text{Ca}^{2+}$  channels in muscles and neurons are under feedback controls by intracellular  $\text{Ca}^{2+}$  concentrations ( $[\text{Ca}^{2+}]_i$ ), which include both  $\text{Ca}^{2+}$ -dependent inactivation and potentiation. Little is known, however, about interrelationships between these two opposite functions, and the levels of  $[\text{Ca}^{2+}]_i$  required. With simultaneous optical monitoring of  $[\text{Ca}^{2+}]_i$  using fura2, we investigate at the single-channel level how tonic changes in  $[\text{Ca}^{2+}]_i$  modulate cardiac L-type  $\text{Ca}^{2+}$  channels. When cytosolic  $\text{Ca}^{2+}$  concentration of myocytes under  $\text{K}^+$ -depolarization is altered through changes in both  $\text{Ca}^{2+}$  concentration, activity of  $\text{Ca}^{2+}$  channels is reversibly potentiated as  $[\text{Ca}^{2+}]_i$  exceeds  $\approx 2$  times the resting level, until it reaches the "inactivation" level shortly below the threshold for contraction. We also find that  $\text{Ca}^{2+}$ -dependent potentiation is equipped with short term "memory" which is resistant to transient  $\text{Ca}^{2+}$ -induced inactivation. The present study provide analysis of  $\text{Ca}^{2+}$ -dependence of  $\text{Ca}^{2+}$  channel activity for the first time in direct and quantitative way.

## Tu-P00405

TWO KINDS OF L-TYPE  $\text{Ca}^{2+}$  CURRENTS AND ENDPLATE CURRENT IN CELL LINE H9c2 FROM RAT HEART. Takeshi Nakamura, Wei Wang and Rikuo Ochi. Department of Physiology, Juntendo University School of Medicine, Hongo, Tokyo, Japan 113.

Until the recent reports describing the existence of cardiac-type L type  $\text{Ca}^{2+}$  channel the H9c2 cell line derived from rat heart had been regarded to behave electrically as skeletal muscle (Kimes and Brandt, 1976). We recorded single  $\text{Ca}^{2+}$  channel currents from cell-attached patches on the H9c2 cells cultured for 20-50 days. The pipettes contained 100 mM  $\text{Ba}^{2+}$  as the charge carrier and (+)202-791 (1  $\mu\text{M}$ ). With patches containing more than two channels, clear two different conductance levels, 12 pS and 22 pS, were detected. We obtained mean currents for the two different conductance levels from the idealized open-shut transitions. The mean current of the low conductance openings rised very slowly with the peak time of about 200 ms and that of the high conductance openings rised one order faster at the test pulse to 0 mV, suggesting that the former openings represented not the subconductance but those of skeletal type L-type channels. Also the appearance of endplate current by acetylcholine indicates that the H9c2 has characteristics of the skeletal muscle.

## Tu-P00407

HIGH SOLUTION KINETICS OF L-TYPE  $\text{Ca}^{2+}$ -CHANNEL-LIGAND BINDING USING FLUORESCENT RESONANCE ENERGY TRANSFER. ((W. Berger, J. Striessnig, H. Prinz, H.C. Kang, R. Haugland and H. Glossmann)) Inst. f. Bioch. Pharmakologie, Univ. Innsbruck, Austria; Molecular Probes, Eugene, OR, USA; Max Planck Institut f. Ernährungsphysiologie, Dortmund, Germany. (Spon. by H. Glossmann)

Fluorescent  $\text{Ca}^{2+}$ -antagonists were synthesized, that allow the selective and stereospecific labeling of the dihydropyridine (DHP) and phenylalkylamine binding domain of L-type  $\text{Ca}^{2+}$ -channels. The specific interaction of these fluorescent drugs with the  $\alpha_1$ -subunits of the purified rabbit skeletal muscle channel was directly quantitated by measuring fluorescent resonance energy transfer (FRET), which occurs between the bound drugs (energy acceptors) and tryptophan (W) residues (energy donors) of the  $\alpha_1$  subunits. This method does not require the separation of bound and free ligand and therefore allows on-line measurement of drug binding. For FRET experiments, W-residues of the  $\alpha_1$ -subunit were excited at 285 nm and emission of drug fluorescence was measured at 517 nm. The FRET-signal was proportional to the amount of receptor-bound drug and was modulated by non-fluorescent  $\text{Ca}^{2+}$ -channel drugs with the expected pharmacological profile. This technique will not only allow the detection of conformational changes of the  $\alpha_1$ -subunit but also enabled us to study the association and dissociation kinetics of drug binding at very high time resolution ( $< 1$  data point/sec). FRET analysis revealed complex binding kinetics of DHP  $\text{Ca}^{2+}$ -antagonists that cannot be detected using conventional binding techniques. These data will be discussed in terms of a mathematical model which describes a complex interaction of DHPs with their binding domain. This work was supported by grants (to H.G.) from the FWF (S45-01), by the Bundesministerium für Wissenschaft und Forschung and by the Dr. Legerlotz-Foundation (to J.S.).

## Tu-Pos408

**DEFECTS IN G<sub>i</sub> REGULATORY PROTEIN LEADS TO UP REGULATION OF CARDIAC Ca<sup>2+</sup> CURRENTS.** ((L.A. Sorbera and M. Morad)) Department of Physiology, University of Pennsylvania, Philadelphia, PA 19104-6085.

The cardiac Ca<sup>2+</sup> channels are thought to be up and down regulated by G<sub>i</sub> and G<sub>o</sub> regulatory proteins following exposure of the myocyte to adrenergic or cholinergic hormones. Cardiac hypertrophy has been reported to be accompanied by prolongation of the action potential (Aronson, R.S. *Circ. Res.* 47:443, 1980; Thollon, C. *et al.* *Cardiovasc. Res.* 23:224, 1989), enhancement of I<sub>Ca</sub> density (Keung, E.C. *Circ. Res.* 64:733, 1989), and decreased responsiveness to β-adrenergic stimulation (Scamps, F. *et al.* *Circ. Res.* 67:199, 1990). We investigated the regulation of the Ca<sup>2+</sup> channel in spontaneously hypertensive rats (SHR) which develop significant cardiac hypertrophy by 18 weeks of life (Owens, G.K. *Hypertension* 9:178, 1987). Isolated ventricular myocytes from SHR and normotensive rats were whole cell clamped and cell capacitances and Ca<sup>2+</sup> current densities were measured. In SHR myocytes average cell capacitances were 250.3 ± 25.0 pF (n=11) compared to 151.6 ± 13.7 pF (n=75) in normotensive rats. The L-type Ca<sup>2+</sup> current density also increased in SHR myocytes from -7.2 ± 0.4 pA/pF (n=75) in normotensive rats to -15.3 ± 1.4 pA/pF (n=11) in SHR myocytes. Exposure of myocytes to 1 μM isoproterenol, while markedly enhancing I<sub>Ca</sub> in normotensive myocytes failed to potentiate I<sub>Ca</sub> significantly in SHR myocytes. Dialysis of control and SHR myocytes with 1-2 nM GDPβ-S, although producing little or no effect in normotensive myocytes, markedly suppressed I<sub>Ca</sub> (-4.3 ± 1.1 pA/pF, n=6) in SHR myocytes. Incubation of myocytes in solution containing 500 ng/ml pertussis toxin for 6 hrs. at room temperature, produced little or no effect in SHR myocytes, but enhanced I<sub>Ca</sub> densities from -2.5 ± 0.4 (n=6) to -11.9 ± 0.6 pA/pF (n=6) in normotensive myocytes. Isoproterenol-enhanced I<sub>Ca</sub> in normotensive myocytes was suppressed by 1 μM acetylcholine (ACh) resulting from the activation of G<sub>i</sub> regulatory proteins (Fischler, J. *et al.* *Pflügers Arch.* 407:182, 1986). Consistent with a suppressed G<sub>i</sub> regulatory pathway, I<sub>Ca</sub> was not suppressed by ACh in SHR or PTX-treated normotensive myocytes. Our results show that genetically-induced cardiac hypertrophy is accompanied by up regulation of I<sub>Ca</sub> resulting in turn from down regulation of PTX sensitive regulatory G<sub>i</sub> protein. (Supported by NIH grant no. HL16152)

## Tu-Pos410

## A HODGKIN-HUXLEY MODEL OF THE SLOW CALCIUM CURRENT

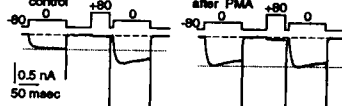
((D. Renald Lemieux, Jacques Beaumont and Fernand A. Roberge)) Institute of Biomedical Engineering, University of Montreal, Montreal, Canada, H3C 3J7.

The slow Ca current (I<sub>Ca,L</sub>) of the cardiac cell sarcolemma is represented by an Hodgkin-Huxley model. The model parameters are estimated from peak current values under voltage clamp, assuming that such experimental measurements are reasonably accurate. Two sets of data are used to estimate steady-state activation (d<sub>∞</sub>) and inactivation (f<sub>∞</sub>) and their degree: Figure 8A of Hagiwara *et al.*, *J. Physiol.*, 1988, 395:233-253, and Figure 6 of Isenberg & Klöckner, *Pflügers Arch.*, 1982, 395:30-41. Parameter values estimated by our general optimization procedure differ from those obtained by normalization, particularly for d<sub>∞</sub>. Next, our optimization procedure allows us to estimate the time constants of activation and inactivation, as well as the maximum conductance. The range of experimental voltage-clamp potentials used in these studies is barely sufficient to carry out the optimization procedure with a reasonable degree of confidence. The need for specific additional data is indicated.

## Tu-Pos412

**PROTEIN KINASE C MODULATES G PROTEIN INHIBITION OF NEURONAL CALCIUM CHANNELS** ((Kenton J. Swartz)) Harvard Med. Sch., Boston, MA 02115 (Spon. D. Goodenough)

In rat superior cervical ganglion, hippocampal CA3, and cerebral cortical neurons, activation of protein kinase C (PKC) with phorbol-12-myristate-13-acetate (PMA; 500 nM) enhanced whole-cell Ca channel current and dramatically reduced G protein-mediated inhibition of Ca channels by neurotransmitters (including those acting at glutamate, GABA<sub>B</sub>, adenosine, muscarinic and α-adrenergic receptors). Both enhancement of Ca channel current and knockout of transmitter inhibition by PMA were blocked when PKC was inhibited with internal PKC19-ss. Receptor-independent G protein-mediated inhibition of Ca channels could be induced by internal GTP-γ-S (300 μM). The amount of G protein inhibition was measured by transiently removing it with depolarizing pre-pulses to +80 mV ('pre-pulse facilitation', figure, left). In these cells the Ca channel current inhibited by G proteins, and subsequently facilitated by voltage, was sensitive to ω-CgTx-GVIA (N-type channels). PMA both qualitatively and quantitatively mimicked the effects of pre-pulse facilitation and occluded subsequent facilitation by voltage (see figure), suggesting that PKC can disrupt G protein inhibition of N-channels when transmitter receptors are bypassed. Tonic G protein inhibition of N-channels could often be seen under control conditions (in the absence of transmitters and with 300 μM internal GTP). In these cells PMA enhanced Ca channel current while removing facilitation, suggesting that enhancement is at least partly due to disruption of tonic G protein inhibition.



Charge carrier is 25 mM Ba. Internal solution contains 300 μM GTP-γ-S.

## Tu-Pos409

**EFFECTS OF ADRENALINE ON BARIUM CURRENTS IN TONIC SKELETAL MUSCLE FIBERS OF THE FROG.** ((M. Huerta, C. Vélez and X. Trujillo)) Centro Universitario de Investigaciones Biomédicas, Universidad de Colima, Apdo. Postal 199, 28000 Colima, Col. Méx.

In tonic fibers, the adrenaline potentiates K<sup>+</sup> contractures (Huerta, *et al.*, 1991: *Jon J. Physiol.* 41:851). This potentiation of tension could be due to adrenergic modulation of calcium channels. We have analyzed the effects of adrenaline on inward barium currents. Experiments were done on cruralis muscle of *Rana pipiens*, using three-microelectrode voltage-clamp technique. The solution contained (mM): TEA(CH<sub>3</sub>SO<sub>3</sub>), 120; Ba(CH<sub>3</sub>SO<sub>3</sub>)<sub>2</sub>, 10; 3,4-DAP, 5 and sucrose, 350. The pH was adjusted to 7.4 with imidazole-Cl. Experiments were performed at room temperature (20-22°C). Adrenaline was added from stock solutions (10<sup>-3</sup> M). Muscle fibers were identified according to their passive electrical properties. The cell holding potential was maintained at -100 mV and 1 s pulses of variable amplitude were delivered. Application of adrenaline (1 μM) to the bath increases the amplitude of barium current in approximately 23% (n=2); adrenaline (5 μM) produced an additional enhancement of about 44.6±10% (n=5). A larger increase of barium current was observed until 52.6±9.7% (n=3) with 10 μM of adrenaline. These effects of adrenaline were observed after a 5 minutes exposure and they were more clearly observed when membrane was depolarized in the range of -10 to 0 mV. The present results show that adrenaline causes an increase of the inward barium current in tonic muscle fibers of the frog.

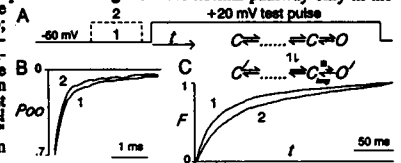
\* CONACYT Fellowship

Supported by SEP C89-01-0150 and CONACYT d111-904366.

## Tu-Pos411

**Ca-SENSITIVE INACTIVATION OF L-TYPE Ca CHANNELS: KEY ROLE OF AN ENDURING CLOSED STATE OUTSIDE THE NORMAL ACTIVATION PATHWAY** ((J.P. Imrody and D.T. Yue)) Johns Hopkins University, Baltimore, MD 21205

An important negative feedback element in Ca<sup>2+</sup> signalling is the Ca-sensitive inactivation of many high-threshold Ca channels. From the analysis of individual cardiac L-type Ca channels, we have recently established that this inactivation mechanism involves an unusual phenomenon (*Science* 250:1735, 1990): even if a channel manages to open after a period of Ca entry, it will subsequently be closed with a greater probability than would be found after openings without prior Ca influx. Open probabilities conditioned on first openings in a test pulse (P<sub>1</sub> in B) illustrate the effect explicitly: the P<sub>1</sub> following a channel-activating prepulse (A&B, case 2) is clearly depressed relative to the analogous P<sub>1</sub> without a prepulse (A&B, case 1) (5 patch means). One explanation is that Ca entry permits the channel access to an alternate open state (O') that communicates readily with a long-lived closed state (C<sub>slow</sub>). We now confirm this mechanism by demonstrating prepulse-dependent slowing of the first latency distribution function F (probability of a 1st test pulse opening before t), which is characteristic of trapping in a stable closed conformation (panel C, 5 patch means normalized for comparison). The prepulse insensitivity of F when Ba<sup>2+</sup> carries charge argues that access to C<sub>slow</sub> relates intimately to Ca-sensitive inactivation. The peculiar form of the retardation of F, appearance of a slow exponential component following a brisk initial rise, argues strongly that C<sub>slow</sub> resides along an activation scheme distinct from the normal pathway (C inset, top row). Moreover, the insensitivity of Ca channel gating currents to elevated intracellular [Ca<sup>2+</sup>] (*J Physiol* 444:257, 1991) places C<sub>slow</sub> next to O', in an activation sequence differing from the normal pathway only in the diminished final opening rate (C inset, ■ in lower row); other topologies entail Ca-dependent charge immobilization. We therefore propose that Ca-sensitive inactivation results from Ca-dependent redistribution of a channel between two "gating modes" distinguished primarily by an enduring closed state.



## Tu-Pos413

**ADENOSINE MODULATES VOLTAGE-GATED CALCIUM CHANNELS IN ADULT RAT SYMPATHETIC NEURONS VIA A GUANINE NUCLEOTIDE BINDING PROTEIN.** ((Yu Zhu & Stephen R. Ikeda)) Department of Pharmacology & Toxicology, Medical College of Georgia, Augusta, GA 30912.

Ca<sup>2+</sup> channel modulation by adenosine was investigated in enzymatically dispersed adult rat superior cervical ganglion (SCG) neurons using the whole-cell variant of the patch-clamp technique. Adenosine produced a concentration-dependent decrease in the Ca<sup>2+</sup> current amplitude with an EC<sub>50</sub> of 170 nM and maximum inhibition of 40%. The adenosine-induced Ca<sup>2+</sup> current inhibition was mediated by A<sub>1</sub> purinergic receptor as the EC<sub>50</sub> value for an A<sub>1</sub> receptor selective agonist chloro-N-cyclopropyladenosine was 1000 fold lower than that of an A<sub>2</sub> receptor selective agonist CGS-21680 (33 nM vs. 40 μM). G-protein appeared to be involved in the action of adenosine as: 1) the adenosine-induced current inhibition could be largely relieved by depolarizing voltage prepulses; 2) tail current analysis revealed that adenosine shifted Ca<sup>2+</sup> channel activation to more depolarized potentials; 3) adenosine inhibition was abolished by 2 mM intracellular GDP-β-S or 500 ng/ml pertussis toxin treatment. Adenosine appeared to affect "N" and possibly "P" type Ca<sup>2+</sup> channels as the prolonged tail current component induced by the dihydropyridine "agonist" (+)202-791 (2 μM) was not reduced by adenosine and a portion of the Ca<sup>2+</sup> current (20%) which was resistant to 10 μM ω-conotoxin GVIA was further inhibited by adenosine. Supported by NIH grant HL-43242 and a Biomedical Research Support Grant from Medical College of Georgia.

**Tu-P06414**

**L- AND T-TYPE CALCIUM CURRENTS IN CARDIAC MYOCYTES FROM DWARF (DW4) RATS.** ((E. S. Piedras-Renteria and P. M. Best)) Dept. Physiology and Biophysics, University of Illinois, Urbana, IL 61801.

DW4 rats are mutants that show a selective reduction in growth hormone synthesis and storage. They provide an excellent model to study possible hormonal regulation of ion channel expression.  $Ca^{2+}$  currents in atrial cells from 5 week-old, female DW4 and control (Fischer, F344) rats were studied with whole-cell patch clamp. Bath solution composition (mM) was: 2  $CaCl_2$  (or 5  $BaCl_2$ ), 100 N-methyl-D-glucamine methanesulfonate, 1  $MgCl_2$ , 10 HEPES and 10 glucose, pH=7.4. The pipette solution contained (mM): 140 Cs-Asp, 10 Cs-EGTA, 5  $MgCl_2$ , 1 ATP, 0.3 GTP, pH=7.4. Average capacity was smaller in DW4 cells (22.4  $\pm$  1.51 pF (n=9)) than in F344 cells (32.75  $\pm$  3.28 pF (n=8)) ( $p < 0.01$ ). With  $Ca^{2+}$  as charge carrier, peak T and L current densities were greater in DW4 rats than in controls ( $p < 0.05$  and  $p < 0.1$ , respectively). T current density was  $-2.02 \pm 0.5$  pA/pF (n=7) for DW4 and  $-0.76 \pm 0.14$  pA/pF (n=5) for F344. Similar values were also recorded using  $Ba^{2+}$  as charge carrier. L-type peak current density was  $-4.55 \pm 0.86$  pA/pF (n=7) for DW4 and  $-2.63 \pm 0.5$  pA/pF (n=6) for F344. L currents were sensitive to dihydropyridines, Bay K 8644 and  $CdCl_2$ . Supported by AHA, Illinois Affiliate.

**Tu-P06416**

**DIMERCAPTO COMPOUNDS PREVENT ACUTE LEAD EFFECTS ON NEURONAL L-TYPE CALCIUM CHANNELS.** Gutierrez, Francisco and Bernal, Juan. Physiology Department, University of Aguascalientes. 20100, AGS., Mexico.

Although Dimercapto compounds have been used to treat lead poisoning in humans, the mechanism by which these compounds act at the cellular level is still unclear. Dimercapto compounds such as Meso 2,3-dimercaptosuccinic acid (DMSA) and 2,3-dimercapto-1-propanesulfonic acid (DMPS) were tested on *Helix aspersa* neurons previously intoxicated with lead. The neurons were studied under current and voltage clamp conditions while sodium and potassium currents were blocked. Thus, the Calcium Action Potentials ( $Ca^{2+}$ -AP) and the Calcium Currents ( $ICa^{2+}$ ) were monitored in control conditions and when cells were exposed to the compounds of interest. In all cells tested,  $Pb^{2+}$ -Ac at 50  $\mu$ M reduced the duration of  $Ca^{2+}$ -AP and the magnitude of  $ICa^{2+}$  by  $38.7 \pm 4\%$  S.D. n = 6. Lead effects on calcium signals were found to be reversible when cells were bathed with a solution containing  $Pb^{2+}$ -Ac 50  $\mu$ M along with DMSA (150  $\mu$ M) or DMPS (150  $\mu$ M). These results suggest that Dimercapto compounds may act at cellular membrane level to prevent lead effects.

**Tu-P06418**

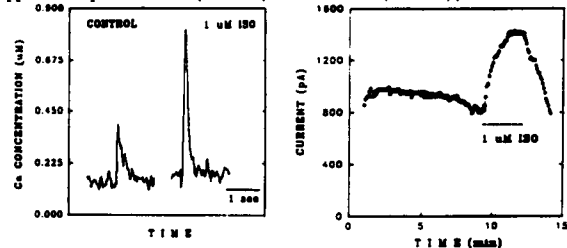
**NEUROPEPTIDE Y POTENTIATES CALCIUM CHANNEL CURRENTS IN SINGLE VASCULAR SMOOTH MUSCLE CELLS.** ((Z.G. Xiong, B.J. Bolzon and D.W. Cheung)) University of Ottawa Heart Institute, Ottawa K1V 4E9. (Spon. by B. Huang)

The effect of neuropeptide Y (NPY) on  $Ca^{2+}$  channel currents in isolated vascular smooth muscle cells was studied with the perforated-patch recording technique. Using  $Ba^{2+}$  (10 mM) as the charge carrier, inward currents sensitive to  $Cd^{2+}$  and nifedipine were potentiated by NPY in a concentration-dependent manner. The threshold concentration for the potentiating effect of NPY was 50 nM and reached a maximum at 150 nM. NPY shifted the steady-state activation curve to less positive membrane potentials by about 6 mV so that the potentiating effect was most prominent near the activation threshold of the current. It had no effect on steady-state inactivation of the current. These results suggest that NPY potentiates vasoconstriction by promoting calcium entry through L-type voltage-dependent  $Ca^{2+}$ -channels.

**Tu-P06415**

**MODULATION OF THE CA TRANSIENT AND THE CA CURRENT IN CARDIAC MYOCYTES ISOLATED FROM NORMAL MOUSE.** ((B.M. Wolaka, G.M. Wahler & R.J. Solaro)) Dept. of Physiology & Biophysics, Univ. of Illinois, Chicago, IL, 60680.

After establishing the procedure of isolation of mouse myocytes, we have measured the Ca transient in fura-2/AM loaded cells and the Ca current in the whole-cell configuration. The mean intracellular diastolic Ca concentration was  $110 \pm 9$  nM (SE) and it increased to  $132 \pm 10$  nM after adding 1  $\mu$ M of isoproterenol (ISO) to the perfusing solution. Under this condition the amplitude of the Ca transient increased from  $265 \pm 22$  nM to  $597 \pm 64$  nM. This increase is statistically significant. ISO also caused an increase in the rate of decline of the Ca transient. The Ca current increased  $177 \pm 27\%$  after adding ISO. In addition to increasing the Ca transient and the Ca current, ISO also enhanced the contractions of cells and the rate of relaxation. Further investigation of these effects of ISO are now in progress. (Supported by HL 22231 (R.J.S.) & HL 42955 (G.M.W.)).

**Tu-P06417**

**CALCIUM CURRENT IN SINGLE SYNAPTIC TERMINALS: CALCIUM-DEPENDENT INACTIVATION.** ((G. Matthews and H. von Gersdorff)) Dept. of Neurobiology, SUNY, Stony Brook, NY 11794

Type I Mbl bipolar neurons from goldfish retina are non-spiking, CNS interneurons with a giant synaptic terminal (8-10  $\mu$ m diameter) that is advantageous for studies of calcium regulation in individual synaptic terminals. Previous work has shown that these terminals have a single type of sustained, dihydropyridine-sensitive Ca current (Heidelberger & Matthews, 1992, J. Physiol., 447, 235-254). In experiments using combined fura-2 and patch-clamp measurements from single terminals, we have found that this Ca current is subject to negative feedback regulation via Ca-dependent inactivation. During prolonged depolarization (> 2 sec), the Ca current was initially constant, and then began to inactivate. The delay to onset, the speed, and degree of inactivation depended on the size of the Ca current and on the Ca buffering conditions. Inactivation was reduced when barium replaced calcium in the external solution, and addition of BAPTA (0.5 - 10 mM) to the pipette solution slowed the onset and reduced the magnitude of inactivation. EGTA was less effective. The effectiveness of BAPTA in reducing inactivation implies that the Ca sensor for inactivation is not directly on the channel. Inactivation produced by a 20-sec depolarizing step was greatest for step voltages ranging from -20 to +20 mV, and declined at more positive potentials. This voltage-dependence of inactivation was similar to the relation between voltage and change in  $[Ca]_i$ . All of these properties suggest that the Ca current in the presynaptic terminal shows Ca-dependent inactivation. Following inactivation, Ca current recovered slowly, along an approximately exponential time-course with a time constant of about 30 sec. The time constant for the return of  $[Ca]_i$  to baseline after an inactivating stimulus was much shorter, averaging about 5 sec. In the intact retina, illumination produces a sustained depolarization of type I Mbl bipolar neurons, and Ca-dependent inactivation of the Ca current in the terminal might contribute to the conversion of this sustained response into the transient response typical of the ganglion cells. (Supported by NIH grant EY03821.)

**Tu-P06419**

**KINETIC DIVERSITY OF L-TYPE CALCIUM CHANNELS IN RAT HIPPOCAMPAL NEURONS.** ((Ege T. Kavalali and Mark R. Plummer)) Biological Sciences, Rutgers Univ., Busch Campus, Piscataway, NJ 08855

L-type calcium channels display diverse gating patterns that can be modulated by dihydropyridines and potentiating voltage protocols. We have used single-cell recordings to examine the re-opening of L-type channels following a voltage pulse. Pyramidal neurons obtained from embryonic day 18 rat hippocampi were placed in tissue culture in defined media and used from 3 to 10 days after plating. Recordings with 110 mM  $BaCl_2$  as the charge carrier in a bath solution of 140 mM K gluconate, 5 mM EGTA, 10 mM HEPES, and 0.5  $\mu$ M (+)-(-)-202-791 revealed that L-type channels show two very distinct forms of gating following a 160 msec voltage pulse to either +20 or +40 mV. The channels either exhibited conventional tail current openings (the channel was open previous to the termination of the voltage, and closed after a delay) or showed re-openings that could occur up to 400 msec after the termination of the pulse. These re-openings occurred in bursts that could continue for as long as 0.5 sec. To date, we have found this to be a non-uniform characteristic of L-type channels: they either showed re-openings (30% of our recordings), or did not, for the entire duration of the experiment. We are presently investigating whether this dichotomy is due to differential modulation of L-type channels, slow transitions between "modes" that show re-openings and those that do not, or the possibility that this reflects differences in the kinetics of distinct subtypes of L-type calcium channels.

**Tu-P0420**

**HIGH  $[Ca^{2+}]_i$  IN THE CYTOSOL DOES NOT ABOLISH  $Ca^{2+}$  INDUCED  $Ca^{2+}$  RELEASE ALTHOUGH IT INACTIVATES SARCOLEMMA  $Ca^{2+}$  CURRENT IN CANINE VENTRICULAR MYOCYTES.** (B. Szabo, T. Banyasz, R. Fugate, C. Rajagopalan, and R. Lazzara, OU Health Sciences Center and VA Medical Center, Okla. City, OK.)

In order to study the effects of high cytosolic  $Ca^{2+}$  concentration ( $[Ca^{2+}]_i$ ) on the action potential (AP),  $I_{Ca}$ , the release of  $Ca^{2+}$  from the sarcoplasmic reticulum (SR), and on contraction, we measured these parameters in canine ventricular myocytes which exhibit AP with "spike and dome" configuration. To minimize intracellular dialysis and rundown, ultrathin microelectrodes (3M KCl) were used for intracellular stimulation and recording  $V_m$  ( $R_e = 30-60$  M $\Omega$ ) and for discontinuous single electrode voltage clamping ( $R_e = 10-15$  M $\Omega$ ). Changes in systolic  $[Ca^{2+}]_i$  transients (CaT) were expressed as normalized values of the uncalibrated fura-2(AM) signal. Contraction was measured with an edge detector. Treatment with ouabain (0.5  $\mu$ M) increased CaT to a maximum at 155% in 3 stages: (1) Within the first 15 min CaT and contraction were increased by 15% and 50%, respectively, with no changes in AP. (2) Between 15-25 min CaT increased by 24% and contraction by 218%. During diastole slowly rising spontaneous  $Ca^{2+}$  release (SCR) occurred without generating delayed afterdepolarizations (DAD). The "dome" in the AP became depressed and the duration of AP became shorter. (3) Between 25-30 min CaT reached a maximum when DAD appeared in combination with more rapidly rising and larger SCR (up to 120% of the control CaT). Individual CaT and contraction were reduced if preceded by an SCR. When AP were elicited during large SCR,  $I_{Ca}$  and the "dome" were completely suppressed and the AP was abbreviated from 250 msec to about 50 msec, yet the AP elicited a CaT as contraction. In conclusion: (1) Depolarization may trigger Ca release from an overloaded SR in the absence of  $I_{Ca}$ . (2) However, diastolic SCR and DAD can deplete  $Ca^{2+}$  from the SR and reduce the releasable amount of  $Ca^{2+}$  for the forthcoming CaT.

**Tu-P0422**

**GLYBURIDE INDUCES TRANSIENT INWARD CURRENT BUT DECREASES  $I_{Ca}$  IN VENTRICULAR MYOCYTES**

(J.S. Pasnani and G.R. Ferrier) Dalhousie University, Halifax, N.S. Canada

The ability of glyburide to induce transient inward current ( $I_t$ ) was examined with discontinuous single electrode voltage clamp conditions in isolated guinea pig ventricular myocytes. A holding potential of -80mV was used. When 5-10 prepulses from -80 to +10mV were used, glyburide (3,10 and 30  $\mu$ M) induced  $I_t$  on repolarisation following depolarising steps to +10 or +50mV in 72% of the cells. This protocol did not induce  $I_t$  in the absence of drug or in the presence of solvent (DMSO). The amplitude of  $I_t$  peaked at approximately -50mV and was greater after depolarising steps to +50mV than +10mV.  $I_t$  was not observed in the presence of glyburide if prepulses were not used.  $I_t$  is caused by intracellular  $Ca^{2+}$  overload which can occur either through increased  $Ca^{2+}$  influx or decreased  $Ca^{2+}$  efflux. Glyburide significantly ( $p < 0.05$ ) decreased  $I_{Ca}$  activated from -40 mV, with incremental steps of 5mV, to +30 mV. This suggests that calcium overload is not due to increased  $Ca^{2+}$  influx through L-type  $Ca^{2+}$  channels. Glyburide increased the magnitude of cell shortening (measured by a video edge detector) elicited after 10 prepulses from a postconditioning potential of -40 mV with incremental steps to +30 mV. These results suggest that glyburide increases intracellular  $Ca^{2+}$  by a mechanism other than L-type  $Ca^{2+}$  channels, possibly by increased sequestration of  $Ca^{2+}$  or decreased  $Na^+-Ca^{2+}$  exchange.

**Tu-P0424**

**FACTORS WHICH MAY EXPLAIN DIFFERENT DEFIBRILLATION THRESHOLDS FOR MONOPHASIC AND BIPHASIC SHOCKS.**

(S.M. Dillon, T. Wang)) Columbia University, New York, NY 10032.

Two sets of experiments used Langendorff perfused rabbit hearts. I) Measurements of defibrillation (DF) threshold for 5 msec monophasic (5M), 2.5 msec monophasic (2.5M) and 5 msec biphasic (5B) shock waveforms (8 hearts) used logistical regression analysis of DF success rate. II) Optical action potentials were recorded on the ventricle (7 hearts) while shocks were applied during 200/min ventricular pacing. Shock strength at the recording site was set to 5, 10, 15 and 20 V/cm. The action potential prolongation (APP) and arrhythmogenicity were measured. The APP for shocks applied during the plateau phase was the delay of phase 3 repolarization following the shock with respect to the unshocked action potential. A shock exhibited arrhythmogenicity if it evoked extra beat(s) following the shock response. Shock voltages at the level of 50% DF success rate were: 5M = 61% 2.5M and 5B = 44% 5M, i.e. DF threshold voltages in rank order were 2.5M > 5M > 5B. The APP produced by the shocks in rank order were 5M > 2.5M > 5B for all shocks before repolarization ( $p < .05$  except for 5V/cm shocks). The number of arrhythmic outcomes for all shocks was 5B = 44% 5M and 5M = 93% 2.5M. Since all waveforms stimulated equally well (not shown) the DF threshold may depend upon the ability to prolong refractoriness, i.e. APP, or produce arrhythmias. 5M and 2.5M waveforms were almost equally arrhythmogenic but the 5M produced more APP, possibly explaining the greater DF efficacy of the 5M waveform. While the 5B waveform produced the least APP, it evoked far fewer arrhythmias than the other waveforms which may explain its greater efficacy.

**Tu-P0421**

**MEMBRANE CURRENTS DURING  $[Ca^{2+}]_i$  OSCILLATIONS IN THE ABSENCE OF  $Na^+$ .**

(K.R. Sipido, G. Callewaert, J. Vereecke and E. Carmeliet) Laboratory of Physiology, Catholic University of Leuven, Belgium.

Transient inward currents ( $I_t$ ) during  $[Ca^{2+}]_i$  oscillations have been ascribed to the Na/Ca exchanger. We have investigated whether other  $Ca^{2+}$ -dependent membrane currents contribute to  $I_t$ .

Enzymatically isolated single ventricular myocytes from guinea pig were studied under whole-cell voltage clamp.  $[Ca^{2+}]_i$  was measured with fura-2. The pipette solution contained (in mM) CsCl 130, HEPES 10, MgCl<sub>2</sub> 1, MgATP 4, fura-2 0.1, pH 7.20. The control external solution contained (in mM) NaCl 130, CsCl 10, HEPES 10, dextrose 10, MgCl<sub>2</sub> 1, CaCl<sub>2</sub> 1.8, pH 7.40.  $[NaCl]_o$  was substituted with either CsCl, LiCl, or NMDGCl.

In the absence of  $Na^+$ , the cell could be loaded with  $Ca^{2+}$  by repetitive depolarizations to +10mV, inducing spontaneous  $[Ca^{2+}]_i$  oscillations. During these oscillations, no inward currents were seen, but instead an outward current shift was observed at potentials between -40mV and +60mV. This outward current shift was not sensitive to substitution of either internal monovalent cations or external Cl<sup>-</sup>. It was however, sensitive to block of  $I_{Ca}$  by verapamil.

In conclusion, during  $[Ca^{2+}]_i$  oscillations in the absence of  $Na^+$ , oscillations of the membrane current result from  $Ca^{2+}$ -dependent, transient, inactivation of  $I_{Ca}$ . We could not identify a contribution of the  $Ca^{2+}$ -activated non-specific cation channel.

**Tu-P0423**

**COMPLEX AND CHAOTIC DYNAMICS OF EARLY AFTERDEPOLARIZATIONS IN SIMULATED PURKINJE FIBERS.**

(Y. Kowtha, M. Boujtir, E.B. Caref, N. El-Sherif, M. Restivo) SUNY Health Science and Brooklyn VA Medical Centers, Brooklyn, NY 11209

Polymorphic ventricular arrhythmias such as torsades de pointes can be induced with agents that prolong the inactivation of the fast inward sodium current ( $I_{Na}$ ). Certain types of these arrhythmias are associated with a bradycardia dependent prolongation of the action potential which progresses until a secondary depolarization occurs prior to repolarization (early afterdepolarization - EAD). The combined role of the action potential lengthening and EAD generation remain unclear. We investigated the generation of EADs in a model of the cardiac Purkinje fiber (modified DiFrancesco-Noble) by delaying inactivation of  $I_{Na}$  ( $\beta_h$ ).  $\beta_h$  was varied such that the inactivation time constant ( $\tau_h$ ) for  $I_{Na}$  was prolonged 1-25 times of control  $\tau_h$  which induced 1 or more EADs. When multiple EADs were present there was an increase in the amplitude of the depolarizations and a decrease in takeoff potential with time. Action potential duration (APD 90%) plotted versus  $\beta_h$  was non monotonic and showed multiple discontinuities. In the voltage range in which EADs were induced, APD could double for a change in  $\tau_h$  of only 2%. Changes in APD were also accompanied by a varying number of EADs during plateau. Rapid pacing shortened the action potential duration and suppressed EADs, but steady state APD was reached only after a sufficient number of beats. A critical reduction in calcium current or sodium calcium exchange resulted in complex and chaotic EAD formation, during which the afterdepolarizations varied in amplitude and takeoff potential. In summary, we found that EADs can be induced by delayed  $I_{Na}$  inactivation that can result from a number of pathological and pharmacological conditions. Conduction of EADs to the surrounding myocardium, combined with the extreme sensitivity of APD to small changes in kinetic properties can result in marked heterogeneity in recovery of excitability and may predispose hearts to complex reentrant ventricular arrhythmias.

**Tu-P0425**

**ELECTROPHYSIOLOGIC PROPERTIES OF SPONTANEOUSLY ACTIVE MYOCYTES FROM RABBIT AV NODE.** (Y. Habuchi and W.R. Giles) Department of Medical Physiology, University of Calgary, Alberta, Canada T2N 4N1

Spontaneously active single cells having an average capacitance of  $41 \pm 2$  pF ( $n=58$ , mean  $\pm$  SE) were enzymatically isolated from the central region of the atrioventricular (AV) node of rabbit heart. Nystatin-permeabilized patch recordings made at 32°C consistently gave spontaneous action potentials with a rate of  $129 \pm 24$  bpm, average maximal diastolic potential (MDP) of  $-56 \pm 1$  mV ( $n=44$ ) and amplitude of  $86 \pm 2$  mV ( $n=44$ ). The majority of these cells had large TTX-sensitive  $Na^+$  ( $I_{Na}$ ), L-type  $Ca^{2+}$  ( $I_{Ca}$ ), delayed rectifier  $K^+$  ( $I_K$ ), and hyperpolarization-activated inward ( $I_h$ ) currents. A  $Ca^{2+}$ -insensitive, 4-aminopyridine-sensitive transient outward current ( $I_t$ ) was also present in most cells. The delayed rectifier,  $I_K$ , was highly selective for  $K^+$ , turned on at approximately -40 mV and had an inwardly-rectifying I-V relationship.  $I_t$  was activated at approx. -70 mV, was blocked by  $Cs^+$  (3mM) and had a linear I-V relationship with a reversal potential of -25 mV. The time- and voltage-dependent properties of  $I_{Na}$  and  $I_{Ca}$  were examined in detail using membrane-ruptured whole-cell recordings.  $I_{Na}$  was blocked by TTX and  $Ca^{2+}$  with  $K_m$  of 1.5  $\mu$ M and 1.6 mM, respectively.  $I_{Ca}$  was blocked by nifedipine ( $2 \times 10^{-6}$  M), and no T-type  $Ca^{2+}$  current was observed even when  $I_{Ca}$  was elicited from negative holding potentials in  $Na^+$ -free solution. The steady-state inactivation curve for  $I_{Na}$  and  $I_{Ca}$  had their midpoints at -86 mV and -30 mV with slope factors of 4.8 mV and 5.3 mV, respectively. (Supported by AHFMR, CHF and MRC)



**Tu-P0426**

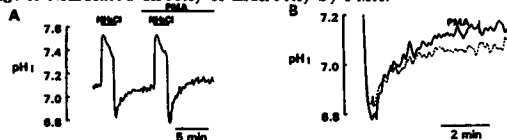
RESPONSES OF  $\beta$ -ADRENERGIC SYSTEM IN INTACT CARDIOMYOCYTES TO SHORT TERM EXPOSURE TO  $\beta$ -AGONISTS. (M. Horackova and Mary G. Murphy), Dept. of Physiology and Biophysics, Faculty of Medicine, Dalhousie University, Halifax, Nova Scotia, Canada B3H 4H7. (Spon. by A.Y.K. Wong)

In a recent study, we demonstrated that the binding of the hydrophilic ligand, CGP-12177, to  $\beta$ -receptors on the surface of the isolated cardiomyocytes was not affected by short-term exposure to physiological levels ( $10^{-9}$  to  $10^{-6}$  M) of  $\beta$ -AR agonists, which label the high-affinity  $\beta$ -adrenoceptors (Horackova & Wilkinson, 1992). In fact, a 2-hr exposure to micromolar quantities of isoproterenol (ISO) or norepinephrine was required to produce a decrease in the density of these receptors. As an extension of these studies of the desensitization process, we have now examined the effects of short-term, repeated exposure of the cardiomyocytes to low concentrations (nM) of  $\beta$ -AR agonists on levels of intracellular cyclic AMP (cAMP). ISO, norepinephrine and forskolin-stimulated cAMP formation have been examined in terms of their abilities to modify the responsiveness of the  $\beta$ -AR to subsequent stimulation. The results of the study demonstrated that both ISO and forskolin stimulate adenylate cyclase as judged by rapid rises in intracellular cAMP in the presence or absence of the phosphodiesterase (PDE) inhibitor, Ro 20-1724. Short-term exposure to either results in desensitization of the  $\beta$ -AR/AC interaction, and this process appears to be homologous in nature. This study was supported by Heart and Stroke Foundation of Nova Scotia. M. Horackova and M. Wilkinson; Pflügers Arch. 1992 - in press.

**Tu-P0428**

EFFECT OF PHORBOL ESTER ON RECOVERY FROM ACID LOAD IN ADULT VENTRICULAR MYOCYTES. (Rita L. Skolnick and Kenneth W. Spitzer) Nora Eccles Harrison CVRTI, University of Utah, Salt Lake City, UT 84112.

Effects of the phorbol ester, PMA, on intracellular pH ( $pH_i$ ) recovery from acid loading were examined in adult resting myocytes (guinea pig) held at 37°C ( $pH_o=7.4$ ).  $pH_i$  was measured with SNARF-1 AM after 10 min loading (15  $\mu$ M) and 30 min perfusion with indicator-free solution containing (mM): NaCl 126, dextrose 11.0, KCl 4.4, MgCl<sub>2</sub> 1.0, CaCl<sub>2</sub> 1.0, Hepes 24.0, NaOH 13.0.  $pH_i$  was determined by the ratio of fluorescence emission (640nm/580nm) during continuous excitation at 515nm. Acid load was imposed by application and removal of 10 mM NH<sub>4</sub>Cl. In the absence of HCO<sub>3</sub><sup>-</sup>/CO<sub>2</sub>, PMA (0.1  $\mu$ M) enhanced the initial rate of recovery from acid load ( $dpH_i/dt$ ) by 82±63% (n=5) (Figure A). Figure B shows the overlay of the recoveries. In the steady state, PMA (0.1  $\mu$ M) caused an intracellular alkalosis of 0.06±0.01 pH units (n=3) after 4 min. This effect was blocked by amiloride (1mM). This suggests that Na/H exchange is stimulated directly or indirectly by PMA.

**Tu-P0430**

EFFECT OF CAPTOPRIL TREATMENT ON Na<sup>+</sup>,K<sup>+</sup>-PUMPING IN RABBIT HEART CELLS. (L.C. Hool, B.G. Robinson, H.H. Rasmussen) Dept. of Cardiology, Royal North Shore Hospital, Sydney, NSW, Australia. 2065.

A variety of hormonal stimuli regulate the Na<sup>+</sup>,K<sup>+</sup>-pump by modifying gene expression or by modifying pre-existing pumps. Since it is unknown if interference with the renin-angiotensin system alters the pump long-term we examined the effect of captopril treatment on the sarcolemmal Na<sup>+</sup>,K<sup>+</sup>-pump. Ouabain-sensitive (50  $\mu$ M) Na<sup>+</sup>,K<sup>+</sup>-pump current ( $I_p$ ) was recorded in single right ventricular myocytes voltage-clamped at -40mV with wide-tipped patch-pipettes. When the Na<sup>+</sup> concentration in the pipette (Na<sub>p</sub>) was 10 mM,  $I_p$  of myocytes from rabbits treated with captopril for 8 days (8mg/kg/24h) was larger than  $I_p$  in controls ( $0.56 \pm 0.04$  pA/pF, n=10 vs.  $0.32 \pm 0.03$  pA/pF, n=9, mean  $\pm$  SE, P<0.001). When Na<sub>p</sub> was 50 mM to near-saturate the pump, there was no difference in  $I_p$  between cells from captopril treated and control animals ( $1.16 \pm 0.10$  pA/pF, n=11 vs.  $1.10 \pm 0.04$  pA/pF, n=7). This suggests that captopril does not induce an increase in sarcolemmal pump density. To support this conclusion we searched for evidence of synthesis of new pump units by measuring mRNAs for the  $\alpha_1$ ,  $\alpha_2$  and  $\beta$  subunits of the Na<sup>+</sup>,K<sup>+</sup>-pump in control rabbits (n=4) and in rabbits treated with captopril for 1 (n=4) or 8 days (n=4). This was performed using quantitative Northern blotting. There was no difference in subunit mRNAs between controls and captopril treated animals at either of the time points. The findings suggest that treatment with captopril causes an increase in Na<sup>+</sup>,K<sup>+</sup>-pump current at 10 mM Na<sub>p</sub> due to an increase in the Na<sup>+</sup> affinity of pre-existing pump units. This may have implications for understanding clinical effects of captopril.

**Tu-P0427**

NEURAL CONTROL OF ADULT RAT CARDIOMYOCYTES IN CO-CULTURES WITH CARDIAC NEURONS. (M. Horackova, M.H. Huang and J.A. Armour). Dept. of Physiology and Biophysics, Faculty of Medicine, Dalhousie University, Halifax, Nova Scotia, Canada. B3H 4H7

Ventricular myocytes as well as stellate and intrinsic cardiac neurons were enzymatically dissociated from adult male guinea pigs and plated together; the cultures were maintained in an incubator for 2-10 weeks. The electrical properties of cultured myocytes and neurons were investigated by means of conventional microelectrode technique and the myocytes' spontaneous contractile activity was recorded by means of a video system. The electrical properties of the cultured myocytes and neurons were similar to those reported in other *in vitro* studies. However, innervated versus non-innervated cardiomyocyte cultures responded differently to various pharmacological interventions. Spontaneous contractions were attenuated by tetrodotoxin ( $4 \times 10^{-7}$  M),  $\beta$ -adrenergic blockade and nicotinic blockade more in co-cultures than in cardiac myocyte cultures alone. On the other hand, the  $\beta$ -adrenergic agonist isoproterenol increased the spontaneous beating in both types of co-cultures more than in myocytes alone. The effects of the muscarinic agonist bethanechol and muscarinic blocker atropine were not significantly different in innervated and non-innervated cultures. Nicotine induced either an increase or decrease in contractile rates of both co-cultures while not affecting non-innervated myocyte cultures. These results demonstrate a functional interaction between both types of neurons and the myocytes and they indicate a presence of adrenergic neurons in both - the extrinsic (stellate) ganglion and in the intrinsic cardiac ganglia. This study was supported by Grants MT 1248 and MT 10122 from Medical Research Council of Canada.

**Tu-P0429**

FUNCTIONAL AND STRUCTURAL STUDIES OF PHOSPHOLAMBAN AS A MODEL ION CHANNEL PROTEIN. Shy Arkin<sup>1</sup>, Edward G. Moczydlowski<sup>2</sup>, Saburo Aimoto<sup>2</sup>, Steven O. Smith<sup>1</sup> and Donald M. Engelman<sup>1</sup>. Departments of Cell Biology<sup>1</sup>, Pharmacology<sup>2</sup>, and Molecular Biophysics and Biochemistry<sup>3</sup>, Yale University School of Medicine, New Haven CT 06510. Institute for Protein Research, Osaka 565, Japan<sup>2</sup>.

Phospholamban is a non-covalent homopentameric membrane protein believed to function in the regulation of the Ca<sup>2+</sup> pump in cardiac SR. It is particularly useful as a model for molecular mechanisms of ion permeation, since its small size (52 residues) makes it amenable to spectroscopic methods of structure determination.

A synthetic peptide corresponding to the transmembrane domain of phospholamban readily incorporates into planar lipid bilayers and exhibits reproducible single-channel fluctuations. The channel is cation specific and selective towards Ca<sup>2+</sup>. It is predominantly in an open state and exhibits several sub-conducting states. The channel forming property of phospholamban may represent the underlying regulatory mechanism acting on the Ca<sup>2+</sup> pump.

In addition, we have expressed phospholamban in a chimeric construct in *E. coli*, which is similar to the native molecule in its pentameric behavior. By PCR mutagenesis we have shown that conservative changes in several residues in the transmembrane domain abolish pentameric association.

Taken together the conductance measurements and mutagenesis data provide an approach for correlating structure and function of this cardiac ion channel.

**Tu-P0431**

THE EFFECT OF  $\beta$ -STIMULATION ON Na/K PUMP CURRENT IN GUINEA PIG VENTRICULAR MYOCYTES IS MEDIATED BY A cAMP-DEPENDENT PKA PATHWAY. (J. Gao, R.T. Mathias, I.S. Cohen and G.J. Baldo) HSC, SUNY at Stony Brook, NY, 11794-8661.

The  $\beta$ -agonist isoproterenol (ISO) increases Na/K pump current ( $I_p$ ) via  $\beta$ -adrenergic receptors when the intracellular calcium concentration ( $[Ca]_i$ ) is above 150nM in acutely isolated myocytes (Gao, Mathias, Cohen and Baldo, 1992). The cellular signaling pathway was characterized using the whole cell patch clamp technique and fixing  $[Ca]_i$  at 1.4  $\mu$ M. The non-specific protein kinase inhibitor H<sub>7</sub> (100  $\mu$ M) eliminated the stimulatory effect of 0.5  $\mu$ M ISO, suggesting a phosphorylation step is involved.  $I_p$  in the presence of 12nM ISO was further increased by the protein phosphatase inhibitor calyculin A (0.5  $\mu$ M). Neither H<sub>7</sub> nor calyculin A had any effect on  $I_p$  in the absence of ISO. These results indicate a low basal phosphorylation, making the effects of H<sub>7</sub> and calyculin A difficult to detect without increasing the phosphorylation level. The stimulatory effect of ISO could be mimicked by bath application of 0.5mM of the membrane-permeant cAMP analog chlorophenylthio-cAMP, the phosphodiesterase inhibitor IBMX (100  $\mu$ M), or the adenylyl cyclase activator forskolin (50  $\mu$ M). The synthetic peptide inhibitor PKI (2  $\mu$ M) of protein kinase A (PKA) prevented the effect of ISO or chlorophenylthio-cAMP. These results suggest the effect of ISO is mediated via a phosphorylation step induced by a classical cAMP-dependent PKA pathway. Supported by the AHA and NIH grants HL20558, HL28958 and HL43731.

**Tu-P0432**

**SINGLE-ENDED FIBER OPTIC SYSTEMS FOR RECORDING FROM MYOCARDIUM AND NERVE AXON.** (V. Krauthamer, H.J. Bryant, C.C. Davis) Div Phys Sci (HFZ-133), FDA, Rockville, MD 20857, Dept. Physiol, USUHS, Bethesda, MD, Dept Elec Eng, U of MD, Coll Pk, MD

We developed three systems which use single optical fibers to both excite fluorescence from tissue stained with a voltage-sensitive dye and detect the action-potential-related signals. The first system features a single-mode, 4µm core, fiber. Light from a 633nm laser is passed through a dichroic reflector into the fiber which is placed in immobilized frog heart stained with the oxonol dye WW781. The emitted fluorescence is returned through the fiber and reflected by the dichroic into a photomultiplier tube. This system has the advantage of high spatial resolution, but signal averaging is required. The second system has improved signal/noise ratios and employs a larger (100µm) core fiber, and a 543nm He-Ne laser with a photomultiplier tube that matches the spectral characteristics of improved styryl dyes bound to cell membrane. The results were low-noise, single-trial, action potentials from myocardium stained with RH237, and signal-averaged action potentials from lobster axon injected with RH461. The third system substitutes couplers to simplify construction and permit a dual channel system. The excitation light is first split (1:1), and each of the two fibers transmits part of the excitation light through a second fiber coupler (93% loss) to the heart. The returning red fluorescence is split in the coupler (7% loss) and directed to the photomultiplier tube. With the two-fiber system differences in action potential shape and timing were observed.

**Tu-P0434**

**MOLECULAR CLONING OF A CYCLIC-NUCLEOTIDE GATED CHANNEL FROM MOUSE HEART.** ((MariaLuisa Ruiz, Barry London, Diomedes Logothetis, and Bernardo Nadal-Ginard)) Harvard Medical School, Children's Hospital, Boston MA. 02115

Cyclic nucleotide-regulated channels mediate autonomic regulation of heart rate. We have found, by a combination of library screening and reverse transcription-PCR, a sequence from mouse heart RNA which is highly homologous to the rat olfactory channel cloned by Dhallan, et al. (Nature 347: 184; 1990). The 3' two thirds of the clone was isolated from mouse genomic, as well as fetal heart cDNA libraries. The 5' end contains at least two introns, and we suspect the existence of more introns, as was shown for human retinal cyclic nucleotide-gated channels (Dhallan, et al. J. Neuroscience, 12(8): 3248; 1992). We were able to amplify an overlapping 5' end from reverse transcribed cDNA from mouse heart polyA+ RNA, with primers based on homology to the rat olfactory channel. This ~600 bp fragment starts at the putative methionine start codon of the channel and spans at least two introns, which have been spliced correctly in the message. We are presently expressing the putative heart channel in oocytes, characterizing the genomic organization, and surveying the tissue distribution of the transcript.

**Tu-P0436**

**RESPONSE OF CARDIAC TISSUE TO ELECTRICAL STIMULATION FROM A POINT SOURCE.** ((B. J. Roth and J. P. Wikswo, Jr.)) NIH, Bethesda, MD 20892 and Vanderbilt University, Nashville, TN 37232.

Numerical simulations were performed of the response of cardiac muscle to a point source of current. The bidomain model with unequal anisotropy ratios represented the 3-D tissue; leak and active sodium channels represented the membrane conductance. The wave front propagated faster parallel to the fibers (0.45 m/s) than perpendicular to them (0.18 m/s). For cathodal stimulation well above threshold (e.g., 15 mA, 0.5 ms), however, the wave front originated farther from the cathode perpendicular to the fibers than parallel to them, consistent with the dog bone-shaped virtual cathode observed experimentally by Wikswo et al. (Circ Res, 68:513, 1991). The virtual cathode size and shape are dependent upon both membrane and tissue conductivities. The tissue under the anode was hyperpolarized during anodal stimulation, but activation originated from two depolarized regions 1-2 mm from the anode along the fiber direction (threshold: 0.67 mA, 0.5 ms). The virtual cathode arises from differences in the electrical anisotropy in the intra- and extracellular spaces that are difficult to determine using conventional electrophysiological techniques. The virtual cathode's complexity at high stimulus strengths, and the dependence of its size and shape on stimulus and tissue parameters, suggest that these effects provide a new approach to studying the electrical behavior of cardiac tissue.

**Tu-P0433**

**STEREOSELECTIVE USE-DEPENDENT BLOCKADE OF THE I<sub>f</sub> PACEMAKER CURRENT IN SHEEP CARDIAC PURKINJE FIBRES** ((P.P. Van Bogaert & A. Raes)) Electobiology, University of Antwerp, B-2020 Antwerpen, Belgium.

The bradycardic agent DK-AH 3, a racemic compound, blocks the I<sub>f</sub> pacemaker current in a use- and voltage dependent manner during trains of voltage-clamp pulses from -30 to -120 mV, lasting 1 sec at 0.4 Hz with an apparent K<sub>d</sub> of 7\*10<sup>-9</sup> M (Van Bogaert, P. P. and A. Raes, 1991, Arch. Int. Pharmacod. 310: P191). If bradycardic drugs do block the I<sub>f</sub> current by binding to a specific receptor site associated with the I<sub>f</sub> channel, I<sub>f</sub> blockade by these drugs should be stereoselective. I<sub>f</sub> blocking potencies of the two isomers i.e. DK-AH 269 and DK-AH 268 were compared in short cardiac Purkinje fibres of sheep, using two micro-electrodes voltage-clamp technique (Di Francesco D. et al., 1991, Pfluegers Arch. 417:611). Both drugs caused an exponential decline of the peak I<sub>f</sub> current during a pulse train. The rate constant of decline A, increased linearly as a function of concentration. The steady state reduction in fully-activated I<sub>f</sub> current amplitude (γ) increased sigmoidally as a function of the drug concentration (x), according to the expression  $\gamma = [1 + (K_d/x)^n]^{-1}$  with n=1 and K<sub>d</sub>=8.9\*10<sup>-9</sup> M in the presence of DK-AH 269. In similar conditions DK-AH 268 induced I<sub>f</sub> block with an apparent K<sub>d</sub>=1.7\*10<sup>-9</sup> M. This significant difference in apparent K<sub>d</sub> is of the same order of magnitude as described in another ionic current in cardiac myocytes (Clarkson, W., 1989, Circulation Res. 65: 1306).

**Tu-P0435**

**INFLUENCE OF STRETCH ON EXCITATION THRESHOLD OF SINGLE FROG VENTRICULAR CELLS**

((Shazhou Zou and Leslie Tung)) Dept. of Biomedical Eng., The Johns Hopkins University, Baltimore, MD, 21205.

The excitation threshold intensity (ETI) of enzymatically dissociated single frog ventricular myocytes (n=6) was measured as a function of cell length (CL) and sarcomere length (SL). Field stimulation with constant current rectangular pulses (2-5ms) was applied through two platinum wire electrodes parallel to the long axis of the cell. ETI was measured as the amplitude of applied current with an error of less than 1%. Single cells were held isometrically by two glass pipettes and wrapped around an optical fiber which served as a force transducer and also was used to control cell length (Tung and Parikh, J Biomech Eng 113:492, 1991). SL was measured using video microscopy and a phase-locked loop system. Changes in CL and SL were induced by mechanical stretch of the whole cell. Bath solution was 1mM calcium Ringer. CL and SL initially were 343±41µm(±SD) and 2.11±0.10µm and increased following stretch to 364±45µm (increase of 6.2±2.4%) and 2.24±0.09µm (increase of 6.3±3.1%) respectively. This increase caused the ETI to decrease by 6.7±3.7% from the initial level (p<0.01, paired t-test). Stretch-activated channels may underlie the stretch-dependent changes in ETI although the influence of geometric changes in cell shape has not yet been ruled out.

**Tu-P0437**

**ICI D7288 INHIBITS THE HYPERPOLARISATION ACTIVATED CURRENT IN SINGLE SINOATRIAL NODE CELLS ISOLATED FROM THE GUINEA PIG.**

((Nicholas C. Sturgees, Robert E. BoSmith and Ian Briggs)) Bioscience II, ICI Pharmaceuticals, Alderley Park, Macclesfield, Cheshire, SK10 4TG. U.K. (Spon. by J.M.H. french-Mullen)

ICI D7288 (4-(N-ethyl-N-phenylamino)-1,2-dimethyl-6-(methylamino) pyrimidinium chloride) is a sinoatrial node (SAN) modulating agent which produces a slowing of the mammalian heart rate. The electrophysiological actions of ICI D7288 on the hyperpolarisation activated cationic current (I<sub>p</sub>) of single, freshly dissociated SAN cells, isolated from guinea pig, were investigated using the patch clamp technique in the whole-cell configuration. Single SAN cells were isolated from guinea pig cardiac tissue. Whole-cell I<sub>p</sub> currents were evoked by hyperpolarising voltage clamp steps from a holding potential of -40 mV, and were subsequently recorded using standard patch clamp procedures in HEPES buffered Tyrode solution. ICI D7288 inhibited I<sub>p</sub> in a concentration dependent manner, such that concentrations of 0.1, 0.3 and 1.0 µM ICI D7288 inhibited the I<sub>p</sub> current by 44 ± 4% (n=15), 65 ± 4% (n=14) and 78 ± 4% (n=9) respectively. The reduction in I<sub>p</sub> resulted from both a shift in the I<sub>p</sub> current activation curve in the negative direction on the voltage axis, and also a reduction in the activation curve amplitude. 0.1 µM ICI D7288 shifted the I<sub>p</sub> half-maximal activation by -6.1 ± 1.1 mV (n=8) and reduced the activation curve maximum by 35 ± 3% (n=8). A concentration of 0.3 µM produced a greater shift of -16.2 ± 1.8 mV (n=5) in the half-maximal activation and a reduction in the maximum of 52 ± 6% (n=5). ICI D7288 did not affect the I<sub>p</sub> channel ion selectivity properties, since the reversal potential remained unchanged in the presence of 0.1 - 0.3 µM of the drug (n=3). Blockade of the I<sub>p</sub> current by 0.3 - 1.0 µM ICI D7288 was not use-dependent (n=3). These results show that ICI D7288 reduces I<sub>p</sub> by affecting the gating properties of the I<sub>p</sub> channel, and that this inhibition may account for this agent's bradycardic properties.

## Tu-Pos438

THE PACEMAKER CURRENT  $i_f$  EXISTS IN ADULT MAMMALIAN VENTRICULAR MYOCYTES. ((H. Yu, F. Chang, and I.S. Cohen)) Dept. of Physiology & Biophysics, HSC, SUNY at Stony Brook, NY 11794-8661.

Isolated guinea pig and canine ventricular myocytes were studied with the whole cell patch clamp technique. In order to maximize our chances to observe  $i_f$ , cAMP (0.2mM) was added to the pipette solution, and isoproterenol (8μM) and BaCl<sub>2</sub> (8mM) were added to the bathing Tyrode. In both preparations we found a time dependent inward current activated by hyperpolarization, which is reversibly blocked by 4mM CsCl<sub>2</sub>. The activation threshold for this current is extremely negative (-148mV, n=12 in the guinea pig ventricular myocyte, -129mV, n=18 in the canine ventricular myocyte). This current reversed at -41mV in 5.4mM [K]<sub>o</sub> and normal [Na]<sub>o</sub> and the reversal potential showed selectivity to changes in either [K]<sub>o</sub> or [Na]<sub>o</sub>. This negative activation threshold was unlikely to be entirely due to the dissociation procedure since canine Purkinje myocytes had an activation threshold of -89mV, n=10 under the same recording conditions. As a final control we also recorded the  $i_f$  current in the canine ventricular myocytes in the absence of added cAMP to the pipette solution, and in the absence of isoproterenol in the perfusate. Although its activation threshold was 8mV more negative, it was still present. We believe that the presence of  $i_f$  in ventricular myocytes is an important clue to the differentiation of non-pacing regions in the heart and might be arrhythmogenic under pathologic conditions. Supported by grants HL20558, HL28958 and HL43731.

## Tu-Pos440

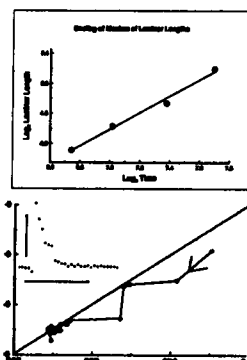
ALPHA-2 ADRENERGIC-MEDIATED ELECTROPHYSIOLOGIC EFFECTS IN ISOLATED CANINE PURKINJE FIBERS ((Ricardo A. Samson, Erwin F. Shibata, and Hon-Chi Lee)) University of Iowa, Iowa City, IA 52242

Alpha-2 adrenergic effects on the electrophysiological properties of the heart have not been previously characterized. Using standard microelectrode techniques, we studied the effects of yohimbine (Yo, 0.1 μM), a selective α<sub>2</sub> antagonist on action potential duration (APD) in isolated canine Purkinje fibers superfused with Tyrode's buffer at 37°C and paced at 2 Hz. In the presence of norepinephrine (NE, 0.5 μM) and propranolol (P, 0.5 μM), APD50 and APD90 were lengthened from 160.9±7.6 and 227.3±7.0 ms (mean±SE, n=6) at baseline to 174.7±5.5 and 241.6±8.9 ms respectively (p<0.05). NE+P+Yo decreased APD50 and APD90 to 165.1±4.9 and 228.1±7.6 ms respectively (p<0.05 vs NE+P). Yo alone did not have significant effects on APD50 or APD90. Resting membrane potential was -91.6±2.2 mV and did not vary significantly between interventions. Similar interventions in canine ventricular myocardium produced no α<sub>2</sub> specific electrophysiological effects. After incubation of Purkinje fibers with pertussis toxin (1 μg/ml) at 37°C for 6 hours, Yo no longer could reverse the effects of NE+P on action potential duration, while prazosin (0.1 μM), a selective α<sub>1</sub> antagonist, produced significant suppression of the NE+P effects. These results suggest that α<sub>2</sub> receptors are present on canine Purkinje fibers and are coupled to a pertussis toxin-sensitive G-protein. Stimulation of α<sub>2</sub> receptors results in significant prolongation of Purkinje fiber action potential and refractoriness.

## Tu-Pos442

TYPE I INTERMITTENCY IN THE RHYTHM OF A HUMAN HEART. ((D.F. Scollan, J.J. Dornig, Rizwan-uddin, J.R. Moorman)) University of Virginia, Charlottesville, VA.

We are analyzing low dimensional deterministic dynamics in the rhythm of a newborn infant who, after heart transplantation, was found to have two interacting atrial pacemaking sites. We here demonstrate type I intermittency, an archetypal form of chaos. As a slowly varying parameter of the system changes (following an inverse tangent bifurcation), epochs of a steady signal (here, constant RR intervals) punctuate the apparently random behavior and become more frequent. The time between the apparently random epochs, or *laminar lengths*, become longer. In a deterministic system, a plot of maximum laminar lengths as a function of the parameter has a power law relationship. A segment of the data was suggestive of intermittency, because areas of noisy bursting of RR intervals became less frequent and were separated by longer laminar lengths until constant RR intervals prevailed. The top figure is a log-log plot of maximum laminar lengths of constant RR interval epochs within four non-overlapping 400 sec windows as a function of time. The straight line is length = time<sup>2</sup>, and fits the data well. Intermittency can be characterized using a plot of RR<sub>n+1</sub> as a function of RR<sub>n</sub> (bottom). As successive points approach the diagonal, they become almost trapped, a characteristic of type I intermittency. This evidence strongly suggests that the dynamics are deterministic chaos.



## Tu-Pos439

NPY DECREASES AND VIP INCREASES THE PACEMAKER CURRENT  $i_f$  IN CANINE PURKINJE FIBERS. ((F. Chang and I.S. Cohen)) Dept. of Physiology & Biophysics, HSC, SUNY at Stony Brook, NY 11794-8661. (Spon. by P. Brink)

We studied canine cardiac Purkinje fibers with the two microelectrode voltage clamp technique. The bathing Tyrode contained 4mM BaCl<sub>2</sub> to block background K<sup>+</sup> permeability and eliminate extracellular [K<sup>+</sup>] fluctuations. We elicited the pacemaker current,  $i_f$ , by hyperpolarizations from a holding potential of -50mV to test potentials from -80 to -100mV. NPY reversibly decreased  $i_f$  while VIP reversibly increased  $i_f$  with this protocol. To determine whether these changes were alterations in conductance or shifts in activation we employed a two pulse protocol (Chang et al., Circ. Res., 1990, 66:633-637). The results of this protocol suggest that NPY shifts  $i_f$  activation in the negative direction and VIP shifts  $i_f$  activation in the positive direction on the voltage axis with no change in maximal  $i_f$  conductance. These actions of NPY and VIP on  $i_f$  activation were reversibly blocked by their specific NPY and VIP receptor antagonists. VIP and NPY are colocalized in cardiac parasympathetic and sympathetic nerve endings respectively. Given this localization these results suggest a potential role for these neuropeptides in controlling cardiac pacemaker current and consequently heart rate. Supported by grants HL20558, HL28958 and HL43731.

## Tu-Pos441

A NEW TECHNIQUE TO MAP REFRACTORY PERIODS IN HEART. ((I.R. Efimov, D.T. Huang, J.M. Rendt and G. Salama)) Department of Physiology, Sch. of Med., University of Pittsburgh, Pittsburgh, PA 15261

Abrupt variations of refractory period (RP) across the myocardium have been invoked as a mechanism to explain the genesis of most arrhythmias. Yet surface electrode(s) combined extra-stimuli techniques have failed to generate reproducible maps of RPs.

Guinea pigs hearts were stained with the voltage-sensitive dye di-4-ANEPPS and imaged on a photodiode array to simultaneously record optical action potentials (APs) from 124 sites. We developed a signal processing technique to map the spread of activation and recovery from fluorescence (F) APs. AP duration was taken as the time interval between depolarization (dF/dt<sub>max</sub>) and the time-point when the AP returns to baseline or some percent thereof. But drifting base-lines and motion artifacts often interfered with the detection of repolarization phases making this approach unsuitable. We have found that the second derivatives of APs contain easily-detectable, stable local maxima (d<sup>2</sup>V/dt<sup>2</sup>)<sub>max</sub> that correspond to inflection time-points between the steepest portion of repolarization and the base-line. With extra-stimuli techniques applied to simulation of Beeler-Reuter model and experiments with guinea pig hearts, we can show that (d<sup>2</sup>V/dt<sup>2</sup>)<sub>max</sub> corresponds to the end of the relative RP. Imaging combined with signal detection of d<sup>2</sup>F/dt<sup>2</sup><sub>max</sub> with voltage-sensitive dyes provide a direct, convenient and accurate technique to study the dynamics of RP & APD in normal and arrhythmic conditions.

## Tu-Pos443

MUSCARINIC RECEPTOR MEDIATED STIMULATION OF THE HEARTBEAT IN CULTURED HEART CELLS. ((H. M. Colcraft, V. K. Sharma, D. J. Williford, L. J. Field, W. C. Claycomb, and S-S. Sheu)) Department of Pharmacology, University of Rochester, 601 Elmwood Avenue, Rochester, NY 14642.

It has become apparent that aside from the pertussis toxin (PTX)-sensitive inhibitory effects of cholinergic agonist application and vagal stimulation on the heartbeat, there is also a PTX-insensitive stimulatory pathway present which is often unmasked when the inhibitory pathway is blocked. The cellular and molecular mechanisms for these two antagonistic responses are still unclear. The purpose of the present study was to develop a single cell model that would allow us to elucidate the mechanisms by which cholinergic agonists evoke positive chronotropic and inotropic responses. To this end we have studied the effects of carbachol (CCh) (50 nM - 300 μM) on Ca<sup>2+</sup> transients of spontaneously beating cultured neonatal rat ventricular myocytes (NRVMs), and the recently described atrial cardiomyocyte cell line, AT-1 cells, developed from transgenic mice. Briefly, cells loaded with fura-2 were mounted in a tissue chamber on the stage of a Nikon Diaphot inverted microscope equipped for epifluorescence. Cells were excited at 380 nm and 340 nm wavelength light from a Xenon-arc UV lamp and the emitted signal at 510 nm counted in a photomultiplier tube. The resulting counts, after digitization, were plotted on a computer screen in real time to yield Ca<sup>2+</sup> transients. In NRVMs, CCh evoked a dose-dependent, reversible decrease in heart rate. These inhibitory effects of CCh were blocked by atropine and the m<sub>2</sub> antagonist, methoctramine. In cells pretreated with PTX (1 μg/ml for 18-24 hrs) to block the m<sub>2</sub>-mediated inhibitory pathway, CCh (300 μM) elicited a reversible positive chronotropic response which was also blocked by atropine. Similarly, in AT-1 cells, CCh induced a dose-dependent, reversible decrease in heart rate which is blocked by methoctramine. However, in AT-1 cells pretreated with PTX, we have been unable to detect any increase in heart rate in response to CCh. We conclude that these two cultured heart preparations provide us with a dynamic *in vitro* system that enables the further investigation of the mechanisms by which cholinergic agonists stimulate the heartbeat.

## Tu-Pos444

## IS PENTOBARBITAL AN APPROPRIATE ANESTHETIC FOR ELECTROPHYSIOLOGICAL STUDIES?

((B. Fermini, Z. Wang, C. Matthews, G. Nicol, S. Nattel)) Montreal Heart Institute, Montreal, Quebec, Canada H1T 1C8.

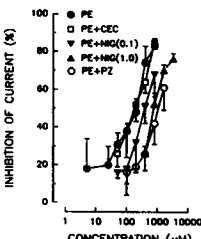
Pentobarbital (PB) is widely used for *in vivo* studies of cardiac electrophysiology, arrhythmia mechanisms and antiarrhythmic drug actions. Yet, PB has been shown to suppress ventricular function, increase action potential duration (APD), and reduce  $V_{max}$  in various cardiac preparations. These actions suggest that PB may have intrinsic electrophysiological effects. We used pharmacological as well as microelectrode and patch clamp techniques to study the effects of PB on the properties of dog and guinea pig ventricular muscle and isolated myocytes from rabbit ventricle. We studied PB washout (by HPLC) from ventricle preparations taken from dogs anesthetized with PB (30 mg/kg). PB concentrations (conc) in myocardium averaged  $43 \pm 2$  mg/kg initially (plasma conc  $34 \pm 1$ ) and showed a first order washout with a  $t_{1/2}$  of  $1.2 \pm 1$  hr. PB (5-25 mg/L) caused conc-related decreases in resting potential (RP  $-97 \pm 3$  mV, control;  $-75 \pm 5$  mV PB 25 mg/L,  $P < 0.01$ ), enhanced abnormal automaticity in canine Purkinje fibers, and increased APD in guinea pig ventricular muscle. In isolated rabbit ventricular myocytes, PB produced a conc-dependent inhibition of the inward rectifier current ( $I_{K1}$ ) at all voltages examined (-90 to -10 mV). When studied at -90 mV, the inhibition of steady-state  $I_{K1}$  by PB averaged  $33 \pm 6$  and  $48 \pm 5\%$  ( $P < 0.05$ ,  $n=5$ ) for 25 and 50 mg/L, respectively. **Conclusion:** 1) Slow PB washout emphasizes caution for its use as anesthetic agent for electrophysiological studies, and for the interpretation of studies using such compounds. 2) PB has significant intrinsic electrophysiological actions at therapeutic concentrations. 3) PB actions appear to be mediated mainly through inhibition of the inward rectifier current ( $I_{K1}$ ).

## Tu-Pos446

## ALPHA ADRENERGIC REGULATION OF BACKGROUND CL-CURRENT IN RABBIT ATRIAL MYOCYTES.

((D. Duan, B. Fermini, S. Nattel)) Montreal Heart Institute, Montreal, Quebec, Canada H1T 1C8.

We have shown that the sustained outward current after  $I_{Na}$  inactivation in rabbit atrial myocytes is due to a background chloride current ( $I_{Cl}$ ). Since  $\alpha$ -adrenoceptor stimulation prolongs action potential duration in rabbit atrial cells, we examined the possible role of  $\alpha$ -adrenergic modulation of Cl-current. Whole-cell patch clamp technique was used to study rabbit atrial myocytes at  $30^\circ\text{C}$  with  $\text{Ca}^{2+}$  substituted for  $\text{K}^+$ ,  $100 \mu\text{M}$   $\text{Cd}^{2+}$  to suppress  $I_{Ca}$ ,  $500 \mu\text{M}$   $\text{Ba}^{2+}$  to block  $I_{K1}$ , and a holding potential of -40 mV to inactivate  $I_{Na}$ . The current-voltage relation for  $I_{Cl}$  was studied by 300 ms step to voltages between -100 and +80 mV. Propranolol (1  $\mu\text{M}$ ) was used to block  $\beta$ -adrenergic effects. The  $\alpha$ -adrenergic agonist phenylephrine (PE) inhibited  $I_{Cl}$  in a concentration-dependent fashion (figure), an action that was blocked by the  $\alpha_1$  receptor antagonist, prazosin (PZ, 2  $\mu\text{M}$ ). The  $\alpha_{1B}$  receptor antagonist chloroethylclonidine (CEC, 100  $\mu\text{M}$ ) did not alter the response to PE, but the  $\alpha_{1A}$  antagonist nigludipine (NIG) inhibited the PE response in a concentration-dependent way. The potency of NIG was of the same order as that of PZ.  $I_{Cl}$  was observed in the absence of cell swelling and agents that generate cyclic AMP, and was blocked by organic Cl-transport blockers (SITS and DIDS). **Conclusions:** 1) Activation of  $\alpha_{1A}$  adrenoceptors inhibits  $I_{Cl}$  in rabbit atrial myocytes. 2)  $\alpha$ -adrenoceptor modulation of  $I_{Cl}$  is a novel and potentially important physiological mechanism.

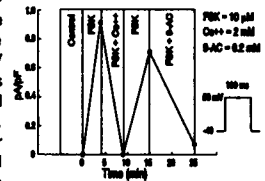


## Tu-Pos445

DIVALENT CATIONS CAN INHIBIT ISOPROTERENOL (ISO) -INDUCED CHLORIDE CURRENT ( $I_{Cl}$ ) IN FELINE VENTRICULAR MYOCYTES

((Ke Zhang, Shin-ichi Kouri, J. A. Wasserstrom and R. E. Ten Eick)) Northwestern University, Chicago, IL 60611. (Spon. by A. Vites)

Divalent cations can modulate the conductance of a number of types of ion channels in heart and other excitable membranes. We have examined the hypothesis that divalent cations can alter the whole-cell-conductance for the ISO-induced  $I_{Cl}$  in isolated feline ventricular myocytes. The findings indicate that 1-2 mM  $\text{Co}^{2+}$ ,  $\text{Zn}^{2+}$ ,  $\text{Mn}^{2+}$ ,  $\text{Cd}^{2+}$  and even  $\text{Mg}^{2+}$  can at least partially inhibit ISO- or forskolin (FSK)-induced, 9-anthracene carboxylic acid (9-AC) sensitive  $I_{Cl}$ . The current-voltage curve was shifted  $\sim 10$  mV by  $\text{Co}^{2+}$ . Even when this shift was accounted for, the current was reduced reversibly in the presence of 1-2 mM  $\text{Co}^{2+}$ . The findings suggest that  $\text{Co}^{2+}$  and other divalents can block the ISO-induced  $I_{Cl}$  and that the block is not due to a shift in the voltage dependence of the activation parameters for the current. Because solutions normally used for electrophysiological studies on cardiac myocytes ordinarily contain  $\text{Ca}^{2+}$  and  $\text{Mg}^{2+}$  and occasionally may contain divalents (e.g.  $\text{Cd}^{2+}$  and  $\text{Co}^{2+}$ ) intended to block  $I_{Ca}$ , failure to find ISO-induced  $I_{Cl}$  should not be interpreted necessarily to mean that Cl<sup>-</sup> channels are absent or non-functional. The molecular basis for this ion-channel interaction remains to be elucidated.



## Tu-Pos447

## PHARMACOLOGICAL INHIBITION OF THE SWELLING-INDUCED CHLORIDE-SENSITIVE CURRENT IN DOG ATRIAL CELLS.

((S. Sorota)) Columbia University, New York, New York.

Cell swelling activates an outwardly rectifying chloride-sensitive current ( $I_{Cl-SWELL}$ ) in dog atrial cells (Sorota, *Circ. Res.* 70:679-687, 1992). This current might become functionally significant under pathological conditions that are associated with cell swelling, such as ischemia. Identifying effective and specific blockers would aid in defining the consequences of  $I_{Cl-SWELL}$  activation. Putative chloride channel blockers were examined for their ability to block  $I_{Cl-SWELL}$  in dog atrial cells under whole cell patch clamp conditions. Niflumic acid (100  $\mu\text{M}$ ), nitro phenylpropylamino benzoate (10  $\mu\text{M}$ ; NPPB), isomerically pure indanyloxyacetic acid (100  $\mu\text{M}$ ; IAA-94), and racemic indanyloxysulfonic acid (200  $\mu\text{M}$ ; ISA-94/95) could all completely inhibit  $I_{Cl-SWELL}$ . The effects of ISA-94/95 and IAA-94 were slow in onset and occurred with a variable time course from cell to cell (9 to 20 minutes for complete inhibition). Anthracene-9-carboxylic acid (1 mM) inhibited  $I_{Cl-SWELL}$  by  $\sim 67\%$ .  $I_{Cl-SWELL}$  recovered on washout of each compound. Disothiocyanatostilbene-disulfonic acid (DIDS), at 100  $\mu\text{M}$  blocked the current in a voltage-dependent manner. DIDS blocked outward current more effectively than inward current. The complete blockers had nonspecific actions. NPPB activated the ATP-inhibitable potassium current. NPPB also depolarized the resting potential in the presence of 10  $\mu\text{M}$  glybenclamide. ISA-94/95 and IAA-94 depressed plateau amplitude but had no effect on resting potential. Niflumic acid partially inhibited the L-type calcium current but did not affect steady state currents. Niflumic acid, ISA-94/95 and IAA-94 might be useful for functional studies on the effect of  $I_{Cl-SWELL}$  on resting potential. None are specific enough for studies on the effects of  $I_{Cl-SWELL}$  on action potential parameters.

## RHODOPSIN AND BACTERIORHODOPSIN

## Tu-Pos448

CONTROLLING THE SCHIFF BASE  $pK_a$  OF VISUAL PIGMENTS BY SYNTHETIC RETINAL ANALOGS

((Jie Liang<sup>1</sup>, Gali Steinberg<sup>2</sup>, Mordechai Sheves<sup>2</sup> and Thomas G. Ebrey<sup>1</sup>))

<sup>1</sup>Dept. of Physiology and Biophysics, University of Illinois at Urbana-Champaign, Urbana, IL 61801. <sup>2</sup>Dept. of Organic Chemistry, The Weizmann Institute of Science, Rehovot, 76100, Israel

In visual pigments, meta II intermediate is responsible for activation of transducin. Its formation is accompanied by the deprotonation of the Schiff base linkage. Understanding of the Schiff base  $pK_a$  is thus crucial to clarify the mechanism of visual pigments function. In bacteriorhodopsin, it has been demonstrated that the artificial pigment derived from 13CF<sub>3</sub> retinal analog reduces the Schiff base  $pK_a$  from 13.3 to 8.0. 14F-9-*cis* retinal is another retinal analog bearing a strong electron withdrawing group. In solution, the protonated Schiff base  $pK_a$  of this chromophore is reduced by 2.2 units relative to 9-*cis* retinal protonated Schiff base. Recent studies using artificial bovine rhodopsin pigments pointed to the possibility that the Schiff base  $pK_a$  of bovine rhodopsin is above 17. In this work we studied the octopus photoreceptor microvilli and gecko cone pigment P521. Both native pigments show a blue shifted spectral change when the pH is raised to 10.0. We found that the artificial octopus pigment in microvilli derived from 14-F-9-*cis* retinal has a significant change in  $pK_a$  of such spectral change, indicating that the titration observed in the native system is associated with Schiff base titration. Results with the artificial gecko cone pigment P521 will also be discussed.

## Tu-Pos449

## EARLY RETINAL SCHIFF'S BASE DEPROTONATION IN RHODOPSIN.

((T. E. Thorgeirsson, J. W. Lewis, S. E. Wallace-Williams, D. S. Klier)) University of California Santa Cruz, Santa Cruz, CA 95064.

Photolysis of sonicated disk membrane samples from bovine retinas was used to study the photointermediates of rhodopsin. Metarhodopsin II is generally believed to be the activated form of rhodopsin that interacts with transducin. Metarhodopsin II is characterized by an unprotonated Schiff's base, and its formation is accompanied by a large increase in volume and net proton uptake. According to the traditional scheme,  $\dots \text{Lumi} \rightarrow \text{Meta I} \rightleftharpoons \text{Meta II}$ , all these changes take place in a single concerted reaction during the transition from Meta I to Meta II.

To study the formation kinetics of Metarhodopsin II in detail, transient absorbance measurements were made using multichannel detection with microsecond time resolution following photolysis with a 7 ns (477 nm) laser pulse. Spectra were collected at 5 different temperatures between 15 and 35  $^\circ\text{C}$ , and analyzed using singular value decomposition and multiexponential fitting.

The traditional mechanism cannot adequately account for the observations. To explain the results within the framework of first-order kinetics it is necessary to modify the traditional scheme by including a new intermediate that has a similar absorption spectrum as does Metarhodopsin II, but is formed much faster. This leads to the general kinetic scheme:

$\dots \text{Lumi} \rightarrow [X_{380} \rightleftharpoons \text{Meta I}] \rightleftharpoons \text{Meta II}$   
where the relative amount of the new intermediate,  $X_{380}$ , increases with temperature. Several kinetic schemes that include this new intermediate (branched, sequential, etc.) are presented and discussed.

## Tu-P0450

**STERIC CONSTRAINTS IN THE SENSORY RHODOPSIN-I RETINAL BINDING POCKET.** ((Bing Yan<sup>1</sup>, Aihua Xie<sup>2</sup>, G. Ulrich Nienhaus<sup>2</sup>, Shaojiang Lin<sup>3</sup> & John L. Spudich<sup>1</sup>) <sup>1</sup>Univ. of Texas Medical School, Houston, TX 77030; <sup>2</sup>Univ. of Illinois at Urbana-Champaign, Urbana, IL 61801; <sup>3</sup>Rice Univ., Houston, TX 77251.

Molecular interactions and steric constraints within the retinal binding pocket of sensory rhodopsin-I (SR-I) were investigated by low temperature flash photolysis of SR-I and by studies of SR-I pigments made by replacing retinal with retinal analogs in SR-I. SR-I-K intermediate formation depends greatly on temperature. Below 220K, K formation decreases and is totally blocked at 100K indicating a very tight retinal pocket, while in BR K formation is not affected in this temperature range. K formation is also blocked at room temperature in an analog SR-I pigment formed with 13-desmethyl retinal. Another analog SR-I reconstituted with 13-ethyl retinal exhibits a 30-fold slower binding rate and an altered photochemical reaction. These results indicate that one of the tight steric interactions is at the retinal 13-methyl, in accordance with the steric requirement for SR-I activation identified previously (Yan et al., PNAS 88:9412-9416, 1991). This interpretation is supported by a structural model of SR-I constructed assuming homology with BR and by energy minimization calculations. Different from BR, the model predicts a steric interaction also near the 6-ionone ring introduced by His135 in SR-I at the homologous position for Met145 in BR. Consistent with this model, an analog SR-I formed by a retinal analog without the ring lost both photochemical and physiological activities, while the corresponding BR analog was previously shown to be functional. Photoisomerization of retinal within the protein interior alters protein surface conformations as detected by the viscosity dependence in the latter half of the SR-I photocycle.

## Tu-P0452

**FLUORESCENCE TRANSFER IN IRBP.**

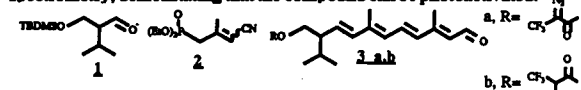
((E.S.Hazard<sup>1</sup>, R.K.Crouch<sup>1</sup>, B.Wiggert<sup>2</sup> and G. Chader<sup>2</sup>) <sup>1</sup>Medical University of South Carolina, Charleston SC 29425 and <sup>2</sup>NEI, NIH, Bethesda MD 20892.

Fluorescence transfer from aromatic residues to bound fluorescent ligands has been a powerful tool for studies in various retinoid binding proteins. Adler et al., J.BIOL.CHEM. 260:4850,1985 provided the first comprehensive biophysical analysis of IRBP but reported no detectable fluorescence energy transfer. Recently, Wiggert (pers. comm.) has reported that bound fluorescent-labeled fatty acids are excited via energy transfer from the protein fluorophores. Hazard et al., BIOPHYS. J. 59:329A, 1991 have presented evidence for a competition between fatty acids and all-trans retinol (ATR) for one class of binding sites on IRBP. We report here that fluorescence transfer is present for all levels of bound ATR. Excitation spectra (emission @ 470nm) show peaks at 340nm AND 280nm. Emission spectra (excitation at 285nm) show protein fluorescence at 334nm as well as at 470nm. The peak at 334nm decreases with incremental addition of ATR while the peak at 470nm increases. Protein fluorescence CAN provide useful information about the ATR binding site(s) of IRBP. Supported by an MUSC Intramural Grant and NIH EY04939 and HL07260.

## Tu-P0454

**A BACTERIORHODOPSIN ANALOGUE PIGMENT FORMED WITH A PHOTOAFFINITY LABELED ACYCLIC RETINAL.** ((J. Oatla, D. Knapp, R. K.Crouch, R. Govindjee and T. G. Ebrey)) Medical University of South Carolina, Charleston, SC 29425 and University of Illinois at Urbana-Champaign, Urbana, IL 61801.

The all-trans acyclic retinal 3a was synthesized from 1 and 2 via two Wadsworth Emmons coupling - DIBALH reduction cycles, followed by removal of the TBDMS group and esterification with the 3,3,3-trifluoro-2-diazopropionyl chloride. The structure was fully characterized by 400MHz NMR and mass spectrometry. Upon photolysis in cyclohexane, the crosslinked adduct 3b was produced, as shown by liquid secondary ion mass spectrometry, demonstrating that the compound can be photoactivated.



A stable pigment was formed in good yield with the apoprotein of bacteriorhodopsin with an initial  $\lambda_{max}$  of 448nm. A slight shift to 450nm occurred on light exposure with a further, irreversible shift to 453nm on dark adaptation. The acyclic retinal is in the native binding site as shown by its slow displacement by all-trans retinal to form a 560nm pigment. The pigment shows some photochemistry with a blue-shifted M intermediate (double peak at 345/360nm). Protein coupling experiments will be discussed. Supported by NIH grants EY04939 and EY08239 and Research to Prevent Blindness.

## Tu-P0451

**REDUCED ACTIVITY OF 9-DESMETHYL RHODOPSIN IN LIGHT-DEPENDENT PHOSPHORYLATION.** ((D.F. Morrison<sup>1</sup>, T.D. Ting<sup>2</sup>, Y.K. Ho<sup>2</sup>, R.K. Crouch<sup>3</sup>, D.W. Corson<sup>4</sup> & D.R. Pepperberg<sup>1</sup>) Depts. of <sup>1</sup>Ophthalmology & Visual Sciences and <sup>2</sup>Biochemistry, Univ. of Illinois, Chicago, IL 60612; and Depts. of <sup>3</sup>Ophthalmology & <sup>4</sup>Pathology, Medical University of South Carolina, Charleston, SC 29425

The 11-cis isomer of 9-desmethylretinal combines with opsin to form a bleachable pigment (9-desmethyl rhodopsin). Previous studies have shown that the photoactivated form of this pigment (9-desmethyl R\*) exhibits low activity in transducin activation<sup>1</sup> and mediates a photocurrent response of abnormally long lifetime<sup>2</sup>. We examined the ability of 9-desmethyl R\* to function as a substrate in the enzymatic phosphorylation reaction that supports visual pigment deactivation *in vivo*. Bleached bovine ROS membranes were incubated with 11-cis retinal or 11-cis-9-desmethylretinal. Light-dependent phosphorylation of regenerated rhodopsin and 9-desmethyl rhodopsin was analyzed in assays employing ATP- $\gamma$ -<sup>32</sup>P and bovine rhodopsin kinase. Quantitation (SDS-PAGE) of <sup>32</sup>P-opsin product indicated phosphorylation of the 9-desmethyl R\* to be less than half that of R\*. The data suggest that the electrophysiological finding<sup>2</sup> reflects the sluggish activity of 9-desmethyl R\* as a substrate for phosphorylation. <sup>1</sup>Ganter et al. *Biochem.* 28:5954 (1989). <sup>2</sup>Corson et al., *Biophys. J.* 61:A9 (1992).

Supported by Research to Prevent Blindness, Inc. and NIH Grants EY06368, EY05494, EY01792, EY04939, EY07543 & EY05788.

## Tu-P0453

**PREPARATION, PURIFICATION AND CHARACTERIZATION OF RHODOPSIN CONTAINING A FLUORESCENT DERIVATIVE OF PALMITATE.** ((Susan J. Moench, David H. Stewart, Cristina E. Terry and T. Gregory Dewey)) Department of Chemistry, University of Denver, Denver, CO 80208

Two tandem cysteine residues in the carboxyl terminal region of rhodopsin have been shown to be palmitoylated (1). We have incorporated a fluorescent analogue of palmitate into the protein in high yield (>40%) through pre-treatment of bovine rod outer segments with hydroxylamine and subsequent incubation with 16-(9-anthroyloxy) hexadecanoyl coenzyme A ester. Covalent incorporation of probe into protein was demonstrated by SDS PAGE. Proteolytic digestion of labeled rhodopsin in the disc membrane with papain and thermolysin verified the C-terminal location of the probe. Labeled unbleached rhodopsin was purified from excess probe by chromatography over hydroxyapatite and Concavalin-A agarose and reconstituted into dimyristoyl phosphatidyl choline vesicles. Preliminary fluorescence quenching, polarization and energy transfer studies have revealed that the fluorescence probe is rigidly held in close proximity to the retinal and partially accessible to lipophilic quenchers.

(1) Ovchinnikov, Y.A. et al. *FEBS Lett.* (1986) 230, 1-5.

## Tu-P0455

**RAMAN SPECTROSCOPIC STUDY OF BACTERIORHODOPSIN AT HIGH PRESSURE.** ((L. Bradley II, Y. Dai, A. Schulte, C. Williams)) Department of Physics and Center for Research in Electro-Optics and Lasers, University of Central Florida, Orlando, FL 32817.

We have measured the effect of high pressure on the Raman spectrum of bacteriorhodopsin in solution. Using excitation in the near infrared (840 nm), we monitor the isomeric ratio between all-trans and 13-cis retinal in dark-adapted bacteriorhodopsin. The relative intensity of the ethylenic bands provides direct spectroscopic evidence that the fraction of all-trans isomers decreases with increasing pressure. We will also present Raman spectra of photocycle intermediates as a function of pressure and temperature.

## Tu-Poe456

PROTON DIFFUSION STUDIED BY SOLID STATE 2D AND 3D MAS <sup>1</sup>H-NMR.

((L. Zheng, K. W. Fishbein, R. G. Griffin and J. Herzfeld))  
Department of Chemistry, Brandeis University, Waltham, MA  
02254-9110; Francis Bitter National Magnet Laboratory and  
Department of Chemistry, MIT, Cambridge, MA 02139-4307.

Two dimensional and three dimensional solid state MAS proton NMR techniques are being developed to study proton diffusion in bacteriorhodopsin. High resolution solid state <sup>1</sup>H NMR spectra were obtained by combining deuterium spin-dilution (proton:deuterium ~ 5:95) and high-speed magic angle spinning (MAS ~ 10kHz) using a 400 MHz home-built spectrometer. Reverse cross-polarization of protons from deuterons was used when necessary to reduce the proton spin-lattice relaxation time in these magnetically dilute samples. 2D <sup>1</sup>H NOESY spectra and 3D <sup>1</sup>H NOESY-NOESY spectra were used to follow proton exchange. Rapid proton exchange observed in model compounds by these means was linked to the strength of hydrogen bonds. Proton exchange was also observed in lyophilized purple membranes from the Halobacterium halobium on similar time scales.

## Tu-Poe458

## THE ROLES OF ASP85 AND ARG82 IN THE CATALYSIS OF CHROMOPHORE ISOMERIZATION AND PROTON RELEASE IN BACTERIORHODOPSIN. ((S. Balashov, R. Govindjee, M. Kono, T. G. Ebrey, Y. Feng\*, R. K. Crouch\*, and D. R. Menick\*)) Center for Biophysics and Dept. of Cell and Struct. Biology, UIUC, Urbana, IL 61801, and \* Medical Univ. of S. Carolina, Charleston, SC 29425.

The study of R82A mutant expressed in *H. halobium* led to the following conclusions: 1) Dark adaptation (spontaneous trans  $\leftrightarrow$  13-cis isomerization in bR) proceeds through the transient protonation of Asp85 (formation of a blue species). We have found that the strong pH dependence of the dark adaptation rate shifted from the pH range 3-6 in the WT to pH 8 in the mutant. In this region the rate decreases 10 times per pH unit. This shift correlates with the shift in the pK of the purple to blue transition (pK of Asp85) from 2.8 in the WT to 7.5 in R82A (in 150 mM KCl). This correlation indicates that transient protonation of Asp85 catalyzes the trans  $\leftrightarrow$  cis isomerization in bR. 2) Arg82 is associated with the proton release process in bR. Proton release is delayed ~30 times in R82A membranes as compared to that in the WT (~30 ms versus 1 ms, at pH 7.2, 2M NaCl), while proton uptake is not affected. 3) Substitution of positively charged Arg82 by neutral Ala dramatically affects not only the pK of Asp85 but also the kinetics of M formation and Schiff base deprotonation, apparently due to electrostatic interaction. The rise time of the formation of the M intermediate drastically decreased in the mutant (1  $\mu$ s in R82A vs 100  $\mu$ s in the WT at pH7) and does not depend on the pH (while in the WT it changes from 100  $\mu$ s to 6  $\mu$ s when pH is increased to 10). This suggests that the loss of a positive charge in the active site of bR is responsible for the change in kinetics at alkaline pH (fast M formation, decrease in the rate of dark adaptation and alteration of proton release pathway).

## Tu-Poe460

## SPECTRAL AND PHOTOCHEMICAL PROPERTIES OF Y57N MUTANT OF BACTERIORHODOPSIN. ((R. Govindjee, M. Kono, E. Lukashov, S. Balashov, T. G. Ebrey, J. Soppa\*, J. Tlitor\*, and D. Oesterhelt\*)) Center for Biophysics and Dept. of Cell and Structural Biology, University of Illinois, Urbana-Champaign IL 61801, USA and \*Max-Planck Institut für Biochemie, Martinsried, Federal Republic of Germany.

Tyrosine 57 is conserved in the structure of bacteriorhodopsin, halorhodopsin and sensory rhodopsin. In bR it is located near Asp212 and the Schiff base. In order to clarify the functional role of Tyr57, we have studied the Y57N mutant obtained in *H. halobium* cells. The main findings are: 1) Absorbance changes in the near UV region (240 nm) due to increase of pH indicate that the tyrosine residue, deprotonating in the WT with pK ~9, is missing in the mutant. This suggests that Tyr57 deprotonates at pH 9-10 in bR. 2) In contrast to the WT, light adaptation induces photoisomerization in both directions in Y57N; that is not only from 13-cis to trans but also from trans to 13-cis, producing a mixture of these isomers. The ratio depends on the wavelength of illumination. The absorption maximum of all-trans-bR of Y57N (562 nm) is blue shifted 6 nm as compared to the WT. 3) The flash induced concentration of M (absorption maximum is at 411±2 nm) is very small at neutral pH (less than 3%), it increases to 20% that of the WT at higher pH values and salt concentrations. The pH dependence of the light induced absorption increase at 410 nm has a titration-like curve with pK 8.5 (in 2 M salt). This is similar to the pH dependence of the fraction of fast forming M in the WT. One may assume that the amino acid controlling the rate of M formation in bR is present in the mutant. 4) The rise time of M is much slower in Y57N compared to the WT (60  $\mu$ s vs. 6  $\mu$ s at pH 10). 5) The lifetimes of L, M and apparently N intermediates are unusually long in Y57N (~500 ms). These data indicate that Tyr57 is involved in catalyzing the formation of M intermediate and subsequent steps of the photocycle.

## Tu-Poe457

SOLID STATE <sup>13</sup>C NMR ROTATIONAL RESONANCE DISTANCE MEASUREMENT IN THE M PHOTOINTERMEDIATE OF BACTERIORHODOPSIN: DETERMINATION OF THE CONFIGURATION ABOUT THE SCHIFF BASE

((K.V.Lakshmi\*, M. Auger\*, J. Raap\*, J. Lugtenburg\*, R.G.Griffin\* and J.Herzfeld\*)) \*Department of Chemistry, Brandeis University, Waltham, MA 02254-9110, \*Francis Bitter National Magnet Laboratory and \*Department of Chemistry, MIT, Cambridge, MA 02139, \*Department of Chemistry, University of Leiden, The Netherlands.

Previous solid state <sup>13</sup>C NMR studies of bacteriorhodopsin (bR) have used the chemical shifts of [14-<sup>13</sup>C] retinal and [ε-<sup>13</sup>C] lysine<sub>216</sub> resonances to deduce the C=N configuration of the retinal-lysine Schiff base (SB) linkage in the photocycle intermediates of bR. The configuration about the Schiff base linkage in the dark- and light-adapted states in the photocycle has been confirmed by measuring the 14-<sup>13</sup>C-retinal to ε-<sup>13</sup>C-lysine<sub>216</sub> distance using rotationally driven magnetization exchange. In the present study, we apply the same rotational resonance technique to the M photointermediate of bacteriorhodopsin.

The M photointermediate was cryogenically trapped in 0.3M guanidine-HCl at pH 10.0. The [ε-<sup>13</sup>C]lysine<sub>216</sub> chemical shift of M at 60.1 ppm is upfield from the [14-<sup>13</sup>C] retinal chemical shift at 125.2 ppm and downfield from the 6 non-Schiff based lysines (at 40.0 ppm). The distance between the [ε-<sup>13</sup>C] lysine<sub>216</sub> and [14-<sup>13</sup>C] retinal atoms in the M intermediate was determined by simulating the magnetization transfer and found to be 3.9 ± 0.2 Å. We conclude that the M photointermediate contains a CN-anti Schiff base configuration.

## Tu-Poe459

## PHOTOCONVERSION OF THE N INTERMEDIATE OF BACTERIORHODOPSIN AT LOW TEMPERATURE. ((S. P. Balashov, E.S. Imasheva, and T. G. Ebrey)) Center for Biophysics and Dep. of Cell and Struct. Biol., Univ. of Illinois, Urbana, IL 61801.

The N intermediate of the bacteriorhodopsin photocycle can be accumulated and stabilized in aqueous suspensions of purple membrane by warming the M intermediate from -70°C to -30°C (pH 10, 0.2 M KCl) or by illumination of light adapted purple membrane at > 630 nm during cooling. Using the latter procedure it is possible to convert about 70% of bR into N. Photoconversion of N: 1) The N intermediate transforms into a bathoproduct K<sup>N</sup> with maximum absorbance at 600-605 nm upon illumination at 77K at 510 nm. K<sup>N</sup> can be photoreversed with illumination at > 650 nm. Illumination at longer wavelengths (> 680 nm) indicates that K<sup>N</sup> is a mixture of at least two species, K<sup>N</sup><sub>1</sub> and K<sup>N</sup><sub>2</sub>. 2) With high light intensity irradiation at 500-650 nm, N is transformed into a product, designated as P<sup>N</sup>, with an absorption maximum at 610 nm. Quantum yield of P<sup>N</sup> is at least 2 orders of magnitude less than that of K<sup>N</sup>. In contrast to K<sup>N</sup>, P<sup>N</sup> is not photoreversible. Only a fraction of N (~50%) can be converted into P<sup>N</sup>, which indicates that there are two pools of N, or two N intermediates in the photocycle, N<sub>1</sub> and N<sub>2</sub>. 3) At temperatures higher than -100°C K<sup>N</sup> transforms in the dark into a slightly blue shifted intermediate (absorption maximum at 585 nm, which can be considered as an L product of N, L<sup>N</sup>. Photochemically L<sup>N</sup> is very much like N. Under low light intensity irradiation at 510 nm it transforms into a bathoproduct (K<sup>L</sup>), which is similar to K<sup>N</sup>, but unlike K<sup>N</sup> it is stable at -60°C. Under high intensity irradiation L<sup>N</sup> converts into a nonphotoactive photoproduct P<sup>L</sup>, similar to P<sup>N</sup>. No significant amount of M or initial all-trans-bR was formed upon illumination of N at -60°C. Light apparently isomerizes the 13-cis chromophore of N into trans-configuration. However it does not cause drastic acceleration of initial bR formation, which indicates that conformational changes of the protein are the limiting steps in the N to bR conversion.

## Tu-Poe461

## REVERSAL OF PROTON RELEASE AND UPTAKE IN THE MUTANT R82A OF BACTERIORHODOPSIN

((U. Alexiev, P. Scherrer, H. Otto, M. P. Heyn, T. Marti\*, M. P. Krebs\*, R. Mollaghababa\*, H. G. Khorana\*)) Biophys. Group, Freie Univ. Berlin D-1000 Berlin 33, Germany, \*Dept. of Biology and Chemistry, M.I.T., Cambridge, Massachusetts 02139, USA

The rates of proton release and uptake in the R82A mutant of bacteriorhodopsin were measured in a) micelles of R82A (expressed in *E. coli*) with the pH-indicator fluorescein attached to G72C on the extracellular surface and with the bulk pH-indicator pyranine, b) patches of R82A (expressed in *H. halobium*) with pyranine at pH 7.6 and with the pH-indicator xylenol blue at pH 8.5. In all samples proton uptake preceded release, confirming the results of Otto et. al. (PNAS 87 (1990), 1018-1022). The time constants for release and uptake measured with pyranine were close together. In patches the release and the uptake times of approximately 7 and 4 ms may be correlated with the decay of O and the N to O transition respectively. The reversed order of release and uptake and the values of the time constants suggest a role for R82 in the proton release mechanism. The time constants measured with the surface dye were more widely separated (800 $\mu$ s/40 $\mu$ s). At pH 8.5 R82A is fully in its purple form and the times for release and uptake detected with xylenol blue were 10ms and 150  $\mu$ s, clearly separated. For R82A/G72C-AF in the pH range 6.7-7.6 (purple-blue transition) the amplitude of the proton signal was proportional to the amount of M.

**Tu-P0462****CHROMOPHORE MOVEMENT IN THE TRANSITION BETWEEN THE GROUND-STATE AND THE M-INTERMEDIATE OF BACTERIORHODOPSIN.**

((T. Haus, M.P. Heyn, G. Büldt and N.A. Dencher)) Freie Universität Berlin, D-1000 Berlin 33, Germany.

Chromophore movement in the transition between the light-adapted ground-state and the M-intermediate was studied by neutron diffraction of purple membranes regenerated with selectively deuterated retinals. In-plane neutron diffraction data were collected at 85°K in both states. The photocycle was slowed down by the addition of guanidine hydrochloride at alkaline pH. Within experimental error the position of the cyclohexene ring is the same in both states. With 5 deuteriums near the Schiff base (C(20) methyl, C(14), C(15)), the in-plane position of the label moves in the direction of the ring by about 1.4 Å. The apparent length of the projected chromophore is thus shorter in M. This change in position cannot be explained by an isomerization at the end of the polyene chain with the C(5) to C(13) part of the chain staying fixed, since this would leave the label position unchanged. The data are consistent with an increase in tilt angle of the polyene chain by about 11°, leading to a displacement of the C(20) methylgroup towards the cytoplasm. Whether this movement is due to isomerization alone or to isomerization followed by a protein conformational change is at present unclear.

**Tu-P0464****CLASSIFICATION AND CHARACTERIZATION OF Ca<sup>2+</sup> BINDING SITES IN BACTERIORHODOPSIN**

((Y. N. Zhang, M. A. El-Sayed)) Dept. of Chem. & Biochem., Univ. of Calif., Los Angeles; ((M. L. Bonet, J. K. Lanyi)) Dept. of Physiol. and Biophys., Univ. of Calif., Irvine; ((M. Chang, B. Ni and R. Needleman)) Dept. of Biochem., Wayne State Univ.

The binding constants and stoichiometry of Ca<sup>2+</sup> ions in recombinant bR (1) (D85N, D212N and R82Q/D85N) as well as in papain-treated bR (2) are determined by means of potentiometrical titration using Ca<sup>2+</sup> sensitive electrodes. The results are compared with those of wild type bR, which was found (3) to have two high affinity Ca<sup>2+</sup> binding sites and 4-6 low affinity ones. The effects of removing metal cations on the retinal absorption of the different recombinant bR were also investigated.

The important results are: 1) Removing metal cation from the recombinant proteins shifts the retinal absorption to blue, opposite to the effect on wild type bR; 2) Residue replacement is found to reduce the binding affinity of the two high affinity sites, but does not affect the values of binding constants of the four low affinity ones; 3) The D212N protein has the largest reduction in the association constants of the two high affinity sites (by a factor of ~1/15); 4) The removal of the C-terminus in bR by papain-treatment eliminates most of the low affinity Ca<sup>2+</sup> binding sites and leaves the two high affinity sites unaffected. The above results suggest that the two high affinity sites are close to one another and to the retinal pocket, whereas the weakly bound sites are away from it, e.g. on the membrane surface. While none of D85, D212 or R82 is individually directly involved in the binding of Ca<sup>2+</sup> in these two sites, they might all participate in it. Together with the protonated Schiff base, they seem to form an electrostatically coupled system which forms part of the cavity that controls the color and function of bR.

1. Y. N. Zhang, M. A. El-Sayed, M. L. Bonet, J. K. Lanyi, M. Chang, B. Ni and R. Needleman. Submitted to Proc. Natl. Acad. Sci. USA for publication.

2. Y. N. Zhang and M. A. El-Sayed. Submitted to FEBS Letts. for publication.

3. Y. N. Zhang, L.L. Sweetman, E. A. Awad and M. A. El-Sayed. Biophys. J. 61, 1201-1206.

**Tu-P0463****CHROMOPHORE-PROTEIN INTERACTION STUDIES ON BACTERIORHODOPSIN BY MUTATIONS.**

((Y. Feng,<sup>1</sup> R.K. Crouch,<sup>1,2</sup> B. Katz,<sup>2</sup> and D.R. Menick<sup>1,3</sup>)) Dept. of Biochemistry and Molecular Biology,<sup>1</sup> Dept. of Ophthalmology,<sup>2</sup> and Division of Cardiology,<sup>3</sup> Medical University of South Carolina, Charleston, SC 29425. (Spon. by G. Cooper, IV)

Bacteriorhodopsin (bR) has been studied by site-directed mutagenesis and reconstitution with synthetic retinal analogues. Mutant bRs containing the following single replacements R82A, R134A, R134K, and R134Q have been expressed in L33, a bR<sup>-</sup> strain of *H. halobium*. Their recombinant genomic bacterio-opsin genes with individual single substitution have been confirmed by PCR and dideoxynucleotide DNA sequencing. The regenerated R82A pigment by all-trans retinal has a  $\lambda_{max}$  of 582 nm with a recovery rate of 66%, non-responsive to the light/dark adaptation. The R82A apoprotein forms pigment with 13-desmethyl retinal and 4-hydroxyl retinal with absorption maximized at 578 nm and 547 nm, respectively. The R82A/13-desmethyl pigment red shifts 6 nm under illumination. No change is found with R82A/4-hydroxyl retinal. Interestingly, the R134A and R134Q bacterio-opsins do not form pigments in host L33, while the R134K bacterio-opsin partially forms a functional pigment *in vivo* and could regenerate an extra pigment at 628 nm with all-trans retinal *in vitro*. Therefore, it appears that Arg134 might play an important role in pigment formation along the chromophore binding site. These data demonstrate the power of coupling the reconstitution of retinal derivatives with site-specific bR mutants and underscore the importance of homologous expression of bR. (Supported by NIH grants EY04939 and HL44202, and Research to Prevent Blindness).

**PHOTOSYNTHESIS****Tu-P0465**

**PICOSECOND IR SPECTROSCOPY OF REACTION CENTERS : EFFECT OF HYDRATION ON BACKBONE DYNAMICS AND ELECTRON TRANSFER RATES** ((S. Maiti, G.C. Walker, B.R. Cowen, C.C. Moser, P.L. Dutton and R.M. Hochstrasser)) Department of Chemistry and Johnson Research Foundation, University of Pennsylvania, Philadelphia, PA 19104.

Protein and chromophore dynamics following visible excitation of the photosynthetic reaction center have been investigated as a function of humidity by picosecond infrared spectroscopy. IR spectral changes observed in reaction centers in solution and in partially dehydrated films (<15% relative humidity) appear distinctly different. The most notable difference is the presence of a pronounced negative band at 1665 cm<sup>-1</sup> observed only in the hydrated protein. Visible transient spectroscopy reveals markedly different electron transfer kinetics in these two preparations. The rate of Bph → Q<sub>A</sub> electron transfer in the hydrated preparations is 235 ps, while in the films it is biphasic with time constants of 200 ps (40%) and 900 ps (60%). Furthermore, the 1665 cm<sup>-1</sup> band in the amide I region of the hydrated protein appears to develop faster (τ~165 ps) than the rate of electron transfer, suggesting this is a backbone relaxation associated with the formation of BChl<sub>2</sub><sup>+</sup>BPh<sup>-</sup>Q<sub>A</sub> state that is inhibited at lower humidity. We are investigating the effect of chemical modifications of Q<sub>A</sub> on this relaxation.

Sponsored by NIH grants to R.M.H. and P.L.D.

**Tu-P0466****PROTEIN MOTIONS AND ELECTRON TRANSFER IN PHOTOSYNTHETIC REACTION CENTERS STUDIED BY ULTRAFAST INFRARED SPECTROSCOPY**

((B. R. Cowen, G. C. Walker, S. Maiti, C. C. Moser, P. L. Dutton, and R. M. Hochstrasser)) Department of Chemistry and Johnson Research Foundation, University of Pennsylvania, Philadelphia, PA 19104

The ultrafast transient infrared (IR) absorption following optical excitation of *Rb. sphaeroides* R-26 reaction centers in the amide and carbonyl spectral region, 1550-1750 cm<sup>-1</sup> was measured. To accomplish this a transient IR spectrometer based on Ti:Sapphire with 300 fs time resolution, tunable from 1550-2000 cm<sup>-1</sup> and having 10<sup>-5</sup> OD sensitivity was developed. Electron transfer kinetics differing from those established by optical spectroscopy are evident from our observations of the special pair ketone carbonyls (e.g. at 1702 cm<sup>-1</sup>). Besides the expected 3.5 ps component we observed a comparably intense component at ca. 12 ps. The transient IR method is ideally suited to studies of the protein relaxation induced by the primary charge separation and a full study of this region explores both chromophore and amide transitions of the protein. The electron transfer rate measured on our solution samples with optical probes was conventional. The IR transient absorption is also being measured in regions where BChl/BChl shows static absorption differences in model systems, in search of clear spectral evidence for the chlorophyll monomer in the electron transfer process.

Sponsored by NIH grants to R.M.H. and P.L.D.

## Tu-Po467

**TIME-RESOLVED IR SPECTROSCOPY OF PROTON TRANSFER IN NATIVE AND MUTANT REACTION CENTERS OF *Rb. SPHAEROIDES*.**\* ((R. Hienerwadel) Inst. für Biophysik, Universität Freiburg, 7800 Freiburg, Germany; ((M.Y. Okamura, M.L. Paddock, S.H. Rongey, G. Feher)) Dept. of Physics, Univ. of Calif., San Diego, La Jolla, CA 92093, USA; ((J. Breton and E. Nabdryk)) SBE/DBCM, C.E.N. Saclay, 91191 Gif-sur-Yvette Cedex, France; ((W. Mäntele)) Inst. für Biophysik, Universität Freiburg, 7800 Freiburg, Germany.

Time-resolved IR signals associated with  $Q_B$  reduction in *Rb. sphaeroides* RC were measured in the region of protonated carboxyl group absorption ( $1700\text{ cm}^{-1}$  to  $1760\text{ cm}^{-1}$ ) for native and EQ L212 (Glu L212  $\rightarrow$  Gln) or DN L213 (Asp L213  $\rightarrow$  Asn) mutants. Two signals corresponding to protonation reactions could be identified at around  $1725\text{ cm}^{-1}$  and  $1735\text{ cm}^{-1}$  and two corresponding to deprotonation at around  $1702\text{ cm}^{-1}$  and  $1715\text{ cm}^{-1}$ . These signals exhibit different kinetic components with half times of 1-2 msec, but, at least in the case of the  $1735\text{ cm}^{-1}$  signal, with an additional 120-150  $\mu\text{sec}$  kinetics of  $Q_A \rightarrow Q_B$  electron transfer. Matching kinetics of protonation and deprotonation suggests either the involvement in a proton pathway, or indicates that the groups experience the same change of environment. The variation of the maxima of these signals points to a large range of environments, from solvated ( $1702\text{ cm}^{-1}$ ) to more buried ( $1735\text{ cm}^{-1}$ ) COOH groups. The signals from native, EQ L212, and DN L213 mutants are analyzed in terms of a model for a proton pathway to  $Q_B$ . \*Work supported by NSF, NIH and EEC (SCI \*0335-C) grants.

## Tu-Po469

**FTIR SPECTROSCOPY OF BACTERIAL REACTION CENTERS: EFFECT OF MUTATIONS NEAR THE PRIMARY DONOR.**

E. Nabdryk<sup>1</sup>, J. Allen<sup>2</sup>, H. Murchison<sup>2</sup>, A. Taguchi<sup>2</sup>, J. Williams<sup>2</sup>, N. Woodbury<sup>2</sup> & J. Breton<sup>1</sup>

<sup>1</sup>SBE/DBCM, C.E.N. Saclay, 91191 Gif-sur-Yvette Cedex, France

<sup>2</sup>Dept of Chemistry and Biochemistry and Center for the Study of Early Events in Photosynthesis, Arizona State University, Tempe, AZ 85287-1604 USA

Light-induced P+QA-/POA FTIR difference spectra of RCs have been obtained from chromatophores of *Rb. sphaeroides* wild type (Wt) and for mutants designed either to introduce a hydrogen bond to the ring V keto group of one of the bacteriochlorophylls of the primary donor P (Leu to His at L131 or Leu to His at M160) or to cause the loss of the hydrogen bond to the ring I acetyl C=O of PL (His to Phe at L168). For these mutants, the largest changes are observed in the  $1720\text{--}1660\text{ cm}^{-1}$  region, indicating a strong perturbation of the environment of the keto C=O of P or of the charge density on ring V in P and P+. In the mutant LH(M160), two large differential signals are observed at  $1718/1696\text{ cm}^{-1}$  and  $1678/1664\text{ cm}^{-1}$ . They are assigned to the free and hydrogen-bonded keto C=O of PL and PM<sub>1</sub>, respectively, although a protein contribution can also be present at  $1664\text{ cm}^{-1}$ . The frequencies of PL and P+ in LH(M160) are comparable to those of the heterodimer HL(M200) [Nabdryk et al., 1992, Biochemistry, in press] suggesting that the spin density distribution in P+ is more asymmetric in LH(M160) than in Wt. In the LH(L131), the much reduced amplitude of the  $1684\text{ cm}^{-1}$  signal compared to the large negative signal (occurring at  $1683\text{ cm}^{-1}$ ) in Wt is presumably due to the formation of a strong hydrogen bond between HisL131 and the keto C=O of PL. While a small signal at  $1620\text{ cm}^{-1}$  is present in Wt, it is absent in HF(L168). In Wt, this band could correspond to the 2a acetyl of PL hydrogen-bonded to HisL168. This interaction would be lost in HL(L168). Supported in part by NSF and NIH.

## Tu-Po471

**FLASH-INDUCED PROTON UPTAKE IN NATIVE AND MUTANT REACTION CENTERS FROM *RHODOBACTER SPHAEROIDES*, MEASURED BY GLASS ELECTRODE.**

((V. Shinkarev, E. Takahashi and C. Wraight)) Dep of Physiol and Biophysics UIUC, Urbana, IL 61801

In the presence of exogenous electron donor, actinic flashes induced binary oscillations in proton uptake by photosynthetic reaction centers. The extent of H<sup>+</sup> uptake was dependent on the pH of the medium and salt concentrations. Increasing salt concentrations led to 7-fold decrease in the relative amplitude of first compared to the second flash-induced proton uptake, at neutral pH. The dependence of first flash-induced proton uptake on salt concentration is explained by a salt screening effect of the  $Q_B$  semiquinone electric potential, leading to diminution of the pK shifts of amino acid residues. The observed dependence may partially explain the discrepancies in earlier measurements of the stoichiometry of protons taken up after the first flash in the presence of donor. The evidence to date supports the major involvement of a small number of residues in the H<sup>+</sup>-binding stoichiometry of  $Q_B$  at alkaline (pH > 9.5) and acid (pH < 6.5) and a distributed response over many residues at neutral conditions ( $6.5 < \text{pH} < 8.5$ ).

## Tu-Po468

**LIGHT-INDUCED FTIR DIFFERENCE SPECTROSCOPY OF PROTON TRANSFER MUTANTS OF *Rb. SPHAEROIDES*.**\* ((E. Nabdryk, J. Breton)) SBE/DBCM, C.E.N. Saclay, 91191 Gif-sur-Yvette Cedex, France; ((R. Hienerwadel, W. Mäntele)) Institut Biophysik, Universität Freiburg, 7800 Freiburg, Germany; ((M.L. Paddock, S. H. Rongey, G. Feher and M.Y. Okamura)) Department of Physics, Univ. of Calif., San Diego, La Jolla, CA 92093-0319, USA

Light-induced FTIR absorption changes associated with the photoreduction of  $Q_B$  were measured at pH 5.8 - 9.4 in native R26 reaction centers (RCs) and RCs from mutants EQ L212 (Glu L212 to Gln) and DN L213 (Asp L213 to Asn) which display reduced proton transport to  $Q_B$ . In the region of protonated carboxyl groups ( $1700\text{--}1760\text{ cm}^{-1}$ ), the  $Q_B/Q_B$  IR difference spectrum of native RCs is characterized by a main positive band at  $1728\text{ cm}^{-1}$  (at all pH values), with negative lobes at  $1740$  and  $1712\text{ cm}^{-1}$  (which disappear at pH 9.4). All the absorption changes were normalized to the  $1480\text{ cm}^{-1}$  semiquinone anion band. Compared to native RCs, the band at  $1728\text{ cm}^{-1}$  is larger in DN L213 and is strongly diminished in EQ L212 indicating that it is due to Glu L212. The bands at  $1740$  and  $1712\text{ cm}^{-1}$  are still present at pH 7.2 in both mutants and therefore cannot be due to Asp L213 or Glu L212. These results suggest that the  $1740$  and  $1712\text{ cm}^{-1}$  bands are due to either changes of protonation states or to absorption shifts of residue(s) other than Asp L213 and Glu L212. For native RCs and the DN L213 mutant, the carboxyl absorption change at  $1728\text{ cm}^{-1}$  is interpreted in terms of the protonation of Glu L212 upon  $Q_B$  formation. \*Work supported by NSF, NIH and EEC (SCI \*0335-C) grants.

## Tu-Po470

**LIGHT-INDUCED FTIR DIFFERENCE SPECTROSCOPY OF BACTERIAL REACTION CENTERS RECONSTITUTED WITH CHEMICALLY MODIFIED QUINONES: THE QA VIBRATIONS**

J. Breton, J.-R. Burie, C. Berthomieu, G. Berger and E. Nabdryk SBE/DBCM, C.E.N. Saclay, 91191 Gif-sur-Yvette Cedex, France

Photoreduction of the primary electron acceptor QA in *Rp. viridis* and *Rb. sphaeroides* RCs has been characterized by FTIR spectroscopy (1). However, these spectra cannot be directly interpreted in terms of the quinone vibrations inasmuch as any bond (e.g. of the protein) affected by the photoinduced change of state of QA will also contribute to the spectrum. We have thus characterized the QA-/QA vibrations of *Rb. sphaeroides* RCs reconstituted with a series of 1,4-naphthoquinones (NQ). The QA-/QA FTIR spectra of QA-depleted *Rb. sphaeroides* RCs reconstituted with the native ubiquinone (UQ<sub>10</sub>) and of untreated RCs are identical. Upon reconstitution with vitamin K<sub>1</sub> (2-Methyl-3-phytyl-NQ), the QA-/QA spectrum is practically identical to that of native RCs in the region where protein contributions dominate (e.g.  $1550\text{ cm}^{-1}$ ). It exhibits a triplet of positive bands at  $1478$ ,  $1444$  and  $1388\text{ cm}^{-1}$  in the region of absorption of the C...O and C...C vibrations of the quinone anion, instead of a broad structured band at  $\approx 1466\text{ cm}^{-1}$  for native RCs. This triplet of bands compares remarkably well with that reported for the QA-/QA FTIR spectrum of native *Rp. viridis* RCs (1) which contain menaquinone 9 (2-Methyl-3-isoprenyl-NQ). Comparison of these QA-/QA FTIR spectra, together with the absorption spectra of the isolated quinones leads to assign the *in vivo* neutral C=C vibrations of QA at  $1585$  and  $1601\text{ cm}^{-1}$  for *Rp. viridis* and *Rb. sphaeroides*, respectively. Additional comparison with spectra of *Rb. sphaeroides* RCs reconstituted with NQ, 2-Methyl-NQ and 2-3 Dimethyl-NQ allows for a tentative assignment of a band at  $1636\text{ cm}^{-1}$  to a C=O mode of QA in *Rp. viridis*. ([1] J. Breton et al. 1991, FEBS Lett., 278, 257)

## Tu-Po472

**AN ANALYSIS OF PHOTOSYSTEM II BEHAVIOR, BASED ON MISSES, ESTIMATED FROM QUASI-EQUILIBRIA ON THE DONOR AND ACCEPTOR SIDES OF REACTION CENTER.**

((V. Shinkarev and C. Wraight)), Dep. of Physiol. and Biophys., UIUC, Urbana, IL 61801

Flash-induced oxygen evolution in the thylakoids of plants and algae exhibits damped oscillations with period four. These are well described by the S-state model of Kok et al. (1970), with damping provided by empirical misses and double hits in the reaction center (RC) of Photosystem II. Here we apply a mechanistic interpretation of misses as arising from two sources. (1) Reaction centers that are inactive at the time of the flash due to the presence of either P<sup>+</sup> or  $Q_A$ , according to the electron transfer equilibria on the donor and acceptor sides of the RC and (2) charge recombination before equilibrium reached. The calculated misses are different for each flash-induced RC transition. Identification of these mechanisms underlying the miss factor for each transition leads to the recognition of two different reaction sequence cycles of Photosystem II, with different transition probabilities, producing an intrinsic heterogeneity of Photosystem II activity.

## Tu-P0473

Q<sub>y</sub>-EXCITATION RESONANCE RAMAN STUDIES OF BACTERIAL PHOTOSYNTHETIC REACTION CENTERS.

((V. Palaniappan and David F. Bocian)) Department of Chemistry, University of California, Riverside, CA 92521.

Q<sub>y</sub>-excitation resonance Raman (RR) spectra in the 30-1800 cm<sup>-1</sup> region are reported for chemically reduced and oxidized photosynthetic reaction centers (RCs) from *Rb. sphaeroides* 2.4.1. at 201 and 25 K. The RR spectra were acquired using a number of excitation wavelengths in the 675-925-nm range that spans the Q<sub>y</sub>-bands of the special pair (P), accessory bacteriochlorophylls (BChls) and bacteriopheophytins (BPhs). Analysis of the RR spectra in 1430-1800 cm<sup>-1</sup> region indicates that the chemical (or photo) oxidation of P effects specific structural rearrangements near BPhs and accessory BChls, the rearrangements near BPh<sub>1</sub> being the largest. Evidence also indicates that BPh<sub>1</sub> is intrinsically stabilized toward anion formation. There seems to be several structural motifs present on and around the L-branch chromophores that facilitate the charge separation down the L-branch rather than M-branch. Qualitative excitation profiles constructed for the low-frequency modes of P indicate that the intensities of these modes follow the absorption contour of the P<sup>+</sup> absorption band. RR intensities of the low-frequency modes of P are ~5-15 times stronger than those of the analogous modes of the accessory BChls. This result indicates that a number of low-frequency modes are strongly coupled to the Q<sub>y</sub> electronic transition of P. However, it remains to be determined whether these low-frequency modes of P are coupled to the charge separation process as well.

## Tu-P0475

SPECTROSCOPIC STUDIES OF PURIFIED PHOTOSYSTEM II FROM A PHOTOSYSTEM I INACTIVATED STRAIN OF SYNECHOCYSTIS 6803 ((M.P. Espe, N.R. Bowlby, M. Mac, J.L. McCracken, L. McIntosh and G.T. Babcock)) Dept of Chemistry and USDOE Plant Research Lab, Michigan State University, East Lansing, MI 48824.

For spectroscopic analysis of Photosystem II (PSII) particles, a preparation virtually free of Photosystem I (PSI) is preferred. In order to bypass rigorous biochemical purification of PSII, which can reduce or eliminate enzymatic activity, we have genetically inactivated PSI. The new strain was generated by inactivating the *psaA* gene. The purification of PSII from this strain results in the high yield of protein recovery and high rates of oxygen evolution. Magnetic resonance techniques have been applied to characterize these PSII samples.

EPR signals from the dark stable tyrosine, Y<sub>D</sub>, and cyt b<sub>559</sub> are identical to that detected in the PSI containing strain. In addition the multiline signal arising from the manganese ensemble of PSII is also detected and is the same as that observed for the PSI containing strain as well as from spinach. Application of pulsed EPR techniques to Y<sub>D</sub> yield results identical between the PSI<sup>-</sup> system and spinach PSII. The spectra show a set of low frequency peaks which appear to come from an interaction between Y<sub>D</sub> and a nearby nitrogen. Previous models have proposed the source of the hydrogen bond to Y<sub>D</sub> to be a histidine side chain. From the spectroscopic similarity as well as the normal oxygen evolution rates we propose that a normal PSII is assembled in the PSI<sup>-</sup> strain.

## Tu-P0477

A NOVEL MEMBRANE-ASSOCIATED C-TYPE CYTOCHROME INVOLVED IN CYT C<sub>2</sub>-INDEPENDENT PHOTOSYNTHETIC GROWTH IN *RHODOBACTER CAPSULATUS* ((Francis E. Jenney Jr., Roger C. Prince\* and Fevzi Daldal)) Department of Biology, Plant Science Institute, University of Pennsylvania Philadelphia, PA 19104. \*Exxon Research and Engineering, Annandale, NJ 08801.

The bacterium *Rhodobacter capsulatus* utilizes cyclic electron transport during photosynthetic growth. The soluble cytochrome c<sub>2</sub> (cyt c<sub>2</sub>) was believed to be the sole donor of electrons to the photooxidized reaction center (RC). However, *R. capsulatus* strains in which the *cycA* gene encoding cyt c<sub>2</sub> was inactivated by mutagenesis are still able to grow photosynthetically (Ps<sup>+</sup>), unlike the closely related *R. sphaeroides* which is Ps<sup>-</sup> in the absence of cyt c<sub>2</sub>. A genetic screen was used to clone the gene required for cyt c<sub>2</sub>-independent growth in *R. capsulatus* by complementing a cyt c<sub>2</sub><sup>-</sup> Ps<sup>-</sup> *R. sphaeroides* strain to Ps<sup>+</sup> growth with a *R. capsulatus* chromosomal library. The complementing 1.2 Kb fragment encodes a novel, membrane-associated c-type cytochrome cyt c<sub>γ</sub> based on DNA sequence, difference spectra and SDS-PAGE analysis. The cyt c<sub>γ</sub> *R. capsulatus* strain is Ps<sup>+</sup> under conditions tested, however the double mutant cyt c<sub>γ</sub><sup>-</sup> c<sub>2</sub><sup>-</sup> is Ps<sup>-</sup> and complemented to Ps<sup>+</sup> growth by either cyt c<sub>2</sub> or cyt c<sub>γ</sub> in *trans*, demonstrating that cyt c<sub>γ</sub> is necessary for cyt c<sub>2</sub>-independent Ps<sup>+</sup> growth in *R. capsulatus*. Preliminary spectroscopy experiments with these mutants indicated that unlike the cyt c<sub>2</sub><sup>-</sup> or cyt c<sub>γ</sub><sup>-</sup> single mutants, there is no flash-oxidizable c-type cytochrome in the double mutant cyt c<sub>γ</sub><sup>-</sup> c<sub>2</sub><sup>-</sup>, in agreement with their Ps<sup>-</sup> growth phenotypes. The predicted amino acid sequence of cyt c<sub>γ</sub> is unusual in that the NH<sub>3</sub>-terminus is hydrophobic and the COOH-terminus has strong homology to soluble cyt c mainly from plant and animal mitochondria rather than prokaryotic cyt c<sub>2</sub>. This work was supported by DOE grant DE-FG02-91ER20052.

## Tu-P0474

SPECTROSCOPIC, KINETIC AND THERMODYNAMIC PROPERTIES OF THE MUTATION L121(PHE→HIS) IN REACTION CENTERS OF RHODOBACTER SPHAEROIDES ((X. Wang\*, Y. Jia\*, Y. Zhang\*, M. Thurnauer\*, J. R. Norris†, G.R. Fleming† and C. A. Wright\*) University of Illinois\*, University of Chicago†, Argonne National Lab

Spectroscopic, kinetic and thermodynamic properties of RCs from *Rb. sphaeroides* have been compared for wildtype (Wt) and a mutant, L121FH (Phe →His). The mutation is located near rings III and V of the active bacteriochlorophyll (BChl). (1) Optical absorption spectra: a small shift from 802 to 803 nm in the Q<sub>y</sub> band of the monomer bacteriochlorophyll spectrum. (2) Transient kinetics of stimulated emission: the fast components of the P<sup>+</sup> lifetime were similar (τ = 2.5 ps and 3.0 ps for wildtype and L121FH, respectively), but the slow components were distinctly different (τ = 15.8 ps and 38.8 ps for wildtype and L121FH mutant, respectively). (3) The light induced P<sup>+</sup> radical EPR signal and the light-induced triplet signal in QA-reduced RCs: the linewidth of P<sup>+</sup> cation radical showed a small increase (~5%) in mutant RCs; the triplet signal in the mutant (g = 2.00211, ID = 201.45 and EI = 39.18) showed a small increase in rhombicity compared to wildtype (g = 2.0022, ID = 202.95 and EI = 36.75). (4) The rate of recovery of the flash-oxidized primary electron donor, P<sup>+</sup>, from the state P<sup>+</sup>QA<sup>-</sup>: at 295K, in 100 mM KCl and in the presence of o-phenanthroline, the rates of recombination for L121FH were 13 s<sup>-1</sup> at pH 7 and 16 s<sup>-1</sup> at pH 10; wildtype rates were 9 s<sup>-1</sup> and 13 s<sup>-1</sup>, respectively. Between 310K and 275K, the rates of recovery were temperature-independent for both wildtype and L121FH. (5) Extraction of QA and reconstitution with anthraquinone: in L121FH mutant RCs, P<sup>+</sup>QA<sup>-</sup> decay was still temperature independent while wildtype RCs showed temperature-dependent behavior. The activation energy, indicating the enthalpy between P<sup>+</sup>I<sup>-</sup> and P<sup>+</sup>QA<sup>-</sup>, was estimated to be about 0.15 to 0.2 eV larger than for wildtype. (6) The P/P<sup>+</sup> redox midpoint potential: E<sub>m</sub>(P/P<sup>+</sup>) for L121FH was 450 mV, compared to wildtype value of about 490 mV. These measurements indicate a significant change in the energy gap between P<sup>+</sup>I<sup>-</sup> and P<sup>+</sup>QA<sup>-</sup> in L121FH mutant RCs. Supported by NSF

## Tu-P0476

ELECTRIC FIELD EFFECTS ON THE INITIAL CHARGE SEPARATION IN ORIENTED FILMS OF PHOTOSYNTHETIC REACTION CENTERS ((C. C. Moser, R. J. Sensen, A. Z. Szarka, S. T. Repinec, R. M. Hochstrasser, and P. L. Dutton)) Johnson Research Foundation and Dept. Chemistry, University of Pennsylvania, Philadelphia, PA 19104

A Langmuir-Blodgett monolayer of reaction centers from *Rb. sphaeroides* is repeatedly deposited on a transparent electrode, building up an oriented multilayer. Evaporation of polyethylene and platinum creates a multilayer capacitor in which applied fields are parallel to the direction of transmembrane fields *in vivo*. Even at field strengths sufficient to result in 5% quantum yield failure of light induced primary quinone reduction, the kinetics of initial charge separation, followed by examining the approximately 3 psec decay of stimulated emission at 940 nm of the excited BChl<sub>2</sub><sup>+</sup> state, are nearly unchanged, with rate changes of less than 25% acceleration and/or deceleration. This is reasonable for a two step mechanism involving electron transfer from BChl<sub>2</sub> to BChl monomer. Larger rate changes are expected in a single step mechanism from BChl<sub>2</sub> to BPh which has a larger transmembrane dipole. We provide evidence that the msec quantum yield failure, which cannot be explained by these minor rate changes, can be affected by a substantial field sensitivity of the <sup>1</sup>BChl<sub>2</sub>+BPh- charge recombination reaction. The large free energy of this reaction appears to access the Marcus inverted region. Supported by NIH Grants GM 41048 (PLD) and GM 12592 (RMH).

## Tu-P0478

CYLINDRICAL AGGREGATES OF PYROCHLOROPHYLL-A COMPARED WITH AGGREGATES OF BACTERIOCHLOROPHYLL-C: MODELS FOR ANTENNA CHLOROPHYLL IN *CHLOROFLEXUS* & *CHLOROBIVUM*. ((D.L. Worcester\*, T.J. Michalski and J.J. Katz\*)) Biology Div., Univ. of Missouri, Columbia, MO, 65211 and Chemistry Division, Argonne National Lab., Argonne, IL, 60439.

Neutron scattering data were obtained for hydrated aggregates of pyrochlorophyll-A and bacteriochlorophyll-C in deuterated octane/toluene solvents. The data show that the main aggregates are hollow cylinders. The bacteriochlorophyll-C cylinders were determined to be 11-12nm diameter, as reported in earlier work (PNAS 83, 3791, 1986). Data for aggregates of pyrochlorophyll-A demonstrate cylinders that are smaller by about a factor of two (5-6nm diameter) and are less distinctly hollow. These two cylinder sizes are of interest since they have been reported in electron microscopy studies of chlorosomes in *Chlorobium* and *Chloroflexus* respectively, and recent work shows that the interior of chlorosomes in *Chloroflexus* does not contain protein (Holzwarth et. al., Z. Naturforsch. 45g, 203, 1990), as had been previously reported by other researchers. Pyrochlorophyll-A and bacteriochlorophyll-C lack the ring V carbomethoxy group present in other chlorophylls, but bacteriochlorophyll-C contains a ring I hydroxyethyl group which appears to be involved in the formation of the 11-12nm diameter cylinders. Molecular arrangements in the hydrated chlorophyll aggregates are proposed, whereby the absence of the hydroxyl group in pyrochlorophyll-A results in the smaller diameter cylinders. Similar chlorophyll interactions are examined for aggregates found in chlorosomes.

## Tu-P0479

LIGHT-HARVESTING BY CAROTENOIDS HAVING DIFFERENT EXTENTS OF  $\pi$ -ELECTRON CONJUGATION. ((Harry A. Frank, Roya Farhoosh, Ronald L. Christensen, Beverly DeCoster, Ronald Gebhard and Johan Lugtenburg)) Department of Chemistry, University of Connecticut, 215 Glenbrook Road, Storrs, CT 06269; Department of Chemistry, Bowdoin College, Brunswick, ME 04011; and Gorlaeus Laboratories, University of Leiden, Leiden, The Netherlands.

Several carotenoids having various extents of  $\pi$ -electron conjugation have been incorporated into the B850 light-harvesting complex of the carotenoidless mutant, photosynthetic bacterium, *Rhodobacter sphaeroides* R-26.1. Carotenoid-to-bacteriochlorophyll (BChl) singlet state energy transfer efficiencies were measured for the complexes using steady-state fluorescence excitation spectroscopy. The results suggest that the position of the carotenoid and BChl energy levels, the magnitude of spectral overlap between the carotenoid  $S_1$  ( $2^1A_g$ ) state emission and the BChl absorption of the native complex, and the dynamics of internal conversion are important in controlling singlet energy transfer. These studies provide a systematic approach to exploring the effect of these factors on the efficiencies of carotenoid-to-bacteriochlorophyll energy transfer in photosynthetic systems. This work is supported in part by a grant from the National Institutes of Health (GM-30353).

## Tu-P0481

ELECTRON SPIN POLARIZATION IN IRON-CONTAINING BACTERIAL REACTION CENTERS. ((S. Snyder, A. Morris, S. Bondeson, Y. Zhang, P.L. Dutton\*, M. Gunner\*\*, J.R. Norris and M.C. Thurnauer)) Argonne National Laboratory, Argonne, IL 60439, \*U. of Pennsylvania, Philadelphia, PA 19104 and \*\*City College of New York, New York, NY 10031

Stable charge separation in the purple photosynthetic bacterial reaction center (RC) occurs by sequential electron transfer:  $PHQFe \xrightarrow{h\nu} P^+H^-QFe \rightarrow P^+H(QFe)^-$ , where P is a pair of bacteriochlorophylls, H is bacteriopheophytin, and Q is ubiquinone. We have observed electron spin polarized (ESP) electron paramagnetic resonance (EPR) signals from  $P^+H(QFe)^-$  in native (Fig. 1) and quinone-replaced RCs. The observations can be described by a model for ESP in sequential electron transfer that includes ESP development on both  $P^+H^-QFe$  and  $P^+H(QFe)^-$ .

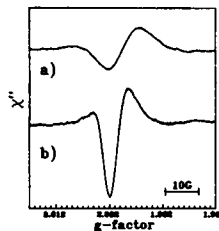


Fig. 1. ESP EPR signals of  $P^+$  in the state  $P^+H(QFe)^-$  from native (a) protonated (b) deuterated RCs.

This work was supported by the U.S. Department of Energy, Office of Basic Energy Sciences, Division of Chemical Sciences under contract W-31-109-Eng-38.

## Tu-P0483

RESIDUES OF THE D1 POLYPEPTIDE THAT INFLUENCE THE ASSEMBLY OR STABILITY OF THE MANGANESE CLUSTER OR THE BINDING OF CALCIUM IN PHOTOSYSTEM II ((H.-A. Chu, A. P. Nguyen and R. J. Debus)) Dept. of Biochemistry, Univ. of Calif., Riverside CA 92521-0129

We have identified seven carboxylate and two histidine residues of the D1 polypeptide that influence the assembly, stability or operation of the Mn cluster in PSII. These residues, identified on the basis of site-directed mutagenesis studies in the cyanobacterium, *Synechocystis* 6803, are Asp-59, Asp-61, Glu-65, Asp-170, Glu-189, Glu-333, Asp-342, His-332 and His-337. The perturbed Mn complexes have been characterized in vivo by measuring the fluorescence changes that follow (i) each of a series of closely spaced saturating flashes, (ii) a single flash given in the presence of DCMU, or (iii) continuous illumination in the presence of DCMU. Most of the mutants appear to contain significant proportions of PSII centers that lack even partially assembled Mn complexes. The balance of the PSII centers in these mutants contain wholly or partially assembled Mn complexes that, in terms of oxygen evolution, are impaired to varying degrees or are nonfunctional. By examining mutants that had been propagated in media having other cations substituted for  $Ca^{2+}$ , we have concluded that Asp-59, Asp-61, His-332, Glu-333, His-337, and Asp-342 directly or indirectly influence the binding of  $Ca^{2+}$  to PSII. Mutations at His-190 appear to interfere with electron transfer from  $Y_2$  to  $P_{680}^+$ , as was reported earlier [Diner et al. (1991) *Curr. Opin. Struct. Biol.* 1, 546-554]. \*Work supported by the NIH (GM-43496).

## Tu-P0480

PLASTOQUINONE MOBILITY IN THYLAKOIDS AND SUBTHYLAKOIDS. ((M.F. Blackwell, C. Gibes, S.F. Gyax, D.J. Roman and B.L. Wagner)) Department of Chemistry, Lawrence University, Appleton, WI 54911.

Laverne, Joliot and their coworkers have recently proposed a domain model of thylakoid membrane microstructure that accounts for a diversity of phenomena, such as the existence of 'fast' and 'slow' PQ pools, the inefficiency of equilibration between the redox states of bound and mobile PQ during electron transport, and the observation of 'active' and 'inactive' PS II reaction centers [P. Joliot, J. Laverne and D. Beal (1992) *BBA* 1101:1-12; J. Laverne, J.-P. Bouchaud and P. Joliot (1992) *BBA* 1101: 13-32.]. They propose that these phenomena be rationalized in terms of a percolation model in which PQ mobility is restricted by thylakoid membrane proteins: the fast pool corresponds to PQ confined to isolated membrane domains in granal regions, whereas the slow pool corresponds to PQ in stromal regions. Here, we provide independent experimental support for the foregoing proposals. We present evidence from pyrene fluorescence quenching studies that the lateral mobility of PQ is highly restricted in thylakoids and subthylakoids, in comparison to its mobility in pure lipid vesicles, and rationalize the decrease in mobility from a purely physicochemical point of view in terms of a percolation model. We propose that integral proteins affect lipid mobility primarily by modifying the nature of lipid/lipid hard body interaction; this modification is represented theoretically by changes in the site occupation probability on the lipid percolation lattice. The percolation model presented here is motivated by experimental studies of probe fluorescence kinetics in liposomes [L. Huang, Y.X. Chen, M. Ge, B.D. Zion and M.F. Blackwell, this meeting], which have yielded results consistent with scaling behavior of diffusion in liposomes and therefore with spatial heterogeneity on the measurement distance scale. Our finding means that PQ is able to move only tens of nanometers on the msec timescale of rapid electron transport from granal PS II to stromal PS I. We conclude that PQ cannot function in long-range, rapid electron transport and presume that plastocyanin must fulfill this role, in agreement with the proposal of Joliot, Laverne and their coworkers. (Supported by ACS-PRF 24266-B4, HHMI 711911-529201 and a Research Corporation Cottrell College Science Grant for the William and Flora Hewlett Foundation).

## Tu-P0482

MUTAGENESIS OF THE MN-STABILIZING PROTEIN OF PHOTOSYSTEM II. ((Robert L. Burnap<sup>1</sup>, J.-R. Shen<sup>2</sup>, Yorinao Inoue<sup>2</sup>, and Louis A. Sherman<sup>3</sup>)) Dept. of Microbiol., Oklahoma State Univ<sup>1</sup>, Stillwater, OK 74078, U.S.A., Solar Energy Group, Inst. for Physical and Chemical Research<sup>2</sup> (RIKEN), Wako, Saitama, 351-01; Japan, Dept. Biological. Sci., Purdue Univ.<sup>3</sup>, West Lafayette, IN, 47907 U.S.A.

Site-directed mutations are being produced at highly conserved amino acid positions of the manganese-stabilizing protein (MSP) of the photosystem II (PSII) reaction center in the cyanobacterium *Synechocystis* PCC6803. The *Synechocystis* strains expressing the mutant MSPs have been characterized with respect to the accumulation of the mutant protein and the impact of these mutations upon the H<sub>2</sub>O-splitting enzyme. Disruption of the disulfide bridge (C20S) [Tanaka & Wada, 1988 *Photosynth. Res.* 17:255] results in the absence of accumulation of MSP despite normal levels of mRNA transcripts. Like the *psbO* deletion strain, the C20S mutant exhibits impaired O<sub>2</sub> evolution activity and greater stability of the S<sub>2</sub> state [Burnap et al, 1992 *Biochemistry* 31, 7404]. The mutation D9K, within the proposed N-terminal binding region [Eaton-Rye & Murata, 1989 *BBA* 977:219] does not affect the accumulation of the protein and only slightly affects the properties of the H<sub>2</sub>O-splitting enzyme. The mutation D159N also did not effect MSP abundance, but resulted O<sub>2</sub> evolution properties intermediate between the deletion mutant and the wild-type. The implications of these results relative to the function and binding of MSP to the PSII will be discussed.

**Tu-Pos484**

**FACILITATION OF RESPONSES TO METABOLICALLY STABLE ANALOGUES OF INOSITOL TRISPHOSPHATE IN LIMULUS PHOTORECEPTORS.** (I. Levitan<sup>1</sup>, R. Payne<sup>2</sup>, B.V.L. Potter<sup>2</sup>, C. Liu<sup>2</sup> and P. Hillman<sup>1</sup>). The Hebrew University, Jerusalem<sup>1</sup>, Israel. The Dept. of Zoology, University of Maryland<sup>2</sup>, College Park, USA. The Dept. Pharmacy and Pharmacology, University of Bath<sup>3</sup>, U.K. (Spon. by S.F. Wood)

Inositol 1,4,5-trisphosphate (InsP<sub>3</sub>) releases Ca from intracellular stores in *Limulus* photoreceptors. The released Ca activates an inward current. We find that small intracellular pressure injections of metabolically stable InsP<sub>3</sub> analogues, which by themselves induce little or no inward current, facilitate the response to subsequent injections of InsP<sub>3</sub> analogues and InsP<sub>3</sub>. This facilitation is in contrast to the desensitization we have previously observed following injections of InsP<sub>3</sub>. We also analyzed the kinetics of the response to InsP<sub>3</sub> analogues. Stable analogues were either rapidly injected into a non-sensitive region of a cell or slowly injected into a sensitive region, creating a slowly-rising ramp of analogue concentration. Either injection method elicited a fast pulse of inward current after a latency of several seconds. The ratio between the latency and duration of the response was greater than 10. Models of InsP<sub>3</sub>-induced Ca release and of the Ca-sensitive process that generates inward current cannot reproduce this ratio unless they include positive feedback. Partial depletion of Ca stores by saturating light flashes reversibly increased the latency of the response to injection of 2,3,5-l-chiro-InsP<sub>3</sub>. Released Ca may initially promote further Ca release from neighbouring InsP<sub>3</sub> receptors before eventually desensitizing them.

**Tu-Pos486**

**Changes in Membrane Protein Phosphorylation in Bovine Retinal ROS as a Function of Disk Age.** <sup>1</sup>K. Roesze-Battaglia, <sup>2</sup>A. D. Albert, <sup>2</sup>P. L. Yeagle. Department of Cell Biology, University of Medicine and Dentistry of New Jersey, School of Osteopathic Medicine, Stratford, NJ 08084 and Department of Biochemistry, University at Buffalo School of Medicine, Buffalo, NY 14214

Rod outer segment (ROS) disk membranes differ in their membrane cholesterol content. This difference reflects the age and position of these membranes in the ROS. Light induced phosphorylation of ROS disk membrane proteins as a function of disk age was investigated using <sup>31</sup>P NMR, SDS-gel electrophoresis and western blotting. <sup>31</sup>P NMR studies showed that the extent of rhodopsin phosphorylation by rhodopsin kinase did not change as a function of disk membrane age, under the bleaching conditions used. Subsequently <sup>31</sup>P NMR magic angle spinning studies showed that when intact ROS were bleached in the presence of endogenously available kinases, membrane proteins were more heavily phosphorylated in disk membranes located at the base of the ROS versus those at the tip. Stains-All, coomassie and silver staining of SDS gels of fractions of the phosphorylated disk membranes revealed a phosphorylated species with a molecular weight of approximately 68-72 kD that was more heavily phosphorylated in disks with a high cholesterol to phospholipid ratio, that is newly formed disk membranes. This particular protein was found to be present along the length of the entire outer segment. Western blot analysis using the 2B6 antibody (generously donated by Dr. R. Molday), revealed this phosphorylated protein to be bovine peripherin. (Supported by EYO3328 and EYO6241)

**Tu-Pos488**

**A SECOND PATHWAY OF CYCLIC GMP SYNTHESIS IN BOVINE PHOTORECEPTOR CELLS INVOLVES NITRIC OXIDE(NO).** (K.-W. Koch and H.-G. Lambrecht) IBI, Forschungszentrum Jülich, Postfach 1913, W-5170 Jülich, FRG

Bovine photoreceptor cells contain a *particulate* guanylate cyclase (GC) that is regulated by the intracellular calcium concentration via the calcium-binding protein recoverin. We here report the existence of a second guanylate cyclase that is *soluble* and sensitive to 1-100 μM sodium nitroprusside (SNP) confirming the results of Margulis et al. (1992) BBRC 185, 909-914. Adding SNP the GC activity increased over tenfold with manganese and over twentyfold with magnesium as cofactor. Furthermore we show that this *soluble* GC can be stimulated in the presence of L-arginine and NADPH in an extract of soluble bovine photoreceptor proteins. The effect is not observed by using D-arginine instead of L-arginine and is inhibited by N<sup>G</sup>-monomethyl-L-arginine and hemoglobin. This indicates that an endogenous NO synthase produces nitric oxide from L-arginine which in turn activates the *soluble* retinal GC. The synthesis of cyclic GMP depends on the concentration of L-arginine and is halfmaximal below 10 μM. The amount of cGMP produced by activation of the NO synthase is 35-100 % compared to the cGMP synthesis after stimulation by SNP. Neither the basal nor the calcium/recoverin regulated activity of the *particulate* GC is directly influenced by SNP or the L-arginine pathway. Interestingly, the NO synthase activity seems to be dependent on calcium/calmodulin, since the effect is abolished by calmodulin antagonists.

**Tu-Pos485**

**EFFECT OF THE LEVEL OF RHODOPSIN PHOSPHORYLATION ON METARHODOPSIN II FORMATION AND G<sub>i</sub> BINDING.**

((Julia Kibelbek and Burton J. Litman)) Department of Biochemistry, University of Virginia Health Sciences Center, Charlottesville, VA 22908

Rhodopsin phosphorylation leads to desensitization in the visual signalling system, as is observed in other G-protein-coupled receptor pathways. ROS kinases, including rhodopsin kinase, catalyze the addition of up to 9 phosphate groups per rhodopsin molecule (P/R) to the C-terminus and possibly other sites on the cytoplasmic surface of rhodopsin, in response to light stimulation. The effect of phosphorylation on receptor conformation was studied using purified pools of rhodopsin containing 0, 4-6, and 8-9 P/R, reconstituted into unilamellar POPC vesicles. K<sub>m</sub> for the metarhodopsin I ↔ metarhodopsin II equilibrium was obtained spectrophotometrically and used to quantify meta II, the G<sub>i</sub>-activating conformation of the photoactivated receptor. In the absence of added G<sub>i</sub>, phosphorylation at the level of 4-6 P/R had little or no effect on K<sub>m</sub> when compared to a K<sub>m</sub> of 0.30 ± .04 for 0 P/R rhodopsin, while 8-9 P/R rhodopsin yielded a K<sub>m</sub> of 0.56 ± .05. Apparent K<sub>m</sub>'s, measured in the presence of added G<sub>i</sub>, were used to measure G<sub>i</sub> binding to meta II. This data suggests a graded reduction in G<sub>i</sub> binding with increasing degree of rhodopsin phosphorylation, with about an order of magnitude difference in K<sub>d</sub> for the meta II-G<sub>i</sub> complex of 0 P/R rhodopsin relative to 8-9 P/R rhodopsin. (Supported by NIH grant EY00548).

**Tu-Pos487**

**DIACYLGLYCEROL ANALOGS SUPPRESS THE CYCLIC GMP-ACTIVATED CONDUCTANCE IN ROD OUTER SEGMENT PATCHES IN THE ABSENCE OF ATP.**

((Sharon E. Gordon and Anita L. Zimmerman)) Section of Physiology, Brown University, Providence, RI 02912.

Although cGMP appears to be the primary second messenger mediating the rod's light response, the inositol phosphate system has also been implicated. We now show that, in the absence of ATP, diacylglycerol (DAG) analogs reversibly suppress the cGMP-activated conductance of multi-channel excised patches from rod outer segments. In the presence of a saturating concentration of the agonist 8-Br-cGMP, the DAG analogs 1,2-dioctanoyl glycerol (1,2-DiC8) and 1,3-dioctanoylglycerol (1,3-DiC8) reduced the agonist-induced current with K<sub>i</sub>'s of about 20 μM. Another C8 analog was much less potent: 100 μM dioctanoyl ethylene glycol (DiC8-EG) reduced the agonist-induced current by about 30%. Similar single-channel currents were recorded before and after treatment with 100 μM 1,2-DiC8. Thus, the large reduction in macroscopic current appeared to reflect a complete block or inhibition of most of the channels, with the remaining channels conducting approximately normally. These findings raise the question of whether light-induced changes in diacylglycerol modulate the cGMP-activated channels *in vivo*.

Supported by NIH EY07774 & NSF RCD-9054722.

**Tu-Pos489**

**Intracellular Ca<sup>2+</sup> Sequestration and Release in Intact Bovine Retinal Rod Outer Segments: A Comparison between Fluo-3 and <sup>45</sup>Ca Flux Experiments.** Paul P.M. Schnetkamp, Xue-Bin Li and Robert T. Szerencsei, Department of Medical Biochemistry, University of Calgary, CANADA

Intracellular Ca<sup>2+</sup> sequestration and release was analyzed in intact rod outer segments purified from bovine retinas (ROS). Ca<sup>2+</sup> influx in Ca<sup>2+</sup>-depleted and fully bleached ROS was mediated exclusively by the Na-Ca+K exchanger and was measured both as a rise in cytosolic free Ca<sup>2+</sup> with fluo-3 and as a total transmembrane Ca<sup>2+</sup> flux with <sup>45</sup>Ca. Ca<sup>2+</sup> fluxes across the ROS plasma membrane were not completely reversible, in small part due to inactivation of the Ca<sup>2+</sup> extrusion mode of the Na-Ca+K exchanger but mostly due to sequestration of cytosolic Ca<sup>2+</sup> into the intradiskal space. Ca<sup>2+</sup> release from the intradiskal space into the cytosol could be induced by low concentrations of the Ca<sup>2+</sup> ionophore A23187 or by addition of ammonium acetate; this intracellular Ca<sup>2+</sup> release gave rise to increases in cytosolic free Ca<sup>2+</sup> by several hundred nanomolar. We conclude that disks within intact ROS contain both a Ca<sup>2+</sup> uptake and a Ca<sup>2+</sup> release mechanism. We discuss possible physiological roles for Ca<sup>2+</sup> sequestration and release from ROS disks. Supported by MRC and RPERF.

**Tu-Pos490**

**LIGHT-INDUCED STRUCTURAL CHANGE IN SQUID PHOTORECEPTOR CELLS.** (Michinori Ichikawa and Gen Matsumoto) Electrotechnical Laboratory, Tsukuba, Ibaraki 305, JAPAN

We have studied squid photoreceptor cells by cryofixation method for electron microscopy. Structural change in squid photoreceptor microvilli accompanied by long period of light illumination has been studied by Tsukita *et al.* (*J. Cell Biol.* 106, 1151-1160, 1988), resulting that there are two states of the microvillar cytoskeletal structure under dark- and light-adapted conditions. In this report we have observed the structural changes as a function of time after the light pulse application. For this experiment, we have developed a new cryofixation device which can combine rapid freezing with electrophysiological measurement. The device cryofixes biological specimen at precisely specified time after the light illumination by driving a small silver block cooled down to 10°K with a computer-controlled actuator; that is, the specimen can quietly be put on an experimental bench while the cooled silver block is rapidly pushed onto it for cryofixation, for letting the physiological manipulation easier and measurement better controlled. As a result, structural change of the microvilli is observed to take place over 50 msec after the light illumination is initiated. The conspicuous change is that the diameter of 70 nm under the dark-adapted condition increases to 120 nm after the light illumination for 5-7% microvilli. The change accompanies the breakdown of the microvillar action filament complex, and is not observed for 20-30 msec light-illuminated photoreceptors. A simple analysis indicates that the photon number of the light is just equal to the number of the structurally-changed microvilli, suggesting each microvillus changes its structure when it is exposed by a single photon. This leads us to an idea that the microvillus works as a single photon detector, together with its cell body as an accumulator for the light-converted signal.

**Tu-Pos491**

**THE LIGHT RESPONSE OF DROSOPHILA PHOTORECEPTORS IS ACCOMPANIED BY AN INCREASE IN INTRACELLULAR CALCIUM** ((E. Suss-Toby<sup>1</sup>, A. Rom-Glas<sup>1</sup>, R. Payne<sup>2</sup> and B. Minke<sup>1</sup>)). Department of Physiology<sup>1</sup>, The Hebrew University-Hadassah Medical School, Jerusalem, Israel. Department of Zoology<sup>2</sup>, University of Maryland, College Park, MD 20742, USA.

Photoreceptors of dissociated *Drosophila* retinae were loaded using the whole cell perfusion technique with 500  $\mu$ M of a fluorescent  $\text{Ca}^{2+}$  indicator (fluo-3 or Ca green 5N with Kd of 0.3  $\mu$ M and 25  $\mu$ M respectively). Simultaneous recordings were made of light-evoked inward current (LIC) and changes in intracellular  $\text{Ca}^{2+}$  concentration for the first time in this preparation. Following the onset of illumination, the LIC accompanied a rapid increase in indicator fluorescence (latency < 10ms). This increase was not observed in cells lacking an electrical response to light or in cells bathed for > 50 mins in an extracellular medium containing no added  $\text{Ca}^{2+}$  and 200  $\mu$ M EGTA. We have, however, observed a rapid, smaller, light-induced increase in fluorescence in cells bathed for shorter periods (5-50 min) in a medium containing no added  $\text{Ca}^{2+}$  + 200  $\mu$ M EGTA. A rapid light-induced increase in fluorescence was also observed in photoreceptors of the transient receptor potential (*trp*) mutant bathed in normal extracellular  $\text{Ca}^{2+}$ . *trp* photoreceptors lack a large fraction of the  $\text{Ca}^{2+}$  permeability underlying the LIC. These results suggest that the light response is accompanied by light-induced  $\text{Ca}^{2+}$  release from a labile intracellular store, in addition to  $\text{Ca}^{2+}$  influx.

**OPTICAL SPECTROSCOPY****Tu-Pos492**

**FLUORESCENCE CORRELATION SPECTROSCOPY UTILIZING TWO-PHOTON EXCITATION.** ((P. T. C. So, C. Dong, K. Berland, E. Gratton)) University of Illinois at Urbana-Champaign, Laboratory for Fluorescence Dynamics, Department of Physics, 1110 W. Green St., Urbana, IL 61801.

Traditionally, fluorescence correlation techniques (FCS) have mainly been limited to two dimensional geometries. The limitation is due to the difficulty of exciting a sufficiently small sample region to obtain measurable fluorescence intensity fluctuations. The recent development of two-photon fluorescence microscopy by Webb's group has demonstrated that fluorescence emission from a sub-micron sample volume can be measured. In addition, the availability of high peak power, femtosecond Ti:Sapphire laser has greatly improved the efficiency of two-photon fluorescence excitation and has made it a practical experimental technique. We have developed two-photon FCS technique to measure diffusion and aggregation of large molecules in bulk solution. This work was supported jointly by the National Institutes of Health (RR03155) and the University of Illinois at Urbana-Champaign.

**Tu-Pos493**

**A MILLISECOND STOPPED-FLOW INSTRUMENT WITH FLUORESCENCE LIFETIME DETECTION CAPABILITIES.** ((S. Eriksson<sup>1</sup>, S. Tetin<sup>2</sup>, E. Voss<sup>2</sup>, E. Gratton<sup>1</sup> and W. Mantulin<sup>1</sup>)) Univ. of Illinois at Urbana-Champaign, <sup>1</sup>Laboratory for Fluorescence Dynamics, Dept. of Physics, & <sup>2</sup>Dept. of Microbiology & Urbana, IL 61801.

Many rapid reactions in biology, and especially in protein folding, have been studied with stopped-flow (or concentration jump) techniques. We have developed an instrument that combines the millisecond stopped-flow mixing capabilities of a commercial unit (Biologic) with the picosecond resolution of fluorescence from a laser-based, frequency-domain fluorometer. The advantages of frequency domain fluorescence lifetime detection of millisecond reaction kinetics include: 1) utilization of the full fluorescence signal (sensitivity equivalent to steady-state measurements); 2) a frequency range suitable for resolution of complex lifetime schemes; 3) at a given frequency, two independent measurements of the lifetime (phase and modulation) are obtained. Our hybrid mixing instrument offers a variable time base, single or multiple shot averaging, facile frequency selection, a variety of detection modalities (transmission; fluorescence intensity, polarization, lifetime or anisotropy). To test its operation in the millisecond regime, we examined the ligand binding of ANS to albumin and fluorescein to IgG 4-4-20. This work was performed at the Laboratory for Fluorescence Dynamics (LFD) at the University of Illinois at Urbana-Champaign (UIUC). The LFD is supported by the NIH (RR03155) and by UIUC.

**Tu-Pos494**

**DISSOCIATION OF LARGE OLIGOMERIC PROTEINS BY HIGH HYDROSTATIC PRESSURE: DYNAMIC LIGHT SCATTERING STUDIES.** ((Gregory Reinhart\*, Enrico Gratton and William W. Mantulin)) \*University of Oklahoma, Department of Chemistry and Biochemistry, Norman, OK 73019; and Laboratory for Fluorescence Dynamics, Dept. of Physics, University of Illinois at Urbana-Champaign, Urbana, IL 61801.

In the study of oligomeric protein association, the combined approach of high hydrostatic pressure perturbation with optical spectroscopic detection has provided great insight into structure and dynamics of these complex systems. Various spectroscopic methods offer advantages in specific cases. For example, a decrease in the light scattering intensity tracks the pressure induced dissociation of oligomeric proteins. However, optical artifacts complicate the interpretation of light scattering experiments under pressure. Dynamic light scattering offers the possibility of directly detecting changes in the translational diffusion coefficient, which change with oligomer dissociation, rather than the total scattered intensity associated with oligomer dissociation. Dynamic light scattering offers greater sensitivity for the study of very large oligomers, that are not readily accessible using other spectroscopic methods. In addition, dynamic light scattering is conveniently used in conjunction with high hydrostatic pressure perturbation. We have performed dynamic light scattering experiments on the pressure dissociation of hemocyanin (gastropod), a very large molecular assembly (approximately  $8 \times 10^6$ ). Under ambient pressure conditions, dynamic light scattering measurements show a heterogeneous oligomer population. The application of about 2 kbar of pressure strongly changes the dynamic light scattering spectrum by depleting most of the low frequency spectral components (large molecular weight oligomers). Supported by NIH RR03155.

**Tu-Pos495**

**SPATIAL RESOLUTION OF TIME-RESOLVED LASER IMAGING.** ((A. Gandjbakhche, R. Bonner and R. Nossal)) NIH, Bethesda, MD 20892.

Several research groups have proposed using time-gated optical detection to determine the existence of tumors whose optical properties differ from those of normal tissue. By detecting early-arriving photons which emerge from a target tissue after irradiation by brief pulses, only very short paths would be selected, which theoretically would dramatically increase resolution. We use photon migration theory to study the resolution of objects imaged in this way, and also to calculate the intensity of detected light. The spread function in the mid-plane of a slab of thickness  $N$  is derived from the joint probability  $\Gamma(\rho, \Delta n)$  that a photon crosses the midplane at a radial point  $\rho$  units away from the point of insertion, and that it has a total path on emerging which is  $n = N + \Delta n$  steps. We find  $\Gamma(\rho, \Delta n)$  to be approximately Gaussian distributed, with a width given as  $2\sigma \approx 1.6(\Delta n)^{1/2}$ . This quantity, which defines the resolution, may be expressed in terms of gating time  $\Delta t$  and real distance  $r$  as  $2\sigma = 1.6(c\Delta t/(1-g))^{1/2}$ , where  $c$  is the speed of light in tissue,  $\Sigma_s$  is the bulk scattering cross-section, and  $g$  is the expected value of the cosine of the scattering angle. Although it thus appears that any given resolution can be achieved by changing  $\Delta t$ , in practice the detected intensity falls precipitously if  $\Delta t$  is much less than the mean transit time of photons detected in dc measurements. We examine these two competing factors to assess the practicality of time-resolved imaging in thick tissues.

**Tu-Pos496**

**FIBER OPTIC-BASED BIOSENSOR: APPLICATIONS FOR ENVIRONMENTAL MONITORING.** ((George P. Anderson<sup>1</sup>, Daya C. Wijesuriya<sup>2</sup>, Robert A. Ogert, Lisa C. Shriver-Lake, Joel P. Golden, and Frances S. Ligler)) Center for Bio/Molecular Science and Engineering, Code 6900, Naval Research Laboratory, Washington, D.C. 20375

The fiber optic biosensor is currently being developed to detect toxins, explosives, and pathogens in environmental samples. Essentially, the biosensor is a fluorimeter which utilizes long clad optical fiber with a short section of core exposed near the distal end to form the sensing region. The sensing region is tapered to improve coupling of the evanescent wave generated fluorescence. Antibodies or other binding proteins are immobilized on the core to provide the mechanism for recognizing an analyte of interest and holding the fluorescent complexes on the fiber surface. Antibodies coated on the fiber are stable for up to two years of lyophilized storage prior to use. A laboratory version of the device is being used for assay development and performance characterization while a portable version is under development. The fiber optic biosensor has been used to measure concentrations of toxins in the parts per billion (ng/ml) range in under a minute. Immunoassays for small molecules and whole bacteria are under development. The fiber can be placed in a flow chamber for rapid measurement of multiple samples. While the probe is disposable, antigen can be washed from the antibody to permit probe reuse. These features yield a device that is fast, sensitive, and permits analysis of hazardous material remote from the instrumentation.

<sup>1</sup>NRL-National Research Council Associate

<sup>2</sup>Georgetown University Postdoctoral Fellow

**Tu-Pos498**

**MEASUREMENT OF ROTATIONAL DYNAMICS OF PROTEINS BY THE NON-LINEAR ANALYSIS OF OPTICAL AND EPR DATA** ((E.J. Hustedt, J.M. Beechem, and A.H. Beth)) Department of Molecular Physiology and Biophysics, Vanderbilt University, Nashville, TN 37232.

An acyl spin-label derivative of 5-aminocoumarin, which allows the measurement of rotational dynamics using both time-resolved optical anisotropy and electron paramagnetic resonance (EPR) techniques, has recently been reported (Cobb et al., *Biophys. J.* in press). This new probe has motivated the development of new methods for the simultaneous analysis of optical and EPR data. Rigid-limit and rotational diffusion models for the simulation of nitroxide EPR spectra have been incorporated into a general non-linear least-squares procedure based on the Marquardt-Levenberg algorithm. These methods have proven useful for the analysis of EPR data from a variety of biological systems. Furthermore, it has been demonstrated, using a spin-labeled eosin / bovine serum albumin complex as a model system, that optical anisotropy and EPR data can be combined and globally fit to an isotropic rotational diffusion model with internally consistent rotational correlation times over a wide range of solution viscosities (Hustedt et al., *Biophys. J.* in press). These methods are now being extended to the analysis of the dynamics of band 3 protein in the human erythrocyte. Preliminary studies have indicated that saturation transfer (ST-EPR) data from spin-labeled band 3 can be reasonably fit to an uniaxial model with a characteristic rotation time of approximately 20 microseconds at 37°C. The ultimate goal of this work is to simultaneously fit ST-EPR and phosphorescence anisotropy decay data to a single motional model in order to define the rotation times and mole fractions of the motional species of band 3 present under a variety of conditions. Supported by N.I.H. grants HL34737, CA43720, RR04075, GM45990, RR05823, and T32 DK07186.

**Tu-Pos500**

**TRACKING OF SINGLE FLUORESCENT PARTICLES IN THREE DIMENSIONS BY A POINT-SPREAD FUNCTION BASED AUTOFOCUS METHOD.** ((H. Pin Kao and A.S. Verkman)) U.C.S.F., San Francisco.

In order to track the motion of fluorescently-labeled subcellular components and microinjected fluorospheres, a single particle tracking (SPT) technique was developed to determine in real-time the  $x, y, z$  position of a  $< 500$  nm fluorescent particle. The cell sample was fixed on the stage of an epifluorescence microscope having paraxial-confocal optics. The fluorescence image was detected by a cooled CCD camera. The axial ( $z$ ) position was tracked using closed loop feedback-control of a microstepper motor which moved the stage vertically. The control algorithm utilized the asymmetric point-spread-function of the objective lens. The system response time was minimized by collection of a rectangular subset of the CCD array and 1-dimensional binning. The planar ( $x, y$ ) position was determined by image analysis. The  $x, y, z$  spatial resolution of the instrument was  $50 \times 50 \times 100$  nm and the tracking time was  $< 0.5$  s. This SPT method was applied to measure particle motion in intact cells: (a) Measurement of water permeability in adherent cultured cells by SPT of a fluorosphere bound to the cell surface, (b) Study of intracellular organization by SPT of fluorospheres microinjected into the cytoplasmic or nuclear compartments, and (c) Analysis of endosomal trafficking by SPT of fluorescently-labeled endocytic vesicles. The SPT method should be useful for analysis of diffusive and directed motions of individual fluorescent particles in living cells.

**Tu-Pos497**

**Functional Localization of Cognitive Responses in the Adult Human Brain.** Z. Zhuang, B. Cohen, Che. Amit, B. Chance. Univ. Pennsylvania, Dept. Biophys/Biochem., Phila., PA 19104

The need for a fast, simple, economical detector of blood volume (or concentration) changes in the frontal region of the human brain is satisfied by a dual wavelength tissue spectrometer (1,2). This device employs two wavelengths that "straddle" the isobestic or crossover point in the Hb/HbO<sub>2</sub> absorption spectrum. The sum of the two absorbances gives the changes of effective hemoglobin concentration at about 2 cm beneath the surface of the left frontal region of the forehead when the light input/output separation is 4 or more centimeters. Responses to visual presentation of abstractions over a 10 minute interval evokes changes of blood concentration in the frontal region over and above those present in a subsequent rest interval of 10 min. These changes are detected by their recurrence frequencies using a fast Fourier transform display in the 0-3 Hz region (as limited by the electronic circuitry). The most prominent "activity" responses are in the 0.5 - 2.5 Hz region. Similar patterns are evoked in a large population of young individuals who are stimulated by the SAT abstractions. One population was reported last year (1). Another population (150 tests) last winter has used noun-verbs. This summer's study of 120 tests used abstractions, the responders are over 85% of three groups studied over 18 months, totaling over 300 tests. A small portion of individuals rejected the abstractions and showed diminished activity. Indifferent individuals show no change. Thus the simple optical probe appears useful in the objective evaluation of localized cognitive function.

1. Chance, B. et al (1992) *Biophys. J.* Abstr 2985

2. Gopinath, S.P., Robertson, C.S. et al (1992) Near-Infrared Spectroscopic

Localization of Intracranial Hematomas. *J. Neuro. Sci.* in press.

This work was supported in part by NSF Grant # RR 03365.

**Tu-Pos499**

**EVALUATION OF TYROSINE TO TRYPTOPHAN RATIOS IN PROTEINS BY LINEAR COMBINATIONS OF SPECTRA** ((E. Waxman, E. Rusinova, G.P. Schwartz, J.B.A. Ross, W.R. Laws, and C.A. Hasselbacher)) Department of Biochemistry, Mount Sinai School of Medicine of CUNY, New York, NY 10029.

Estimation of tyrosine (Tyr) and tryptophan (Trp) content in a protein is often done by measuring the absorbance of the protein at two wavelengths [Edelhoc (1967) *Biochemistry* 6, 1948-1954]. We show that the Tyr to Trp ratio can be more accurately determined from the absorption spectrum of denatured protein (buffer + 6 M Gdm-Cl) using a linear combination of the spectra (LINCS) of model compounds (same solvent). That is, the absorbance as a function of wavelength ( $\lambda$ ),  $A(\lambda)$ , can be fit to  $A(\lambda) = \sum a_i A_i(\lambda)$ , where  $A_i(\lambda)$  are the basis absorption spectra of the model compounds, and  $a_i$  are the relative molar amounts of each basis spectra. The basis spectra are verified and properly scaled (relative extinctions) based on LINCS analyses of polypeptides with known Trp and Tyr content. The method works for binary N-acetyltyrosinamide and N-acetyltryptophanamide mixtures over a 0.01 to 100 Tyr/Trp ratio, and for a set of proteins of known composition. The potential problems of light scatter and disulfides will be discussed. LINCS is an excellent way to quickly screen mutants, establish purity, and estimate Trp content. LINCS can also be used to quantitate the number of Trp residues replaced in a spectrally enhanced protein. Supported by NIH grant GM-39750.

**Tu-Pos501**

**THEORY OF TWO-PHOTON INDUCED FLUORESCENCE ANISOTROPY DECAY IN MACROSCOPICALLY ISOTROPIC OR ORIENTED MEMBRANE SYSTEMS** ((Sun-Yung Chen and B. Wieb Van Der Meer)) Department of Physics and Astronomy, Western Kentucky University, Bowling Green, KY 42101.

We report the first theoretical description for the time-dependent fluorescence anisotropy decay,  $r(t)$ , resulted from two-photon excitation for fluorophores in isotropic or oriented membranes. In case of two-photon excitation, the initial value of fluorescence anisotropy,  $r(0)$ , is a function of the components of two-photon transition tensor ( $S$ ) and the projections of the emission dipole to the principal axes of  $S$ . The components of  $S$  are dependent upon the symmetry of all molecular states relevant to the two-photon absorption process. The maximal value of  $r(0)$  for two-photon excitation is proven to be 4/7 in contrast to 2/5 for one-photon excitation. It is shown that for an extreme case the ratio of the two-photon  $r(t)$  over the conventional one-photon  $r(t)$  may equal 10/7 at all times. The advantages of measuring  $r(t)$  by two-photon excitation for the study of orientational dynamics in membrane systems are discussed from the theoretical point of view. This work is supported by the National Science Foundation EPSCoR program (EHR-9108764).

**Tu-Poe502**

**MULTIPLE SEQUENCE ALIGNMENT METHODS.** ((L.S. Yeh, G.Y. Srinivasarao, and W.C. Barker)) National Biomedical Research Foundation, Washington, DC 20007.

Many methods for automatically constructing multiple alignments of nucleic acid or protein sequences have been described in the recent literature (Higgins et al., 1992 and references therein). As the initial phase of our systematic study, we will compare selected methods such as AMPS, CLUSTAL V, and TREEALIGN for their usefulness in handling different types of protein alignments. Representative sets having fragments, long sequences, and sequences more than 50% different will be studied using each of these alignment programs with varying parameters. For each of the methods, there should be an optimal set of parameters for each sequence set. These results will be tabulated as functions of the pairwise similarity scores among sequences represented in the alignments. In this study, the running times of these methods as a function of sequence similarity, alignment length, and number of sequences will be evaluated. (Supported by NLM grant P41 LM05206 and NSF grant BIR-9107540)

**Tu-Poe504**

**COUPLING POISSON-BOLTZMANN FINITE-DIFFERENCE METHODS WITH MOLECULAR MECHANICS AND MOLECULAR DYNAMICS.** ((Jeffrey D. Madura and Michael K. Gilson)) Department of Chemistry, University of South Alabama, Mobile, AL 36688 and Department of Chemistry, University of Houston, Houston, TX 77204

Finite-Difference solutions to the Poisson-Boltzmann equation have been used in the computation of electrostatic energies of small organic molecules and large biological macromolecules. Along with accurate electrostatic energies, it is now possible to compute accurate atomic forces associated with the Poisson-Boltzmann Equation. The ability to compute these forces make it possible to consider performing energy minimizations and molecular dynamics using continuum electrostatic methods. Continuum methods now have the potential of providing a computationally efficient means of incorporating electrostatic effects of a solvent containing dissolved ions into calculations involving peptides and proteins. To demonstrate the validity and utility of continuum models in molecular mechanics and molecular dynamics we will present results from energy minimizations and molecular dynamics of 1,2-dichloroethane in *vacuo*, in 1,2-dichloroethane, and in water. We also outline the procedures for performing these types of calculations. 1,2-Dichloroethane is a particularly good model because it has profound solvent effects in going from the gas phase to pure liquid or when solvated in an aqueous environment.

**Tu-Poe506**

**SARCOMERE DYNAMICS IN SMALL REGIONS OF CARDIAC CELLS MEASURED BY IMAGE ANALYSIS** ((M.H.P. Wussling)) J. Bernstein Institute of Physiology, University of Halle-Wittenberg, D O - 4020 Halle/Saale

Laser diffractometry has been often used to measure dynamical changes of the sarcomere structure. The number of sarcomeres that generate the diffraction pattern is dependent on the diameter of a commonly focussed laser beam in the region illuminated. In practice, the spot size of a He-Ne laser beam in the focal plane is 100  $\mu\text{m}$  or more. This is in the order of an intact rodlike cardiac myocyte. Thus, it is unjustified to investigate local changes of sarcomere length by laser diffractometry in that preparation.

Spontaneous contractile waves of isolated rat heart cells were analyzed using Fast Fourier Transform (FFT). The data of a CCD camera mounted to an inverting microscope was captured in a Macintosh IIfx computer directly or via an image processor in order to freeze the contractile wave in a distinct portion of the cardiac cell. A VCR was used to store data for dynamical measurements. The "diffraction pattern" obtained by the FFT of the cell's active region clearly differs from that of the relaxed portion even if the number of sarcomeres is less than 10 (i.e. the region of interest is less than 20  $\mu\text{m}$ ). Our results demonstrate that image analysis is an appropriate tool to show local inhomogeneities of the sarcomere structure in cardiac myocytes. (Supported by DFG, Wu 194/1-1)

**Tu-Poe503**

**HYBRID FINITE DIFFERENCE-BOUNDARY INTEGRAL METHOD FOR CALCULATING SOLVATION ENERGIES.** ((P. Beroza, D.R. Fredkin, and G. Feher)) Department of Physics, 0319, University of California, San Diego, La Jolla, CA 92093, USA.

We employed a hybrid finite difference-boundary integral method to calculate solvation self-energies from the Poisson-Boltzmann equation. In continuum electrostatic models the solvation self-energy of a charge in a molecule is calculated from its energy in the reaction field, whose sources are the counterions in solution and the polarization induced in the solvent surrounding the molecule.

We calculated the reaction field potential at the charge from a single finite difference calculation by integrating an expression containing the potential and its normal derivative over the surface of a cube containing the charge. This method avoids the subtraction of large (actually infinite were it not for the discrete grid) quantities from two separate finite difference calculations, as is often done.<sup>1,2</sup> Although the two methods give similar results, the subtraction method, in contrast to ours, lacks mathematical justification.

We confirmed the accuracy of our method on spherical molecules for which exact results are available.<sup>3</sup> We shall discuss the accuracy of the method and its application to the calculation of pK's of amino acids in proteins.

<sup>1</sup>Gilson, M.K. and Honig, B. (1988) *Proteins* 4, 7-18.

<sup>2</sup>Bashford, D. and Karplus M. (1990) *Biochemistry* 29, 10219-10225.

<sup>3</sup>Tanford, C. and Kirkwood, J.G. (1957) *JACS* 79, 5333-5339.

\*Supported by NSF, NIH, and NIH training grant 1T32 GM08326-01.

**Tu-Poe505**

**COMPUTER TOOLKIT FOR FIBER & MEMBRANE DIFFRACTION** ((T.T. Tibbitts)) Physics Dept, Boston University, Boston, MA 02215

A toolkit of general, easy to use computer programs will be described for processing diffraction patterns from oriented biomolecular filaments and membranes, in order to refine structural models of these assemblies to the highest possible resolution. These applications have been written in C for workstations with MOTIF/Xwindows support; the component functions also run standalone using terminal i/o or no display. By dynamically allocating all data arrays at run time, the programs are limited only by the machine resources. All use the madnes image file format (M.Stanton) for autodocumentation of the analysis and easy data exchange across computer platforms. The display package *scope* provides an event-driven interface for finding the pattern origin, refining the specimen tilt angle, correcting for film response, cutting out sections of the pattern, rescaling, rotating, examining pixel values, averaging patterns together, adjusting the color table, editing the file header, and creating postscript output. Additional programs determine background scatter, and correct the patterns for curvature of the Ewald sphere. Using the package *gen*, the processed pattern can be indexed for any repeat distance and/or helical selection rule and an initial deconvolution obtained for a trial coherence length and disorientation. Models based on this deconvolution and/or independent information can then be refined using iterative angular convolution and local regression, which accounts for the effects of cylindrical averaging, specimen disorder, imperfect orientation, and finite beam collimation (Tibbitts & Caspar, *Acta Cryst. A*, in press). Deconvolutions of data from oriented purple membranes containing bacteriorhodopsin (A.Blaurock), and fibers of adhesion pill from *E. coli* (M.Gong & L.Makowski) will be presented.

**Tu-Poe507**

**ANALYSIS OF NOESY SPECTRA OF POLYPEPTIDES BY MEANS OF GLOBAL OPTIMIZATION**  
Yuan Xu and Istvan P. Sugar  
Departments of Biomathematical Sciences and Physiology/Biophysics, The Mount Sinai Medical Center, New York, N.Y. 10029

We recently developed an automated structure refinement method for the analysis of NOESY spectra of polypeptides (Sugar and Xu, Computer Simulation of 2D-NMR-NOESY Spectra and Polypeptide Structure Determination. *Prog.Biophys.Molec.Biol.* 52, 61-84). This new method - an adaptation of the *method of variable target function* - is a successful attempt to overcome the multiple minima problem arising in most of the structure refinement methods.

In this work, the limitations of our structure refinement method for NOESY spectrum analysis is tested. The effects of two parameters, constraint density (CD) and relative fragment length (RFL), on the performance of the method are investigated. CD is the average number of resolved cross-peaks per residue. RFL is the length of the analyzed polypeptide fragment relative to the total length of the polypeptide molecule.

The first set of tests was performed at constant RFL(=1) and different CD values. The structure refinement method resulted in correct polypeptide structures as long as CD was greater than 6. In the second set of tests CD was kept constant (CD=15) and RFL has been varied. In this case we got the correct backbone structure of the polypeptide fragment at  $1 \geq RFL > 0.33$ .

For the purpose of these tests experimental NOESY data have been simulated by using the crystal structure of BPTI.

## Tu-Poe508

A GENERALLY USEFUL METHOD TO SPECIFICALLY LABEL PHOSPHORYLATABLE AMINO ACIDS WITH EXTRINSIC PROBES. (Kevin C. Facemyer, Mark R. Tibeau and Christine R. Cremona), Dept. of Biochemistry and Biophysics, Washington State University, Pullman, WA 99164-4660.

We have developed a method to attach extrinsic probes to amino acids that can be specifically phosphorylated by protein kinases (Facemyer and Cremona (1992) *Bioconjugate Chemistry* 3, 408-413). We have shown that the phosphorylatable ser-19 of the regulatory light chain (RLC20) of smooth muscle myosin can be specifically and stoichiometrically labeled with haloacetyl derivatives. The method involves blocking of the thiols of isolated myosin light chains by reversible or irreversible methods. Following thiol blocking, the protein is specifically thiophosphorylated at ser-19 with myosin light chain kinase. The thiophosphate is then reacted with haloacetyl derivatives to form the stable phosphorothioate ester. If appropriate the oxidized sulfhydryls are then returned to the native reduced form by treatment with reductant. Here we have shown that the rate of reaction of a haloacetate toward the thiophosphate is independent of pH in the pH 6-9 range. We have extended the approach to determine the reactivity of the thiophosphate toward maleimide derivatives. We also show that the phosphorothioate ester can be efficiently cleaved by mercuric acetate, which provides a new technique for photocrosslinking experiments that does not require use of a radioactive photocrosslinking reagent.

## Tu-Poe510

A VERSATILE SPECTRO-FLUOROMETER FOR KINETIC STUDIES OF SINGLE WHOLE-CELL CLAMPED CELLS. L. Cleemann, T. C. L. Tran and M. Morad. Department of Physiology, University of Pennsylvania, Philadelphia, PA.

An inverted microscope used in a single cell patch clamp setup was equipped as a true spectro-fluorometer by introducing rapidly scanning monochromators both into the epi-illumination pathway (Xenon arc lamp) and into the light detection pathway (photo multiplier tube). Each monochromator was based on a diffraction grating next to a servo controlled mirror. This system (including patch clamp amplifier and rapid perfusion manifold) was controlled with a microcomputer using custom designed software which allowed full integration of electrophysiological and optical procedures.

Complete emission and excitation spectra measured from single ventricular cardiomyocytes loaded with the  $Ca^{2+}$ -indicator dye fura-2 could generally be resolved by linear superposition (least squares analysis) of in-vitro spectra from Ca-free and Ca-saturated samples of the dye. Similarly, repeated measurements of excitation spectra during voltage clamp activation showed that the isosbestic point remained stable at the in-vitro value. However, differential measurements of spectra recorded before and after the "balling-up" of the  $Ca^{2+}$  overloaded cell, suggest that of the emission of the fura-2 fraction which does not bind  $Ca^{2+}$  is shifted to slightly longer wave lengths. Spectra from cells dialyzed simultaneously with fura-2 and fluorescein showed that the characteristic spectra of different indicator dyes could be distinguished at the cellular level. Absorption measurements on single cells showed that the non-fluorescent dye ruthenium red diffused very slowly (>10 min) into the cell but could be injected within seconds with gentle back pressure applied to the patch pipette (2-3 MOhm).

It is concluded that this equipment has the flexibility to perform optical measurements at the cellular level in such a way that the acquisition of detailed spectral information can be freely interlaced with rapid kinetic measurements. (Supported by NIH grant HL16152).

## Tu-Poe512

ANALYSIS OF TECHNIQUES USED FOR MEASURING MEMBRANE CAPACITANCE ( $C_m$ ) AS A SINGLE CELL ASSAY OF EXOCYTOSIS. ((K.D. Gillis)) The Jewish Hospital of St. Louis, St. Louis, MO 63110. (Spon. by C.C. Hunt)

The measurement of  $C_m$  permits high resolution monitoring of exocytosis and endocytosis in single cells. Techniques for estimating  $C_m$  involve applying a sinusoidal voltage and then using a "phase sensitive detector" (PSD) to analyze the resulting sinusoidal current. The "phase tracking" technique adjusts the phase ( $\alpha$ ) of the PSD to output a signal insensitive to an induced change in series resistance ( $\Delta R_s$ ). Quantifiable limitations of this technique include an error in  $\alpha$  due to stray capacitance between the bath and ground, variance of  $\alpha$  ("phase jitter") resulting from measurement noise, and artifacts accompanying each update of  $\alpha$ . Another technique uses complex impedance analysis, together with dc information to estimate  $C_m$ . The dynamic range of this approach is extended if automatic capacitance compensation (e.g. EPC-9) is available. An alternative hardware technique to determine  $\alpha$  without the need for  $\Delta R_s$  is from the phase of the complex admittance ( $\beta$ ):  $\alpha = 2^* \beta - \pi/2$ . Calibration of  $C_m$  with the gain relation:  $\omega/(1+\tan^2(\beta))$  does not require adjustment of capacitance compensation circuitry. (Support: NIH DK37380).

## Tu-Poe509

Spatial Localization of Absorbing or Fluorescent Objects Inside Tissue: Progress Using New Photon Density Wave Interference Techniques

A. Knuettel\*, J.M. Schmitt\*, R.L. Barnes+ and J.R. Knutson+

\*BEIP,NCRR) and +(LCB,NHLBI):NIH, 10/5D10, Bethesda, MD 20892

Near-infrared tissue imaging developed in recent years by adapting either time-resolved or frequency domain fluorescence instruments to the recovery of scattered light arrival profiles. Most of the devices operate in transmission only, and their moderate resolution was obtained by laborious and slow mechanical scanning of source/detector or object.

After we introduced the (destructive) interference of diffusive photon density waves as a powerful tool for localization (particularly depth), we extended the method by employing acousto-optic scanning and the electronic control of source power and phase (creating a "phased array" source, in analogy to radar, but having the advantage of amplitude steering in the dispersive medium). Further, we recovered 2D maps of phase and amplitude from a gated, intensified CCD camera modulated at typical frequencies of 250MHz-1GHz. Our reflection-mode instrument can localize either a fluorescent or absorbing probe to better than 1 mm when it is buried 1 cm inside tissue. Our measurements were extensively modeled and verified by both numerical and analytical solutions of the diffusion equation. Recently, we have begun to extend the technique with two overdetermination methods - multifrequency (stretched wiper) and multicolor (FM laser) acquisition. The improved resolution and prospects will be discussed in light of theoretical limits.

## Tu-Poe511

NEW APPLICATIONS AND ADVANTAGES OF DETECTOR ARRAYS IN MULTIFREQUENCY PHASE AND MODULATION FLUOROMETRY ((M.vandeVen, B.Barbieri and E.Gratton\*)) ISS Inc, P.O. Box 6122, Champaign, IL 61826 and \*Laboratory for Fluorescence Dynamics, Physics Dept., Univ. of Illinois at Urbana-Champaign, 1110 W. Green St., Urbana, IL 61801.

Array detectors enable rapid wavelength-resolved accumulation of steady-state and time-resolved fluorescence/phosphorescence emission data. An initial report by Gratton et al. on the technique applied to multi-frequency phase and modulation fluorometry appeared in SPIE 1204, 21-25 (1990). For various instrument implementations we will present the characteristics of most interest to the spectroscopist like attainable frequency-range, signal-to-noise ratio, detection limits and the reduction in measurement time as compared to standard scanning emission monochromator techniques, optical coupling efficiencies and remote sensing. We will show time-, wavelength-, and phase and modulation resolved spectra of some standard fluorophores and several biological samples.

## Tu-Poe513

IMPROVED METHODS FOR LABELLING CELLULAR AQUEOUS COMPARTMENTS WITH FLUORESCENT POLAR DYES S. Yoshikami, Sudhir Sahu, & W.A. Hagins. Lab. of Chemical Physics, NIDDK, NIH, Bethesda, MD 20892.

The usual method for transferring chelating fluorescent indicator dyes to cells is as acetoxyethyl esters (R.Y.Tsien, Nature, 290, 527, 1981). Where there is intracellular esterase activity, the dye cleaves to form the free metallochromic indicator, trapped where it is hydrolyzed. Intensified video microscopy shows that some cells, including most vertebrate retinal rods and cones lack the esterases needed to free significant cytoplasmic amounts of FURA-2 or FLO-3. Yet the same cells load quickly with mM levels of 6-carboxyfluorescein from its diacetate ester. This is mainly due to non-enzymatic transacylation of free -NH<sub>2</sub> and -SH groups and is not useful for staining cells with Tsien's dyes.

We find that t-butyl dimethylsilyl (TBDMS) esters of a variety of fluorochromic indicator dyes uniformly label the cytosols of many cell types by traversing the cell membrane lipids and spontaneously hydrolyzing by non-enzymic reaction with H<sub>2</sub>O to yield >10  $\mu$ M of free dyes. At 50  $\mu$ M levels, the silylated dyes and the silanols produced are non-hemolytic and do not affect electroretinograms of frog retinas. TBDMS esters of iminodiacetic acids hydrolyze with half-times of 40 m, allowing good equilibration of cellular compartments before hydrolysis and permitting theoretical estimation of free dye concentrations in them. The wide range of hydrolysis rates among available types of silyl groups permits a range of tissue thicknesses to be stained by this method. HPLC and fluorescence micrographic studies of the dyes in lymphocytes, protozoa, fibroblasts, and retinas will be shown. The method seems to be generally useful in transferring extracellular polar molecules to the cytosol.

**Tu-Pos514**

**RESOLUTION OF ABSORBING SPHERES IN A HIGHLY SCATTERING MEDIUM: FREQUENCY-DOMAIN STUDIES AND A TOMOGRAPHIC RECONSTRUCTION SCHEME.** ((John Maier and Enrico Gratton)) University of Illinois at Urbana-Champaign, Laboratory for Fluorescence Dynamics, Department of Physics, 1110 W. Green St., Urbana, IL 61801.

We performed frequency-domain studies of the diffraction of a photon density wave, traveling in a homogeneous, highly scattering medium, by spherical and disk shaped absorbing objects. Measurements were made with light intensity modulation frequencies in the 10 to 120 MHz range. The source was a diode laser emitting at 810 nm. Skim milk was used as the scattering medium. The effect of the object's size, position, and shape were studied in the transillumination geometry. Spheres as small as 0.8 mm radius were detected with a source-detector separation of 5 cm. A collection of small absorbing spheres was also studied. The spatial characteristics of the bundle of photon migration paths were mapped, in the frequency domain, from source to detector on the surface of the scattering medium (backscattering geometry). The results lead to a model for tomographic reconstruction of objects deep in a scattering medium, made from measurements taken at the surface. This model involves constructing a 3-dimensional density histogram, based on a model bundle and measurements of amplitude, phase, and modulation made at the surface. Supported by National Institutes of Health (RR03155) and UIUC.

**Tu-Pos516**

**INERT GLUE IN THE SURFACE FORCE APPARATUS? WHERE ARE THE CONTROLS?** ((V.A. Parsegian, N.L. Gershfeld)), NIAMS/NIDDK/DCRT, NIH, Bethesda, MD 20892

During the past several years, the 'surface force apparatus' (SFA) has been widely regarded as a means to study interactions between mica and coated-mica surfaces. Some observations, e.g., electrostatic double layer decay lengths, have been consonant with earlier expectation. Others, e.g., the "long-range hydrophobic force", have many elicited frustrating attempts at explanation. Seeking a simpler explanation for unexpected results, we noted few reports in the SFA literature of the kind of control measurements that invariably accompany more conventional surface chemical studies. We therefore began control measurements for the SFA with an examination of the adhesive commonly used to fasten mica to the optical glass - the commercial Epon or Epikote 1004 - using four glue samples from three different SFA laboratories.

*Our observations indicate that the glue is not inert but rather creates a measurable amount of water-soluble material that is also surface active.*

- \* Grains of glue send out a film onto the air/water interface.
- \* Glue dissolves in distilled water.
- \* Glue from solution adsorbs to freshly cleaved mica.

Any consideration of the consequences of glue contamination in the interpretation of SFA results should probably be deferred until the actual magnitude of neglected contamination is adequately determined.

**Tu-Pos518**

**TRANSMEMBRANE VOLTAGE CONTROL IN LIPOSOMES: THE USE OF BACTERIORHODOPSIN AS A LIGHT-DRIVEN CURRENT SOURCE** ((Eduardo Perozo and Wayne L. Hubbell)) Jules Stein Eye Inst. and Dept Chemistry and Biochemistry, UCLA Los Angeles CA 90024.

We present a new general method for the development and control of transmembrane potentials ( $\Delta\psi$ ) in reconstituted vesicles.  $\Delta\psi$  were measured using two independent techniques. Electron Paramagnetic Resonance (EPR) spectroscopy was used to monitor the distribution and binding of spin-labeled phosphonium ions. Additionally, the distribution of tetraphenylphosphonium (TPP<sup>+</sup>) was followed using electrodes with a PVC-based ion exchange resin. The light-driven proton pump, Bacteriorhodopsin (BR) from *Halobacterium halobium* was used as the current source of the system, where the intensity of light controls the magnitude of the  $\Delta\psi$  at any given time. A stable, steady state bias or holding potential was generated using gradients of anions of limited permeability, in the presence of a highly impermeable cation. Using the polymer Polyethyleneimide (PEI) or N-Methyl Glucamine (NMG) as the impermeable cation, the sequence of permeabilities for egg phosphatidylcholine vesicles was (from the least permeable):  $\text{SO}_4^- < \text{Br}^- < \text{F}^- < \text{NO}_3^- < \text{SCN}^-$ .  $\text{NO}_3^-$  and  $\text{SCN}^-$  were most effective in producing large (> -60 mV) negative potentials. In the presence of a  $\text{NO}_3^-$ -based negative holding potential (-70 mV), BR is capable of depolarizing the membrane to at least the 0 mV level within a few seconds. Effective and fast depolarizations can be achieved by the application of a brief intense illumination preceding the preset illumination level (Supercharging). The technique can be applied to study most voltage-dependent processes by fusion of reconstituted systems with BR-containing liposomes. We report voltage activation of unmodified, reconstituted eel Na<sup>+</sup> channels using this technique. Supported by the PEW Charitable Trust.

**Tu-Pos515**

**BREAKDOWN OF THE DIFFUSION APPROXIMATION IN DESCRIBING PHOTON MIGRATION THROUGH RANDOM MEDIA.** ((Joshua B. Fishkin, Peter T.C. So, and Enrico Gratton)) University of Illinois at Urbana-Champaign, Laboratory for Fluorescence Dynamics, Department of Physics, 1110 W. Green St., Urbana, IL 61801.

The diffusion approximation to the Boltzmann transport equation is valid only in the multiple scattering regime. We determined at what scatterer concentration and distance from a light source that light propagation through random media is described by this approximation. We performed frequency-domain measurements in the MHz to GHz range in which we studied the properties of intensity-modulated light propagating through media containing different concentrations of light scatterers and absorbers. The experimental data are compared to the predictions of the diffusion approximation to the Boltzmann transport equation. The scattering and absorption conditions under which the diffusion approximation fails are compared with typical scattering and absorption conditions found in animal tissues. This work was performed at the Laboratory for Fluorescence Dynamics (LFD) at the University of Illinois at Urbana-Champaign (UIUC). The LFD is supported jointly by the National Institutes of Health (RR03155) and by UIUC.

**Tu-Pos517**

**TWO NEW INSTRUMENTS FOR MONOLAYER STUDIES: A PIEZOCERAMIC FORCE TRANSDUCER FOR SURFACE TENSION MEASUREMENTS AND A LEAK-FREE TROUGH FOR SURFACE PRESSURE-AREA ISOTHERMS.** ((R. Qiu and R.C. MacDonald)) Department of Biochemistry, Molecular Biology and Cell Biology, Northwestern University, Evanston, IL (Spon. by L. Lorand).

With the appropriate electronic circuit, an inexpensive (\$10) piezoelectric ceramic bender (2.5" x 0.1") is a sensitive force transducer for accurate surface tension measurements. These devices are not suitable as steady-state transducers; however, this is no obstacle when the Wilhelmy method is used in the detachment mode. Under such conditions, the voltage output of the transducer is linearly related to the applied force at millivolts or more per dyne. Tension measurements have a precision of <1 dyne/cm. Because of the low cost, dozens of simultaneous measurements can be done simultaneously using common computer multiplexing interface boards.

The problem of barrier leakage in pressure-area measurements has been overcome with a trough in which the sample is compressed within an initially circular band of teflon-covered spring steel strip. A computer-controlled stepping motor drive applies force to one side of the ring, and it deforms from a circle to a "V" shape. Because the band undergoes an unusual distortion, calibration is most conveniently done with a computer-interfaced video imaging system. Surprisingly, the change in area is very close to a linear function of the displacement of side of the band. The area change can be up to 4:1 and is repeatable to 2%. The design greatly simplifies the design of surface troughs and completely obviates the possibility of leakage at high surface pressures.

**Tu-Pos519**

**AFM OF DNA, MEMBRANE AND MEMBRANE PROTEINS**

((Jie Yang\*, Lukas K. Tamm\*, Thomas W. Tillack†, Kunio Takeyasu† and Zhifeng Shao\*)) Departments of \*Physiology and †Pathology, University of Virginia, Box 449, Charlottesville, VA 22908; †Dept. of Med. Biochem. and Biotech. ctr, Ohio State University, Columbus, OH 43210.

We have successfully applied atomic force microscopy (AFM) on a range of biological specimens. With DNA-cytochrome C complexes on carbon-coated mica directly imaged by AFM in air, a resolution of 4 - 6 nm was routinely obtained for a force of 3 - 10 nN, and a resolution better than 3 nm was achieved when the force was below 3nN (mostly in an organic solvent). Synthetic lipid bilayers (DAPC, DSPC, DPPC, DMPC, DPPE, DMPE and POPE) transferred to freshly cleaved mica surfaces in a Langmuir trough were imaged by AFM in aqueous solutions. For polymerized bilayers of the diacylene lipid DAPC a ridge structure of 1.1 nm periodicity was readily observed. For the other bilayers, good patches of flat bilayers were observed only occasionally. When cholera toxin (complete and B-subunit oligomers) was bound to mixed bilayers of DAPC and the receptor glycolipid GM1, the pentameric subunit structure was well resolved by AFM in buffer, without crystallization. The resolution is better than 2 nm with excellent reproducibility for a probe force of 0.3 - 0.5 nN. These results indicate that AFM can indeed be used to study macromolecular structures at physiological conditions, if suitable specimen preparation techniques can be found. Work supported by grants from the Whitaker Foundation, the US Army Research Office, NIH, and the Jeffress Trust.

**Tu-Poe520**

**DETECTION AND LOCALIZATION OF OPTICAL HETEROGENEITIES OBTAINED BY TISSUE-LIKE SCATTERING FROM FREQUENCY-DOMAIN MEASUREMENTS OF PHASE-SHIFT DIFFERENCE AND REDUCED MODULATION.** ((E.M. Sevick, J.K. Frisoli, C.L. Burch, and J.R. Lakowicz)) Department of Chemical Engineering, Vanderbilt University, Nashville, TN 37235; \*\*Center for Fluorescence Spectroscopy University of Maryland, Baltimore, MD 21201.

Previously, we have demonstrated the capacity to "image" a 3 mm diam. absorber obscured by tissue-like scattering from maps of phase-shift difference,  $\Delta\theta$  ( $\theta_{\text{presence}} - \theta_{\text{absence}}$ ) and reduced modulation,  $M_r$  ( $M_{\text{presence}}/M_{\text{absence}}$ ) reconstructed from 2-D, multi-pixel  $\theta$  and  $M$  frequency-domain measurements in the absence ( $\theta_{\text{absence}}$  and  $M_{\text{absence}}$ ) and in the presence ( $\theta_{\text{presence}}$  and  $M_{\text{presence}}$ ) of the absorber (Sevick, et al., *Photochem. Photobiol.*, 1992). These 2-D images suggested a physical model for photon migration imaging (PMI) which to date has been untested. In this study, single-pixel measurements and Monte Carlo predictions of  $\Delta\theta$  and  $M_r$  are presented to provide verification of the frequency-domain PMI model in reflectance geometry. Measurements and simulations demonstrate that  $\theta$  and  $M$  display significant changes due to the presence of perfect light absorbing and transparent volumes that are predictable from the physical model of frequency-domain PMI. Results furthermore illustrate that the changes in  $\theta$  and  $M$  are dependent upon modulation frequency and may provide unique three dimensional localization information from two dimensional reflectance measurements. The frequency-dependence of previous multi-pixel measurements compare well with the single-pixel experimental and simulated values of  $\Delta\theta(f)$  and  $M_r(f)$ . Supported in part by NIH-BSRG 2 S07 RR01201-12 (EHS).

**Tu-Poe522**

**A NOVEL IN VITRO TRANSLATION SYSTEM FOR PREPARATIVE SCALE CUSTOM PROTEIN SYNTHESIS.** ((B.R. MOZAYENI<sup>1,2</sup>, E.S. NAJEM<sup>1,2</sup>, J.A. FERRETTI<sup>1</sup>, and F.M. RICHARDS<sup>3</sup>)) 1) Structural Biophysics Section, LBC, NHLBI, NIH, Bethesda, MD; 2) Dep't of Molecular Biophysics and Biochemistry, Yale School of Medicine, New Haven, CT; 3) Dep't of Radiology, Johns Hopkins School of Medicine, Baltimore, MD

A high expression rate (17mg/ml lysate/6hrs) for globin mRNA endogenous to reticulocyte lysate was achieved by dialysis-ultrafiltration of the lysate with a modified substrate feed solution in a novel bioreactor. To reproduce optimized conditions and to modify reaction parameters in real-time response to the translation rate for any given mRNA construct, a flexible computerized process control system was designed and implemented. Metabolic parameters which govern preparative scale *in vitro* translation of globin were controlled to optimize its expression. Our control of the reaction conditions was sufficiently robust to permit globin production even with micrococcal nuclease-treated lysate. These results suggest that exogenous mRNA for a protein of choice can be expressed at a rate comparable to that achieved for globin. Since mRNA may be transcribed from PCR-derived linear cDNA and because artificial codons can be introduced by site-directed mutagenesis, this system will permit production *in vitro* of site-specifically labelled recombinant proteins in sufficient quantities for conformational determinations by high resolution nuclear magnetic resonance spectroscopy.

**Tu-Poe524**

**A PROTOTYPE ON-LINE RAYLEIGH INTERFEROMETER FOR THE XLA ANALYTICAL ULTRACENTRIFUGE.**

((T.M. Lauc, A.L. Anderson and P.D. Demaine)) Dept. of Biochemistry, University of New Hampshire, Durham, NH 03824.

A Rayleigh interference optical system has been developed for the Beckman XLA analytical ultracentrifuge. The interference optics have been arranged so that absorbance and refractive data may be acquired simultaneously. The pulsed laser diode light source fits in the chamber and is modulated to allow data acquisition from multiple cells. A solid-state television camera serves as the detector. The intervening optics are arranged to provide a 1.4-fold magnified image of the cell at the camera, yielding a radial data spacing of about 9  $\mu\text{m}$  in the cell coordinate system. Fringe displacements are measured using a discrete, single-frequency Fourier analysis, providing a precision better than  $\pm 0.005$  fringe. Less than 20 seconds are required to acquire a scan spanning an entire cell ( $\approx 2000$  data points), save the data to a disk file and present the graph. All operations are controlled from a Windows-based program operating on a PC.

Supported by NSF DIR 9002027.

**Tu-Poe521**

**ELECTROROTATION OF COMPLEX STRUCTURES.**

(( M. Egger and E. Donath\*)) Physiologisches Institut, Universitt Zrich, Winterthurerstr. 190, CH - 8057 Zrich, Switzerland; \* Institut fr Biophysik, FB Biologie, Humboldt-Universitt zu Berlin, Invalidenstr. 42, D-O-1040 Berlin, Germany.

Electrorotation is a convenient method to measure the polarizability of single particles as a function of the frequency of the applied rotating electric field. It provides information about the membrane capacity, the membrane conductivity and the internal conductivity. Since up to now there were only theoretical models describing the electrorotation behavior of spherically or cylindrically symmetrical particles, the interpretation of some experimental results with biological particles was difficult. Therefore we calculated: the electrorotation behavior of (1) particle doublets in the dipole approximation as a function of an interaction parameter, and (2) a large number of aggregated particles again as a function of the intensity of aggregation expressed by the dielectric parameters of the gap between the particles.

The first model was experimentally verified with pollen and human erythrocytes. The second, theoretical model was used to interpret the behavior of an exocytotic cell, an aggregate of cells, and an aggregate of droplets, either water in oil or oil in water.

**Tu-Poe523**

**FLUCTUATING MEMBRANE POTENTIAL, RECORDED BY THE WHOLE CELL PATCH CLAMP TECHNIQUE, OF HUMAN T LYMPHOCYTE CELL LINES; EVIDENCE THAT IT IS A FRACTAL OF THE KIND PRODUCED BY FRACTAL BROWNIAN MOTION.** ((W.A. Gottschalk, S. Yeandle, A.M. Churilla<sup>1</sup>, L.S. Liebovitch, L.Y. Selector<sup>2</sup>))

<sup>1</sup>Naval Medical Research Institute <sup>2</sup>Columbia Univ.

Recently, Maltsev has reported that the T lymphocyte membrane potential oscillates (Immunology Letters, 26 (1990) 277-287). We have seen fluctuations in the membrane potential of 3 T lymphocyte cell lines. The appearance of these fluctuations, both in the time and the frequency domains, differ greatly from cell to cell. The result of Rescaled Range Analysis for a number of experiments yield values of the Hurst parameter H in the range of .86 to .95. In this method the difference R between the maximum and the minimum of a record within a time window T divided by the standard deviation S of the record in that window gives R/S which for a fractal process is proportional to T<sup>H</sup> (See Fractals by J. Feder). We have also observed that for frequencies f above 1 Hz that the power is about proportional to f<sup>(-b)</sup> where b ranges between 1.5 and 3.5. These results suggest that the fluctuations in the T lymphocyte membrane potential have the statistical properties of fractional brownian motion.

**Tu-Poe525**

**CONFOCAL FLUORESCENCE MICROSCOPY OF LIVING CELLS.**

((S.M. Doglia, L. Bianchi, and A.M. Villa)) Physics Department of University and Consorzio Bioricerche, Milano (Italy) (Spon. by F. Bruni)

New insights in the distribution of fluorescent drugs and dyes in single living cells can be achieved through confocal fluorescence microscopy. Results obtained by the laser scanning confocal microscope MRC-600 (Bio-Rad, Microscience Ltd., U.K.) with laser argon excitation and photon counting detection mode will be presented. The high level of confocality employed in the optics has allowed to image the cell within a narrow depth of focus (0.5 micron) and to obtain optical sectioning in the z-direction. Under these conditions high quality images from low drug concentrations of pharmacological significance can be obtained. As an example we will present the study of doxorubicin a fluorescent anthracycline with excitation at 480 nm and emission ranging from 500 to 650 nm, in different cell types (K562, L1210, 3T3). The following results will be discussed: 1) the drug accumulates in the nucleus only at high concentrations (10<sup>-6</sup> M); at low concentrations (10<sup>-9</sup> M) is mainly concentrated in the cytoplasm; 2) the nuclear fluorescence at high drug concentration is confined in the perinuclear region and in condensed chromatin zones around nucleolar structures.